Galanin neurons modulate stress responses in zebrafish larvae

Inaugural-Dissertation
to obtain the academic degree
Doctor rerum naturalium (Dr. rer. nat.)

submitted to the Department of Biology, Chemistry, Pharmacy
of Freie Universität Berlin

by

Laura Corradi

2022

The present work was carried out under the supervision of Dr. Alessandro Filosa and Dr. Suphansa Sawamiphak from October 2017 to January 2022 at the Max Delbrück Center for Molecular Medicine in the Helmholtz Association.

Data described in section 5.5.1 were obtained in collaboration with Prof. Dr. Marco dal Maschio and PhD candidate Matteo Bruzzone from University of Padua.

Herewith I certify that I have prepared and written my thesis independently and that I have not used any sources and aids other than those indicated by me. I also declare that I have not applied for an examination procedure at any other institution and that I have not submitted the dissertation in this or any other form to any other faculty as a dissertation.

1st Reviewer: Dr. Suphansa Sawamiphak

2nd Reviewer: Prof. Dr. Mathias F. Wernet

Date of defense: 30/01/2023

Table of Contents

Summary

Stress responses are fundamental for the survival of an organism and constitute an adaptive reaction to a real or perceived threat. Neuronal, endocrine, and behavioral responses are activated after the perception of a stressor and are aimed to re-establish the organism's homeostasis. A complex network of neuronal circuits involving several brain regions orchestrates the activation of the major stress system, the Hypothalamic Pituitary Adrenal (HPA) axis, and most of the neuronal populations that control its activity reside in hypothalamic nuclei.

Activation of the HPA axis starts within the paraventricular nucleus of the hypothalamus, in which a population of peptidergic neurons secretes corticotropin-releasing hormone (CRH) into the circulation, which in turn initiates a signaling cascade culminating with the production of cortisol. The activity of the HPA axis and CRH-producing neurons must be tightly controlled and rapidly modulated to ensure proper responses to threats but also to avoid overactivation of the stress system, which is deleterious for an animal's wellbeing. However, the hypothalamic circuits responsible for the activation and termination of the stress response and the underlying neuromodulatory mechanisms are still largely unknown.

In this study, I used the zebrafish larva as a model to elucidate the hypothalamic neuronal circuits modulating the behavioral and neuroendocrine responses to acute stress. The transparent and small larval zebrafish brain provides the unique opportunity to study neuronal responses *in vivo*, facilitating the identification of the neuronal populations modulating stress. Importantly the main brain regions and stress axes are conserved between mammals and teleosts. The Hypothalamic Pituitary Interrenal (HPI) axis is homologous to the mammalian HPA axis and its activation is controlled by Crh-producing neurons located in the preoptic area (PoA), homologous to the mammalian paraventricular nucleus.

Among the peptidergic neurons of the hypothalamus that might be involved in the modulation of acute stress, I chose to focus on a population of cells secreting the neuropeptide Galanin (Galn). I identified in the PoA of zebrafish a subpopulation of Galanin-producing neurons ($Galn^{+}$) highly responsive to different types of stressful stimuli. Ablation of $Galn^{+}$ neurons led to exacerbated stress responses, elevated cortisol levels, and caused increased activation of Crh-producing neurons, suggesting an inhibitory effect of $Galn^{+}$ neurons over

the HPI axis. I also found that Galn$^+$ neurons in the PoA of zebrafish larvae are GABAergic, suggesting the possibility that GABA is the neurotransmitter released by Galn$^+$ neurons to inhibit downstream stress-promoting circuits. I further investigated the molecular mechanisms by which Galn$^+$ neurons negatively modulate stress responses by manipulating the peptide Galn. Lack of Galn elicited a diminished response to stress and increased the activity of Galn$^+$ neurons in the PoA. Conversely, overexpression of Galn exacerbated stress-related responses and decreased the activity of Galn$^+$ neurons, suggesting a self-inhibitory action of Galn peptide on Galn$^+$ neurons.

Taken together, the results reported in this study indicate that Galn$^+$ neurons in the PoA negatively modulate Crh$^+$ neurons, likely through GABAergic transmission, to prevent overactivation of the HPI axis. In parallel, the neuropeptide Galn mediates an additional modulatory control within this hypothalamic circuit, reducing the activity of Galn$^+$ neurons through an autocrine mechanism. This dual system likely regulates a balance of activation and inhibition over Crh$^+$ neurons, which allows fine-tuning of the HPI axis activity and mediate behavioral responses to stress.

Zusammenfassung

Stressreaktionen sind für das Überleben eines Organismus von grundlegender Bedeutung und stellen eine adaptive Reaktion auf eine reale oder wahrgenommene Bedrohung dar. Neuronale, endokrine und verhaltensbezogene Reaktionen werden nach der Wahrnehmung eines Stressfaktors aktiviert und zielen darauf ab, die Homöostase des Organismus wiederherzustellen. Die Aktivierung des wichtigsten Stresssystems, der Hypothalamus-Hypophysen-Nebennieren-Achse (HPA-Achse), wird durch ein komplexes Netzwerk neuronaler Schaltkreise gesteuert, an denen mehrere Hirnregionen beteiligt sind, und die meisten Neuronenpopulationen, die ihre Aktivität kontrollieren, befinden sich in den Hypothalamuskernen.

Die Aktivierung der HPA-Achse beginnt im paraventrikulären Kern des Hypothalamus, wo eine Population von peptidergenen Neuronen Corticotropin-Freigebendes-Hormon (CRH) in den Blutkreislauf abgibt, was wiederum eine Signalkaskade in Gang setzt, die in der Produktion von Cortisol gipfelt. Die Aktivität der HPA-Achse und der CRH-produzierenden Neuronen muss streng kontrolliert und schnell moduliert werden, um eine angemessene Reaktion auf Bedrohungen zu gewährleisten, aber auch um eine Überaktivierung des Stresssystems zu vermeiden, die sich nachteilig auf das Wohlbefinden des Tieres auswirkt. Die hypothalamischen Schaltkreise, die für die Aktivierung und Beendigung der Stressreaktion verantwortlich sind, sowie die zugrunde liegenden neuromodulatorischen Mechanismen sind jedoch noch weitgehend unbekannt.

In dieser Studie habe ich die Zebrafischlarve als Modell verwendet, um die hypothalamischen neuronalen Schaltkreise aufzuklären, die die verhaltensbezogenen und neuroendokrinen Reaktionen auf akuten Stress steuern. Das transparente und kleine Larvengehirn des Zebrabärblings bietet die einzigartige Möglichkeit, neuronale Reaktionen in vivo zu untersuchen, was die Identifizierung der neuronalen Populationen, die Stress modulieren, erleichtert. Wichtig ist, dass die wichtigsten Hirnregionen und Stressachsen zwischen Säugetieren und Knochenfischen konserviert sind. Die Hypothalamus-Hypophysen-Nebennieren-Achse (HPI) entspricht der HPA-Achse der Säugetiere, und ihre Aktivierung wird durch Crh-produzierende Neuronen im präoptischen Bereich (PoA) gesteuert, der dem paraventrikulären Kern der Säugetiere entspricht.

Unter den peptidergen Neuronen des Hypothalamus, die an der Modulation von akutem Stress beteiligt sein könnten, habe ich mich auf eine Population von Zellen konzentriert, die das Neuropeptid Galanin (Galn) sezernieren. Ich identifizierte im PoA von Zebrafischen eine Subpopulation von Galanin-produzierenden Neuronen ($Galn^+$), die stark auf verschiedene Arten von Stressreizen reagieren. Die Ablation von $Galn^+$-Neuronen führte zu verstärkten Stressreaktionen, erhöhten Cortisolspiegeln und verursachte eine verstärkte Aktivierung von Crh-produzierenden Neuronen, was auf eine hemmende Wirkung von Galn+-Neuronen auf die HPI-Achse schließen lässt. Ich fand auch heraus, dass Galn+-Neuronen im PoA von Zebrafischlarven GABAerge sind, was die Möglichkeit nahelegt, dass GABA der Neurotransmitter ist, der von $Galn^+$-Neuronen freigesetzt wird, um nachgeschaltete stressfördernde Schaltkreise zu hemmen. Ich untersuchte weiter die molekularen Mechanismen, durch die $Galn^+$-Neuronen Stressreaktionen negativ modulieren, indem ich das Peptid Galn manipulierte. Das Fehlen von Galn führte zu einer verminderten Reaktion auf Stress und erhöhte die Aktivität von $Galn^+$-Neuronen im PoA. Umgekehrt verschlimmerte die Überexpression von Galn stressbedingte Reaktionen und verringerte die Aktivität von $Galn^+$-Neuronen, was auf eine selbsthemmende Wirkung des Galn-Peptids auf $Galn^+$-Neuronen schließen lässt.

Insgesamt deuten die in dieser Studie berichteten Ergebnisse darauf hin, dass Galn+-Neuronen im PoA die Crh^+-Neuronen negativ modulieren, wahrscheinlich durch GABAerge Übertragung, um eine Überaktivierung der HPI-Achse zu verhindern. Parallel dazu vermittelt das Neuropeptid Galn eine zusätzliche modulatorische Kontrolle innerhalb dieses hypothalamischen Kreislaufs, indem es die Aktivität der $Galn^+$-Neuronen durch einen autokrinen Mechanismus reduziert. Dieses duale System reguliert wahrscheinlich ein Gleichgewicht zwischen Aktivierung und Hemmung von Crh^+-Neuronen, dass eine Feinabstimmung der Aktivität der HPI-Achse ermöglicht und Verhaltensreaktionen auf Stress vermittelt.

1 Introduction

1.1 Stress

The biological concept of stress was first introduced almost a century ago by the pioneering studies of Walter Cannon and Hans Selye. Cannon postulated the existence of a physiological reaction of the body to aversive events, which he called ‘‘fight or flight’’ response (Cannon, 1915). A few years later, he coined the term “homeostasis”, inspired by the theory of the French physiologist Claude Bernard that every individual has a *“milieu intérieur”* (internal environment) (Bernard, 1865). According to Cannon, homeostasis is a dynamic equilibrium whose perturbation elicits the activation of the sympathoadrenal system aimed at maintaining or reinstating this inner state (Cannon, 1929).

In 1936, Selye, to whom we own the first definition of stress, published a letter to Nature's journal entitled “A syndrome produced by diverse nocuous agents”. In this short manuscript, Selye described the morphological changes in rats exposed to several severe insults, including enlargement of the adrenal gland (Selye, 1936). He eventually used the word “stress” (Selye, 1950) and described it as the “nonspecific response of the body to any demand made upon it” (Selye, 1976).

After decades of research, the original concept of stress proposed by Cannon and Selye as a state in which aversive clues are sensed and elicit adaptive responses to maintain homeostasis is still in use. Nowadays, stress can be defined as a “consciously or unconsciously sensed threat to homeostasis in which the response has a degree of specificity, depending, among other things, on the particular challenge to homeostasis, the organism’s perception of the stress, and/or the perceived ability to cope with it” (Goldstein and Kopin, 2007).

In modern society, the term “stress” generally carries a negative connotation even though it is a physiological phenomenon beneficial and fundamental for the survival of an organism. On the contrary, “distress”, another term coined by Selye (Selye, 1976), can have deleterious effects on virtually all body organs and is generally caused by prolonged stress or multiple stressful conditions. Chronic exposure to stressors can lead to several pathological conditions, which are not limited to mental health disorders, such as depression and anxiety, but also include cardiovascular diseases, early aging, immunosuppression, metabolic

diseases, and many others (de Kloet, Joëls and Holsboer, 2005; Godoy et al., 2018). In 2017 the World Health Organization declared stress as the "health epidemic of the 21st century" (Fink, 2017), shortly before the Coronavirus disease 2019 (COVID-19) appeared. The global health pandemic caused by COVID-19 has been a considerable source of psychological stress, and it is estimated that during 2020 the incidence of anxiety and depression disorders increased by 25% (World Health Organization, 2022). The rising incidence of health problems caused by chronic stress highlights, besides sociological considerations, the urgency to develop new therapies to treat these conditions, which requires a better understanding of the basic neuronal mechanisms regulating stress responses.

1.1.1 Stress axes

The initiation of any physiological stress response first requires the perception of an aversive stimulus. Real or potential threats lead to the recruitment of different brain regions depending on the type and intensity of the stimulus and whether the threat is physical or psychological (Godoy et al., 2018). Physical stressors threatening homeostasis are mainly processed by the brainstem and hypothalamic nuclei and elicit immediate systemic reactions (de Kloet, Joëls and Holsboer, 2005; Y. Ulrich-Lai and Herman, 2009). Psychological stressors are instead detected by higher brain structures such as the amygdala, hippocampus, prefrontal cortex, and bed nucleus of the stria terminalis and elicit both physical and cognitive responses (Y. Ulrich-Lai and Herman, 2009; Myers *et al.*, 2017). Although distinct brain regions initially process physical and psychological stressors, they both ultimately activate the two main stress systems, the Sympathetic Adreno Medullar (SAM) and the Hypothalamic Pituitary Adrenal (HPA) axes.

Activation of the SAM axis is mediated by the sympathetic division of the autonomic nervous system and constitutes the first phase of the stress response. Sympathetic innervation to the adrenal medulla induces the release of adrenaline and noradrenaline into the systemic circulation and provokes immediate physiological changes such as increased heart rate, blood pressure, and alertness (Sapolsky, Romero and Munck, 2000; Y. Ulrich-Lai and Herman, 2009). This autonomic response provides within seconds a quick and short-term reaction to stress and constitutes the "fight or flight" response described by Cannon and colleagues (Cannon, 1915).

The second response phase is orchestrated by the HPA axis, which is partly responsible for the adrenal gland's morphological changes reported by Selye in his early studies in rats (Selye, 1936). Activation of the HPA axis involves neuronal and hormonal mechanisms which drive an amplified and long-lasting response that allows reinstatement of homeostasis (Goldstein and Kopin, 2007; Y. Ulrich-Lai and Herman, 2009). Although these two major stress axes evoke independent signaling cascades, the neuronal circuits regulating their activation partially overlap to allow a proper and dynamic response to different stressful conditions (Y. Ulrich-Lai and Herman, 2009).

1.1.2 The Hypothalamic Pituitary Adrenal axis

The HPA axis represents the essential link between the central nervous system (CNS) and the endocrine system. In mammals, the main region responsible for eliciting the activation of the HPA axis is the paraventricular nucleus of the hypothalamus (PVN) (Myers *et al.*, 2017). The PVN receives direct synaptic inputs from the brainstem, other hypothalamic nuclei, and peri-hypothalamic regions. Detection of stressors in these brain areas leads to the activation in the PVN of neurons secreting the peptide corticotropin-releasing hormone (CRH). CRH-producing neurons (CRH^+) project to the external zone of the median eminence, where they release CRH and the peptide Arginine Vasopressin (AVP) into the portal circulation (Vale *et al.*, 1981; Sawchenko, Swanson and Vale, 1984; Sawchenko, Imaki and Vale, 1992) (Figure 1). CRH and AVP diffuse to the anterior lobe of the pituitary gland, where they bind to their receptors on the corticotroph cells stimulating the production of the adrenocorticotropin hormone (ACTH) (Antoni, 1986; Wied and Kloet, 1987; Aguilera, 1994). ACTH is released through the hypophyseal portal system and acts on the cortex of the adrenal gland, where it stimulates the synthesis and the release of glucocorticoid hormones (GCs) (Vale *et al.*, 1978), primarily cortisol in humans and corticosterone in rodents (de Kloet, 2004) (Figure 1).

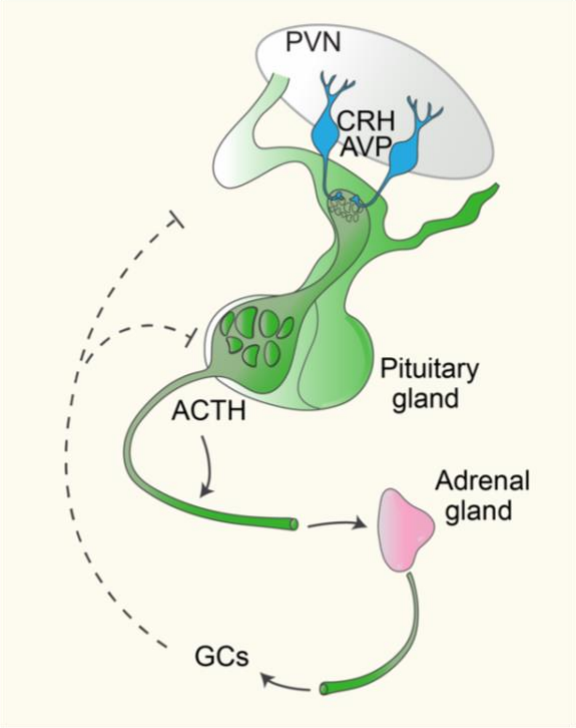

Figure 1: Organization of the HPA axis. Stressors cause the release of CRH and AVP from the PVN of the hypothalamus to the hypophysial portal vessels of the median eminence, which transports the peptides to the anterior region of the pituitary gland. Stimulated corticotroph cells in the pituitary secrete ACTH, which induces the synthesis and release of GCs from the adrenal gland to the systemic circulation. GCs mediate a negative feedback (dashed lines) that reduces the release of CRH and AVP from the PVN neurons and can block the release of ACTH from the pituitary. ACTH adrenocorticotropin hormone, AVP arginine vasopressin, CRH corticotropin releasing hormone, GCs glucocorticoids, PVN paraventricular nucleus. Adapted from (Myers, Jessica M McKlveen and Herman, 2012).

GCs have a wide range of functions and once released into the bloodstream can act on multiple body systems. In the periphery, GCs regulate glucose levels for energy mobilization, alter important immune system components, and affect cardiovascular functions (Timmermans, Souffriau and Libert, 2019). In the CNS, GCs regulate several neuronal functions, including cognitive processes such as learning, memory, cognition, and mood (de Kloet, 2004; Joëls, 2011). The physiological changes elicited by GCs are mediated mainly by glucocorticoid and mineralocorticoid receptors which, upon binding to GCs, can translocate to the nucleus and regulate gene transcription (Weikum *et al.*, 2017).

GCs are also essential for the termination of the stress response inducing a negative feedback mechanism that inhibits the activity of the HPA axis (de Kloet, Joëls and Holsboer, 2005). The most well-characterized inhibitory effects of GCs are mediated by delayed genomic mechanisms, such as repression of the transcription of the *Crh* gene (Julia K Gjerstad, Lightman and Spiga, 2018). In addition, studies in rodents have shown that GCs can regulate inhibition of the HPA axis partially through rapid-non genomic mechanisms which suppress CRH and ACTH secretion (Groeneweg *et al.*, 2011). In the pituitary, GCs can rapidly block the release of ACTH-containing vesicles by regulating membrane potential properties of corticotroph cells (Duncan *et al.*, 2016). In the PVN, it was shown that increased cortisol levels lead to the suppression of excitatory inputs to CRH^{+} neurons (Tasker and

Herman, 2011). This mechanism has been hypothesized to be mainly mediated by cannabinoid receptors in the presynaptic terminals, which upon binding to their ligands, can suppress glutamatergic release into CRH^+ neurons. In addition, a local release of endocannabinoids independent of GCs and inducing the inhibition of CRH^+ neurons has also been observed (Herman et al., 2016).

GCs are synthesized and released not only in response to stress but also throughout the day in circadian and ultradiurnal rhythms (Julia K. Gjerstad, Lightman and Spiga, 2018). This process ensures a circadian-related modulation of the HPA axis, which is crucial to synchronize physiological processes and to enable proper control over energy expenditure. The PVN receives direct inputs from the suprachiasmatic nucleus, which is entrained by exposure to sunlight and affects the circadian rhythm of activation of CRH^+ neurons (Kalsbeek *et al.*, 2012). In turn, CRH affects the release of ACTH, regulating the rhythmicity of cortisol secretion from the adrenal gland (Nicolaides *et al.*, 2014).

Increased and decreased levels of circulating GCs can also be affected by other factors, including whether the exposure to a stressor is acute or chronic. Generally, an acute stressor lasts from minutes to hours and elicits an increase in GCs within 15-30 minutes, which returns to basal levels 60–120 minutes after termination of the stimulus. In contrast, persistent or recurrent exposure to stress generally leads to a chronic secretion of GCs (de Kloet, Joëls and Holsboer, 2005).

1.1.3 Neuronal circuits modulating stress

The activity of the HPA axis is crucial for maintaining homeostasis and requires a continuous balance of excitation and inhibition, which is provided by direct or indirect neuronal inputs to the PVN from several brain regions (Figure 2). Most excitatory PVN-projecting neurons receive inputs from somatic nociceptors, visceral afferents, and sensory pathways to evoke rapid activation of the HPA axis after a stressor is perceived (Herman et al., 2016). Stressors causing homeostatic perturbations are processed mainly by brainstem nuclei, which directly modulate the PVN through monosynaptic ascending projections (Figure 2). Importantly, brainstem afferents to the PVN constitute a large proportion of stress-regulatory inputs to the CRH^+ neuronal population activating the HPA axis (Myers *et al.*, 2017). Brainstem nuclei can modulate the PVN also indirectly through other brain structures,

such as hypothalamic and peri-hypothalamic nuclei (Figure 2) (Herman et al., 2016). For instance, the dorsomedial hypothalamus and the bed nucleus of the stria terminalis both send monosynaptic afferents to the neurosecretory neurons of the PVN (Myers, Jessica M. McKlveen and Herman, 2012).

Unlike homeostatic disturbances, psychological stressors recruit cortico-limbic structures such as the prefrontal cortex, hippocampus, and amygdala, which are connected to the PVN indirectly through hypothalamic and peri-hypothalamic regions. These complex polysynaptic pathways are also crucial for anticipatory responses to threats and to store information about previous stressful experiences which modify the future response to recurring stressors (Y. M. Ulrich-Lai and Herman, 2009).

Inhibition of the HPA axis activity is orchestrated by several GABAergic inputs innervating the PVN and the pituitary corticotroph cells (Myers *et al.*, 2014). This inhibitory control is crucial for preventing overactivation of the HPA axis, yet it must be removed once a stressor is perceived to allow the activation of the stress axis. Although GCs seem to be partially involved in this mechanism, they exert their functions mainly through delayed genomic effects, which are too slow to ensure an immediate response to stress. A rapid removal of inhibitory inputs innervating the PVN appears to be achieved indirectly by excitatory circuits originating in the bed nucleus of the stria terminalis and in the Preoptic Area (POA) of the hypothalamus (Figure 2) (Hewitt *et al.*, 2009). Activation of these neuronal pathways during stress cause depolarization of target cells, making GABAergic inputs largely ineffective.

Inhibitory inputs required for the termination of stress responses arise from hypothalamic regions involved in homeostatic regulation, including the arcuate nucleus, the dorsomedial and lateral hypothalamus, and the POA (Figure 2) (Myers, Jessica M. McKlveen and Herman, 2012). GABA interneurons from the peri-PVN region project into the PVN and receive information from hypothalamic cell groups, serotonergic neurons, and limbic structures. Inhibition of the HPA axis also occurs from limbic sites through the bed nucleus of the stria terminalis, hypothalamic nuclei, and brainstem nuclei that innervate the PVN directly (Figure 2). Overall, hypothalamic inputs constitute the main component of the neuronal network that both excites and inhibits the PVN to maintain systemic homeostasis. However, many of the hypothalamic circuits rapidly modulating the activity of the HPA axis,

especially its inhibition, are not well-characterized mostly due to the difficult accessibility of the hypothalamus and the numerous modulators that are rapidly released during stress.

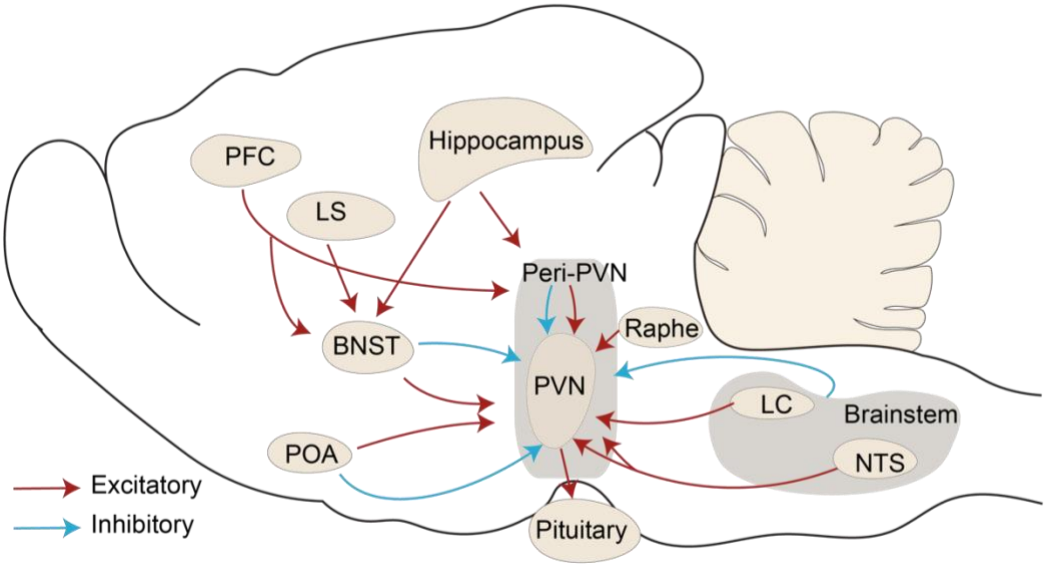

Figure 2: Excitatory and inhibitory inputs modulating stress. Scheme of the lateral view of the mouse brain with the main nuclei sending projections to the PVN to modulate the activity of the HPA axis. Red and blue arrows indicate excitatory and inhibitory inputs, respectively. PVN paraventricular nucleus, PFC prefrontal cortex, LS lateral septum, BNST bed nucleus of the stria terminalis, POA preoptic area, LC locus coeruleus, NTS nucleus of the solitary tract. Adapted from (Heck and Handa, 2018).

1.1.4 Neuronal populations of the Paraventricular Nucleus

Once information from physical or psychological aversive stimuli is processed, the PVN orchestrates the activation of the sympathetic nervous system and the HPA axis. Autonomic regulatory control is exerted through projections from the PVN to autonomic targets in the brainstem and spinal cord, while activation of the HPA axis is mediated by peptidergic inputs from the PVN to the median eminence (Myers *et al.*, 2017). These projections arise from magnocellular and parvocellular neurons, located respectively in the magnocellular and parvocellular divisions of the PVN (Aguilera and Liu, 2012).

CRH^+ neurons are present in both subnuclei of the PVN and distinct CRH^+ neuronal populations regulate autonomic and neuroendocrine responses to stress (Aguilera and Liu, 2012). Parvocellular CRH^+ neurons in the lateral, dorsal, and ventromedial regions project to the brainstem and the spinal cord and are involved in the autonomic control of stress responses. Parvocellular CRH^+ and AVP^+ neurons located in the dorsomedial and anterior

parvocellular nucleus of PVN project to the median eminence and are responsible for the secretion of CRH and AVP into the portal circulation. These neuronal populations are rapidly activated following acute stress and mediate the activation of the HPA axis.

The magnocellular region of the PVN contains magnocellular neurons co-expressing AVP and the neuropeptide Oxytocin (OXT) and/or neurons containing CRH together with OXT. These neurons project to the posterior pituitary through the internal zone of the median eminence and release peptides to the peripheral circulation (Aguilera and Liu, 2012). Contrary to parvocellular cells, magnocellular neurons are activated in response to specific types of stressors. However, it is still uncertain whether their activation occurs in response to the perception of a stressful stimulus or if it is a consequence of the physiological changes elicited by stress. While the release of CRH in response to acute stressors is fundamental for activating the HPA axis, the release of other peptides seems to be mainly implicated in response to chronic stress. For example, in physiological conditions, 50% of parvocellular CRH^+ neurons also co-express AVP, while in chronic stress conditions this percentage increases (Aguilera and Liu, 2012).

1.2 Neuropeptides

Neuropeptides, such as CRH and AVP, have long been known to play a central role as neuromodulators of stress, as well as many other physiological functions. While classic neurotransmitters, such as GABA, mediate fast synaptic transmission, neuropeptides act either as neurotransmitters or hormones and are essential to mediate the communication between the CNS and the endocrine system (Hökfelt *et al*., 2018). Neurotransmitters and neuropeptides have several distinct features, including their modalities of synthesis, release, and degradation, which reflect their different effects on brain signaling.

Neuropeptides are synthesized as prepro-peptides, which are further processed into smaller fragments and undergo post-translational modifications to generate the mature protein (Beinfeld, 1998). Consequently, multiple peptide products can be generated from a single pro-peptide, and each of these molecules can have independent functions. Another difference between neurotransmitters and neuropeptides is the size of these two classes of molecules, as neuropeptides are generally larger than small-molecule transmitters (Nusbaum, Blitz and Marder, 2017). The different size results in different storage, with neuropeptides

being contained in large dense core vesicles (LDCVs) while classic neurotransmitters are generally stored in small secretory vesicles (Zhu, Thureson-Klein and Klein, 1986; Mains *et al.*, 1987).

LDCVs are transported to the axonal terminal and, in response to calcium (Ca^{2+}) influx, fuse with the presynaptic membrane at the synapse or more often extrasynaptically (Ludwig and Leng, 2006; Ludwig *et al.*, 2017). The release of LDCVs generally requires higher firing rates compared to those inducing the release of small-molecule transmitters (Nusbaum, Blitz and Marder, 2017). Once released, neuropeptides bind to G protein-coupled receptors (GPCRs), which mediate their effects on target cells by activating several intracellular signaling pathways. Neuropeptides can also modulate neuronal excitability as their GPCRs can directly affect the opening and closing of coupled channels. For instance, G protein-coupled inwardly rectifying potassium channels (GIRKs) are a family of potassium ion channels that are opened by a signal transduction cascade starting with ligand-GPCRs binding (Glaaser and Slesinger, 2015).

While neurotransmitters are generally considered the messengers between single neurons, neuropeptides mediate communication between entire populations of cells. Neuropeptides have a long half-life in the CNS, in the range of minutes, and are inactivated by extracellular peptidases that are not necessarily located close to the site of release (Ludwig and Leng, 2006). Thus, neuropeptides can diffuse and bind to their receptors situated at a relatively long distance from their release site (Fuxe *et al.*, 2010).

1.2.1 Co-transmission of neuropeptides and classic neurotransmitters

The coexistence of multiple neurotransmitters and/or neuropeptides in the same neurons is considered of crucial importance for the development and function of the CNS (Lundberg and Hökfelt, 1983). Most neuropeptides coexist with classic neurotransmitters, and their combined release enables both immediate and prolonged modulation of brain circuits.

Co-transmission of neuropeptides and neurotransmitters from the same cell can have divergent actions modulating different target neurons (Nusbaum, Blitz and Marder, 2017) (Figure 3A). For example, reticular thalamic GABAergic neurons release Neuropeptide Y (NPY) and GABA, which have divergent inhibitory effects modulating distinct postsynaptic targets (Sun *et al.*, 2003).

Co-transmission of neuropeptides and neurotransmitters can also converge on the same postsynaptic cell, with the two molecules exerting opposite or synergistic effects (Nusbaum, Blitz and Marder, 2017) (Figure 3B). In many cases of convergent co-transmission, the release of the peptide reduces, eliminates, or enhances the effect of the classic neurotransmitters (Wilkinson and Brown, 2015).

Neurotransmitters and neuropeptides can also have opposite effects on the target neuron depending on which molecule is released. For instance, a presynaptic neuron firing at low-frequency releases an excitatory neurotransmitter to the target cell. An increase in the stimulation frequency of the presynaptic neuron would induce the secretion of both the neuropeptide and the neurotransmitter. Binding to its GPCRs on the same postsynaptic neuron, the neuropeptide can cause a hyperpolarization of the target cell, preventing the excitatory effect of the neurotransmitter (Nusbaum, Blitz and Marder, 2017).

Importantly, neuropeptides not only have paracrine effects modulating the activity of neighboring neurons but can also have autocrine functions (Figure 3C). For example, OXT-producing neurons (OXT^+) have been shown to have both autocrine and paracrine actions during birth. Cervical stretch leads to the activation of OXT^+ neurons and somatodendritic secretion of OXT, which binds to autoreceptors and enhances its own release. In addition, OXT stimulates the release of noradrenaline from afferents of OXT^+ neurons, increasing their activity and ensuring a continuous release of OXT into the circulation (Brown *et al.*, 2020). On the contrary, in the magnocellular neurons of the hypothalamus, somatodendritic release of OXT has the opposite effect inhibiting glutamatergic excitatory input by binding to its receptors on the presynaptic membrane (Nusbaum, Blitz and Marder, 2017). Similar to OXT, magnocellular AVP^+ neurons were shown to have an inhibitory autocrine effect on neuronal activity. Upon stimulation, AVP^+ neurons secrete AVP from the axon terminals leading to a systemic increase of the peptide in the circulation. Increased levels of AVP stimulate the somatodendritic release of AVP from the magnocellular neurons. The release of AVP is enhanced until the local extra neuronal concentration of the peptide reaches a threshold sufficient to hyperpolarize AVP^+ neurons or to modulate upstream inhibitory inputs (Ludwig *et al.*, 2017). In addition, AVP can also have paracrine actions on nearby magnocellular neurons (Baribeau and Anagnostou, 2015).

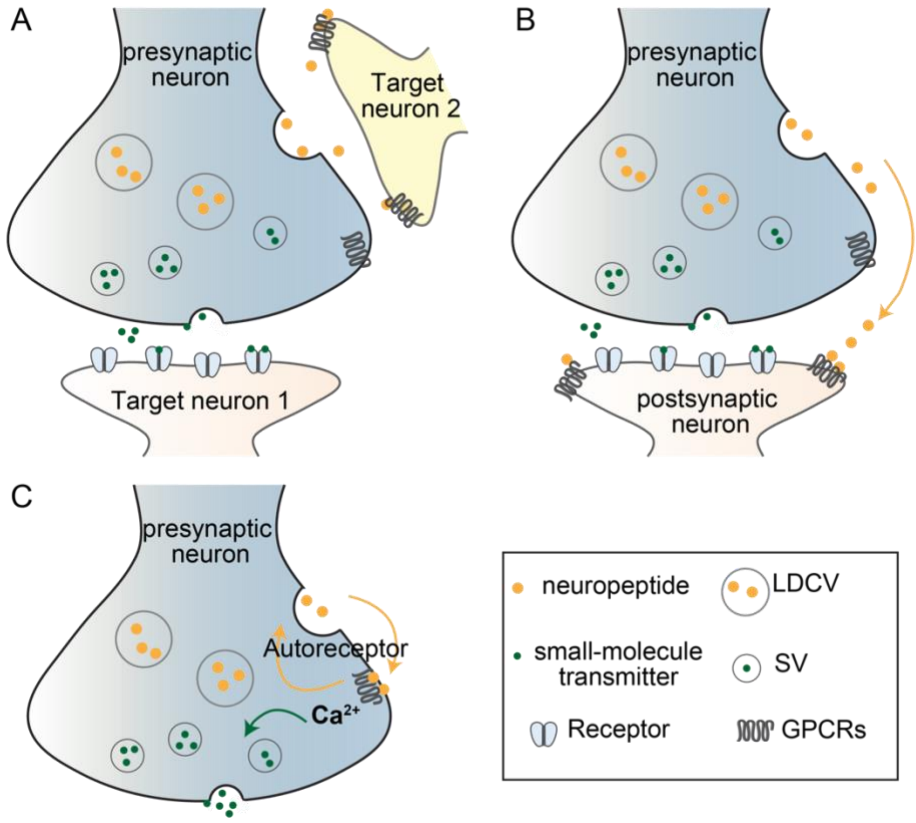

Figure 3: Example of co-transmission of neuropeptides and neurotransmitters. Neuropeptides are stored in large dense core vesicles (LDCVs), which can be released extrasynaptically. In contrast, neurotransmitters are contained in small synaptic vesicles (SVs) released into the synaptic cleft. **(A).** A presynaptic neuron releases a neurotransmitter and a peptide to different targets (divergent co-transmission). **(B).** A presynaptic neuron releases a neurotransmitter and a peptide to the same postsynaptic target neuron (convergent co-transmission). **(C).** A presynaptic neuron releases a neuropeptide which induces a variation in the intracellular Ca^{2+} levels inside the cell and affects the release of both the neurotransmitter and the neuropeptide to the target neuron. Alternatively, the peptide can modulate the activity of the neuron binding to its autoreceptors located on presynaptic cells (not shown).

1.2.2 Neuropeptides and stress

Several features of the neuropeptides reflect their importance in mediating stress and their relevance in stress-related disorders. First, the brain areas containing the highest concentration of neuropeptides are the secretory regions of the hypothalamus and the median eminence, which mediate the activation of the HPA axis (Kormos and Gaszner, 2013). Second, neuropeptides are often co-expressed with small-molecule transmitters involved in mood regulation, such as the monoaminergic neurotransmitters noradrenaline, serotonin, and dopamine (Nusbaum, Blitz and Marder, 2017). However, the co-localization of different

peptides in the same neuron, the co-transmission of neuropeptides and neurotransmitters, and the ability of these molecules to affect several intracellular signaling pathways complicate the identification of their precise function in stress responses. Furthermore, most peptidergic GPCRs display cross-reactivity in the binding of their ligands, which further complicates the identification of each peptide's function (Yang *et al.*, 2021).

While it is established that CRH is the main neuropeptide initiating the HPA axis signaling cascade, several other peptides are released in response to stress, including AVP, NPY, OXT, Urocortin, Neuropeptide S, Somatostatin, Substance P, and Galanin (Kormos and Gaszner, 2013). However, the precise function of most of these molecules and their involvement in stress-related responses is still largely unknown.

AVP is co-released with CRH in the parvocellular neurons of the PVN projecting to the median eminence. The primary function of AVP is to potentiate CRH activity at the corticotroph cells, contributing to the rapid secretion of ACTH from the anterior pituitary in response to stress (Stoop, 2012; Scheng *et al.*, 2021). AVP release is enhanced during prolonged exposure to stressors, and chronic increase of AVP has been connected to anxiety-like behaviors (Beurel and Nemeroff, 2014).

OXT generally acts as a negative modulator of stress, preventing activation of the HPA axis and reducing behavioral responses to acute stress. Although the precise modulatory action of OXT is not clear, it has been hypothesized that it might inhibit CRH^+ neurons or induce the release of GABA from PVN-projecting GABAergic neurons (Smith *et al.*, 2016).

The function of the peptide Urocortin during stress is likely dependent on CRH, as all three Urocortin isoforms bind to CRH receptors in the CNS (Kormos and Gaszner, 2013). Contrary to CRH, Urocortin does not seem to be involved in acute stress responses but rather in long-term adaptation mechanisms (Kormos and Gaszner, 2013).

Peptides mainly involved in energy homeostasis, such as NPY, were also found to affect stress responses. Although this orexigenic peptide is mainly involved in the regulation of feeding, several studies indicate its involvement in anxiety-related states (Reichmann and Holzer, 2016). In rodents, intracerebroventricular injection of NPY can affect hypothalamic *Crh* mRNA levels, and the lack of NPY leads to anxiety-like behaviors both in zebrafish and mice (Reichmann and Holzer, 2016; Shiozaki *et al.*, 2020). Moreover, NPY is involved in sleep through its actions on noradrenergic signaling (Singh, Rihel and Prober, 2017). It is

worth noting that feeding and sleep are both behaviors that can be strongly affected by stress states and are severely disrupted in chronic stress conditions. Thus, it is possible that NPY, like other neuropeptides, might be important to orchestrate different behaviors with respect to ongoing physiological processes. Similar to NPY, a peptide that has been involved in feeding, homeostatic regulation, sleep, and stress-related disorders is Galanin.

1.3 Galanin

Galanin (GAL) is a 29/30 amino acids neuropeptide first discovered by the Mutt group at the Karolinska Institute in Stockholm (Tatemoto *et al.*, 1983). Highly conserved between different species, the *Gal* gene in mammals is structured in six exons encoding for a prepro-precursor peptide (Kofler *et al.*, 1996; Lang *et al.*, 2014). The cleavage of the N-terminal region is followed by a second proteolytic cleavage resulting in the mature GAL peptide and a second peptide named Galanin Message-Associated Peptide (GMAP) (Rokaeus and Brownstein, 1986). The N-terminal region of GAL is highly conserved between species, with the first 19 amino acids displaying over 90% homology from fish to humans (Podlasz *et al.*, 2012). Early pharmacological studies demonstrated the importance of the N-terminal part of GAL for receptor affinity, whereas the C-terminal has been hypothesized to stabilize the peptide, preventing proteolytic degradation (Bedecs, Langel and Bartfai, 1995). GAL and GMAP belong to a family of neuropeptides, together with galanin-like peptide (GALP) and Alarin, another product of the *GALP* gene (Ohtaki *et al.*, 1999; Santic *et al.*, 2006). Residues 9–21 of GALP are identical to the first 13 amino acids of GAL and are essential for binding to GAL receptors. On the contrary, Alarin has no detectable affinity to GAL receptors and lacks homology to GAL (Boughton *et al.*, 2010).

Since its discovery, GAL and its mRNA have been mapped throughout all the CNS of different mammalian species (Skofitsch and Jacobowitz, 1985; Melander, Hökfelt and Rökaeus, 1986; Kordower, Le and Mufson, 1992; Pérez *et al.*, 2001; Lang *et al.*, 2014). High levels of *Gal* transcripts have been reported in the hypothalamus and the brainstem of rats and mice, specifically in the preoptic-, periventricular-, and dorsomedial-hypothalamic nuclei, bed nucleus of the stria terminalis, medial and lateral amygdala, locus coeruleus (LC), and nucleus of the solitary tract. Lower expression of *Gal* mRNA has been detected in the olfactory bulb, septal nuclei, thalamus, and the parabrachial and spinal trigeminal tract nuclei.

Gal mRNA has also been observed in the subventricular zone, the rostral migratory stream, and the subgranular zone of the hippocampus, where it may regulate the proliferation, differentiation, and migration of neural stem cells. In endocrine tissues, GAL was detected in the intestine, in the adrenal medulla, and in the anterior pituitary.

GAL coexists with numerous neurotransmitters, including acetylcholine, dopamine, GABA, glutamate, serotonin, and noradrenaline. In mammals, the peptide has been detected in a portion of serotonergic neurons in the dorsal raphe, in the noradrenergic neurons of the LC, in cholinergic forebrain neurons, in GABAergic and dopaminergic neurons in the hypothalamic arcuate nucleus, in GABAergic neurons in the spinal cord, in glutamatergic dorsal root ganglion neurons, and noradrenergic sympathetic neurons (Nusbaum, Blitz and Marder, 2017; Hökfelt et al., 2018). Co-localization between GAL and other neuropeptides has been extensively observed. For example, in the tuberomammillary nucleus GAL co-localizes with GABA, substance P, and enkephalin. In the hypothalamic arcuate nucleus, GAL is co-expressed with dopamine, growth hormone-releasing factor, and neurotensin, and in the bed nucleus of the stria terminalis with AVP (Kuteeva, 2007; Lang *et al.*, 2014). In some cases, the distribution of *Gal* and its coexistence with specific neurotransmitters was found to be species-specific. For example, *Gal* expression in the dorsal raphe nucleus was detected in rats but not mice. In cholinergic forebrain neurons, *Gal* expression is low in rats but high in monkeys. In mice, *Gal* mRNA and immunoreactivity were detected in the dorsal motor nucleus of the vagus and inferior olive neurons of the mouse but not of the rat (Lang *et al.*, 2014).

The widespread localization of GAL throughout the central and peripheral nervous system reflects the pleiotropic roles of this peptide. GAL is involved in a range of physiological functions, including metabolism, intestinal motility, feeding behavior, cardiac contraction, insulin secretion, energy expenditure, nociception, neuroprotection, neuronal regeneration, cognition, memory, reproduction, water balance, mood, and several other functions (Habecker et al., 2005; Lerner, Sankar and Mazarati, 2008; Lang et al., 2014; Demsie et al., 2020). GAL has also been investigated in several pathological states related to mood disorders, and evidence from animal models suggests GAL involvement in addiction, epilepsy, anxiety, and depression (Ögren *et al.*, 2010; Picciotto *et al.*, 2010; Lang *et al.*, 2014).

1.3.1 Galanin receptors

GAL signaling is mediated via three GPCRs with distinct but partially overlapping patterns of expression, pharmacology, and second messenger systems: Galanin receptor 1 (GALR1), Galanin receptor 2 (GALR2), and Galanin receptor 3 (GALR3). GALR1 and GALR2 are present in different species like primates and fish, while GALR3 has been identified only in some mammals (Lang *et al.*, 2014). GAL displays high affinity for all three receptor subtypes, whereas GALP shows high affinity only for GALR2 and GALR3 (Ohtaki *et al.*, 1999; Berger *et al.*, 2004). The three GALRs differ substantially in the amino acid sequence showing 35-40% identity and can bind to several types of ligands (Gundlach, Burazin and Larm, 2001). For example, the neuropeptide Spexin has been shown to bind to GALR2 and GALR3 (Kim et al., 2014). Several studies indicate the existence of heteromers between GALRs and other GPCRs, resulting in diverse recognition of ligands. For example, GALR1 was reported to form heteromers with serotonergic receptors, NPY receptors, and dopamine-like receptors (Lang *et al.*, 2014) while GALR2 undergoes internalization upon binding to its ligands and can form heteromers with other GALRs (Lang *et al.*, 2014).

Upon ligand binding, GALRs activate multiple transduction pathways, such as stimulation of phospholipase C (PLC) by GALR2, activation of mitogen-activated protein kinase (MAPK) by GALR1 and GALR2, or inhibition of 3′, 5′-cyclic adenosine monophosphate (cAMP) signaling mediated mainly by GALR1 and GALR3 (Figure 4) (Hökfelt et al., 2018). These intracellular pathways are responsible for mediating the effects of GAL on neuronal activity, as GAL is generally considered an inhibitory peptide that reduces the excitability of its target cells.

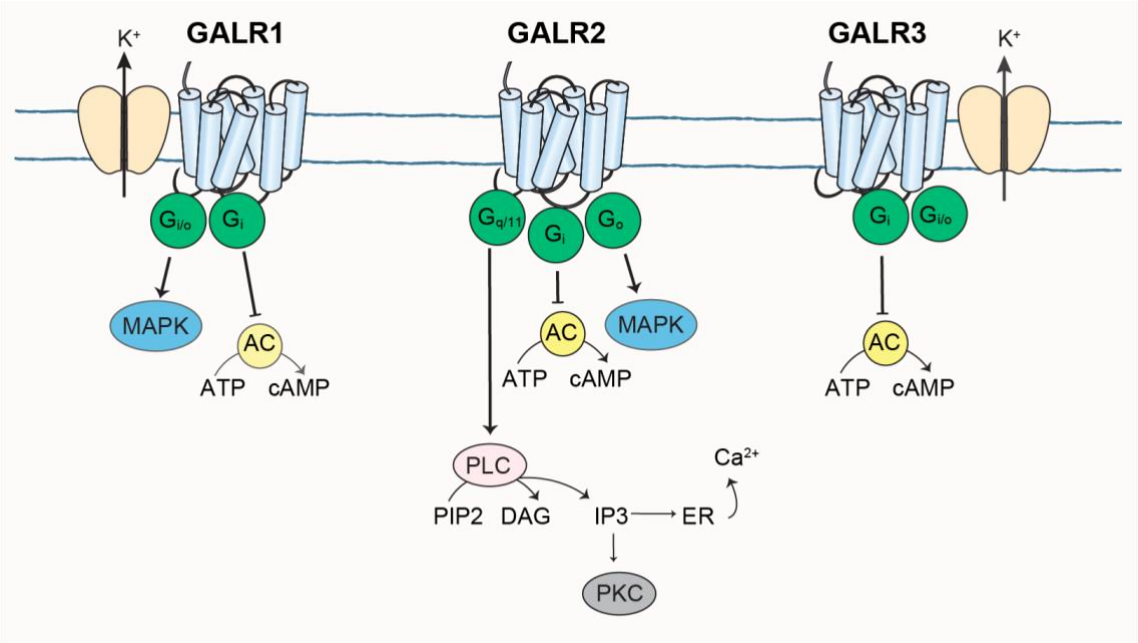

Figure 4: GALRs signaling pathways. GALR1 and GALR3 reduce the concentration of cAMP and induces the opening of GIRK channels leading to membrane hyperpolarization. GALR1 and GALR2 can both stimulate MAPK activity. GALR2 is coupled with the PLC pathway. Activation of the enzyme PLC results in the generation of IP3, which causes the release of Ca^{2+} from the endoplasmic reticulum and activates Ca^{2+}-dependent Cl^- channels. GALR2 can also inhibit the synthesis of cAMP. AC adenylate cyclase, cAMP 3′, 5′-cyclic adenosine monophosphate, ATP adenosine triphosphate DAG diacylglycerol, K^+ G-protein-regulated inwardly rectifying potassium channel, MAPK mitogen-activated protein kinase, sER smooth endoplasmic reticulum, IP3 inositol triphosphate, PIP2 phosphatidylinositol bisphosphate, PKC protein kinase C, PLC phospholipase C. Adapted from (Hökfelt et al., 2018).

Several *in vitro* studies indicate that GALR1 is the main receptor responsible for mediating the hyperpolarizing effect of GAL on target cells. GALR1 is coupled with a pertussis toxin (PTX) sensitive $G_{i/o}$ protein. Activation of GALR1 results in a PTX-sensitive inhibition of adenylate cyclase (AC), which leads to the opening of a GIRK channel resulting in an inward K^+ current (Wang *et al.*, 1997; Smith *et al.*, 1998). Electrophysiological studies in brain slices demonstrated that GAL, acting through GALR1, can decrease spontaneous firings, hyperpolarize membrane potential, and induces outward currents through an increase in K^+ conductance (Pieribone *et al.*, 1995; Ma *et al.*, 2001; Bai *et al.*, 2018). Furthermore, GALR1 inhibits neuronal excitability by closing voltage-dependent Ca^{2+} channels (N- and L-types) (Anselmi *et al.*, 2009). Like GALR1, GALR3 induces the opening of GIRK channels activating $G_{i/o}$ type of G proteins, suggesting that GALR3 is also capable of mediating the inhibitory actions of GAL on neuronal activity (Hökfelt et al., 2018).

Contrary to the other subtypes of GALRs, GALR2 is mainly coupled to $G_{q/11}$-type G-proteins and, upon ligand binding, induces PLC activation and increase in inositol triphosphate (IP3) levels. IP3 interacts with receptors on the intracellular Ca^{2+} stores on the endoplasmatic reticulum and mediates the release of Ca^{2+} and the opening of Ca^{2+}-dependent ion channels (Lang *et al.*, 2014). GALR2 activation may also mediate a modest inhibition of cAMP synthesis in a PTX-sensitive manner through $G_{i/o}$ protein (Webling *et al.*, 2012). Thus, GALR2 can have both stimulatory and inhibitory effects through $G_{q/11}$-types or $G_{i/o}$ type G-proteins, respectively.

GALRs have distinct distribution patterns in the CNS and the peripheral nervous system, which suggest that each receptor mediates some unique physiological functions. Few data are available regarding the distribution of GALR3 in rats and mice, while GALR1 and GALR2 have been extensively mapped, mainly through *in situ* hybridization, northern blot, and reverse transcript polymerase chain reaction (RT-PCR) analysis. *Galr1* expression is high in olfactory structures and subregions of the amygdala, cerebral cortex, and some regions of the hippocampus, thalamus, hypothalamus, and spinal cord (Webling *et al.*, 2012). In the PVN, GALR1 constitutes approximately 90% of all GAL-binding sites, with the remaining 10% being occupied by GALR2 or GALR3 (Zorrilla *et al.*, 2007). Unlike GALR1, GALR2 is distributed in almost all tissues. High levels of *Galr2* mRNA are reported in the dorsal root ganglia, the dentate gyrus of the hippocampus, the cerebellar cortex, and almost all hypothalamic nuclei. In peripheral tissues, *Galr2* expression has been detected in several regions, including the prostate, uterus, ovary, stomach, and large intestine (Webling *et al.*, 2012; Lang *et al.*, 2014). GALR3 is the least abundant of the GALRs, and its mRNA has been mostly detected in peripheral tissues, while in the CNS its expression is limited to the hypothalamus, midbrain, and hindbrain (Freimann, Kurrikoff and Langel, 2015).

Although GALRs have been thoroughly investigated *in vitro*, their distinct physiological roles are still unclear. The most common approach to investigate GALRs signaling is the injection of GAL or GAL chimeric peptides. These molecules often show cross-reactivity between the three receptor subtypes and even between GALRs and other GPCRs. Non-peptide agonists have also been developed, including Galnon and Galmic (Bartfai *et al.*, 2004; Sollenberg, Bartfai and Langel, 2005). However, these molecules display multiple sites of interactions, limiting the study of the physiology and function of the three distinct GALRs subtypes.

1.3.2 Galanin and stress

GAL and its receptors have been linked to anxiety and depression-like behaviors in rat/mouse models and human patients. A cohort study on the European population showed that variants in *GAL* and *GALR1-3* genes confer an increased risk of developing depressive disorders and anxiety in people who experienced recent negative life events or childhood trauma (Juhasz *et al.*, 2014). Noteworthy, a strong correlation between the galaninergic system and depression was detected in highly stressed subjects compared to patients who experienced moderate or low life stress (Juhasz *et al.*, 2014). Further evidence supporting the involvement of GAL in depression comes from an analysis of *post mortem* brain tissues derived from human patients. In the LC and dorsal raphe, transcript and DNA methylation levels of *GAL* and *GALR3* were found significantly altered in depressed patients who committed suicide (Barde et al., 2016). These studies suggest that GAL and its receptors are involved in the pathogenesis of depression in humans, most likely increasing vulnerability to psychosocial stress (Juhasz et al., 2014; Hökfelt et al., 2018).

Studies in animal models of depression have focused mostly on the role of GAL and its receptors in the LC and dorsal raphe regions, as disbalances in monoaminergic transmission are thought to play a major role in the pathophysiology of the disease. GAL is highly expressed in LC neurons, where it co-localizes with noradrenaline (Weinshenker and Holmes, 2016). In brain slices, GAL was shown to hyperpolarize noradrenaline-containing LC neurons (Pieribone *et al.*, 1995), and its inhibitory effect was demonstrated to be mediated mainly by GALR1 through activation of GIRK channels (Bai et al., 2018). GALR2 was also shown to partially inhibit LC neurons, probably affecting intracellular Ca^{2+} levels (Ma *et al.*, 2001). Further studies also indicate that GALR3 might mediate the opening of K^+ channels in LC neurons (Hökfelt et al., 2018).

Interestingly, GAL and its mRNA have been detected within the dendritic processes of LC neurons, suggesting that the peptide might undergo somatodendritic release (Vila-Porcile *et al.*, 2009). It was suggested that GAL, released by soma/dendrites, might bind to autoreceptors on LC neurons, inhibiting their firing and thus modulating the release of noradrenaline, whose disbalance is associated with depression-like behaviors (Hökfelt et al., 2018). GAL effect on LC neuronal activity seems to be enhanced upon exposure to stimuli, as *Gal* was found upregulated in LC of rats and mice following chronic stress and physical exercise (Holmes *et al.*, 1995; O'Neal *et al.*, 2001; Sciolino *et al.*, 2015). Furthermore,

noradrenergic neurons in the LC are involved in other mood-related disorders, such as drug and alcohol addiction, both phenomena associated with GAL and GALRs activity (Picciotto *et al.*, 2010; Weinshenker and Holmes, 2016).

GAL also coexists with serotonin in dorsal raphe neurons, although its expression is lower compared to the LC (Hökfelt and Tatemoto, 2008). Similar to the noradrenergic neurons, GAL was found to inhibit the firing rate of serotonergic neurons, probably via GALR1/3 and activation of GIRK channels (Mazarati *et al.*, 2005). It has been hypothesized that GAL might bind to autoreceptors and inhibits the release of serotonin to postsynaptic neurons, contributing to depression-like behaviors (Hökfelt and Tatemoto, 2008). Contrary to LC neurons, it seems that the effect of GAL on serotonergic neurons is not strictly connected to stress, as *Gal* gene expression in the dorsal raphe nucleus was not found altered by stressful stimuli (Kuteeva *et al.*, 2008).

It is worth mentioning that the original "Monoamine Hypothesis of Depression", claiming that the disease is caused by a deficit in noradrenaline and serotonin levels, is losing consensus (Moncrieff *et al.*, 2022). It is nowadays clear that many different factors, brain regions, and peripheral systems contribute to the etiology of major depressive disorders. Consequently, it would be reductive to think that the implication of GAL in depression can be inferred from its effect on the release of monoamines. Moreover, it is still unknown whether the peptide has a pro- or anti-depressive function, as most studies on animal models report contradictory results. For example, the administration of non-selective GALRs agonists has resulted in both anti-depressive and pro-depressive phenotypes in rats and mice (Weinshenker and Holmes, 2016). In contrast, administration of GAL led to change in the animal behavior in some assays, such as increased anxiety in open-field exploration (Klenerova *et al.*, 2011) but did not cause any change in other behavioral tests, such as elevated plus maze or light-dark exploration (Karlsson *et al.*, 2005; Karlsson and Holmes, 2006).

The incongruency in the behavioral results might be related to the site of administration of the peptide, which might act preferentially on some GALRs as these are differentially distributed throughout the CNS. Indeed, several studies suggest that GAL can exert a pro-depressive effect when acting via GALR1 and/or GALR3, while stimulation of GALR2 has an antidepressant-like effect (Hökfelt et al., 2018). On the other hand, contradicting results were also reported in studies in which no specific substance was administered. For instance,

mice overexpressing *Gal* and mutant mice lacking the *Galr1* or *Galr2* genes did not show spontaneous signs of increased depression-like behaviors (Gottsch et al., 2005). However, *Galr1* knockout mice displayed an anxiety-like state in the elevated plus-maze assay (Holmes *et al.*, 2003). It is worth noticing that several factors can affect the outcome of these assays, including handling of the animals and prior exposure to stressors, which were substantially different among the mentioned studies. Importantly, the significance of GAL in the pathogenesis of depression is mainly thought to be connected to its role in modulating stress, which has not been extensively studied and is still poorly understood.

1.3.3 Galanin in zebrafish

Despite the genome duplication events commonly observed in teleosts, zebrafish has a single *galn* gene (Alsop and Vijayan, 2009), whose structure is highly similar across vertebrates, suggesting that the function of the peptide might be evolutionary conserved in different species. As it was described for mammals, the *galn* gene is structured in six exons encoding a signal peptide, Galn, and GMAP (Podlasz *et al.*, 2012). Alternative splicing of the gene generates two different isoforms, with the longest one containing an intronic insertion downstream of the third exon. The insertion does not change the reading frame of the mature peptide and does not alter the portion of the N-terminal region required for the binding of Galn to its receptors (Podlasz *et al.*, 2012). The amino acid sequence shows 77% of similarities with humans, and the first 13 amino acids are identical between zebrafish and several vertebrate species (Figure 5) (Podlasz *et al.*, 2012).

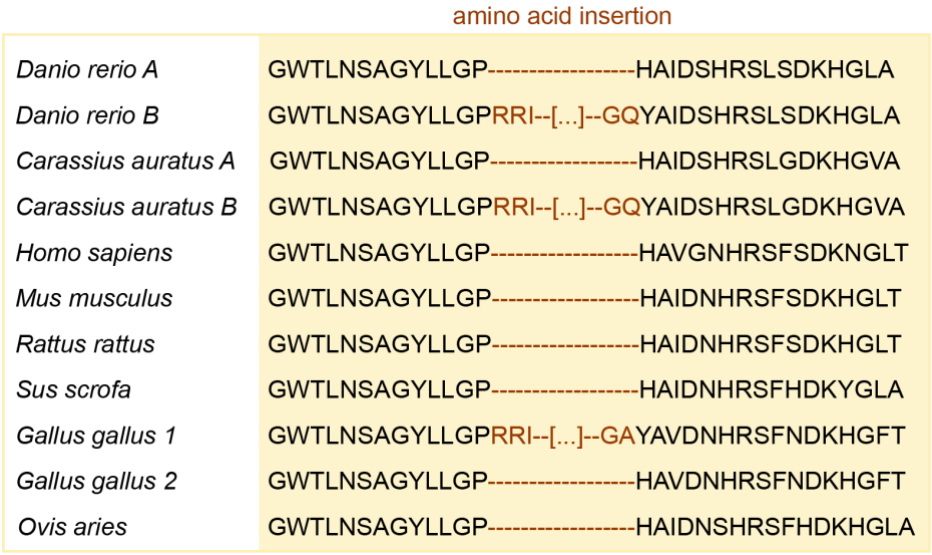

Figure 5: Galn in zebrafish and different species. Scheme showing the alignment of the amino acid sequence of the peptide Galn in zebrafish (*Danio rerio A, B*), goldfish (*Carassius auratus*), human (*Homo sapiens*), mouse (*Mus musculus*), rat (*Rattus rattus*), pig (*Sus scrofa*), chicken (*Gallus gallus*), and sheep (*Ovis aries*). The first 13 amino acids of the N-terminal of Galn are identical in most vertebrate species. Part of the 24 amino acid insertion predicted to generate different Galn isoforms in some species is indicated in brown. Adapted from (Podlasz *et al.*, 2012).

In zebrafish, few studies report the distribution of Galn and its transcripts in the larval brain (Podlasz *et al.*, 2012, 2018; S. Chen *et al.*, 2017). Immunostaining and *in situ* hybridization analysis revealed the presence of the neuropeptide between 4 and 7 days post fertilization (dpf), mostly in the preoptic area (PoA) and in the posterior region of the hypothalamus. Weak expression of Galn was also detected at 5 dpf and 7 dpf in the dorsal telencephalon and in the midbrain tegmentum. At 7 dpf a pair of single fibers were observed innervating the spinal cord, whose source is hypothesized to be the midbrain.

Galn expression was reported to change during larval development, with several galaninergic fibers innervating the spinal cord and the hindbrain at 2 dpf, gradually disappearing at later stages (Podlasz *et al.*, 2012). Although this observation suggests a developmental role for Galn, knockdown of the *galn* gene using morpholino oligonucleotides did not cause any defect in the development or the morphology of the brain (Podlasz *et al.*, 2012). After 5 dpf, Galn expression does not undergo significant changes as data obtained from adult zebrafish brains report Galn immunoreactivity mostly in ventral hypothalamic regions and PoA (Castro *et al.*, 2006; Podlasz *et al.*, 2018). An exception is the presence of the peptide in the midbrain tegmentum and in the dorsal telencephalon which is relatively

abundant in the adult zebrafish, while only a few fibers were observed in the larval brain (Castro *et al.*, 2006).

Few studies have investigated the physiological functions of Galn in zebrafish and none of them have assessed its role in stress responses. Overexpression of *galn* using the *hsp70* heat shock promoter seems protective against seizure, which is in accordance with an anti-epileptic effect of Galn reported in rodents (Lerner, Sankar and Mazarati, 2010; Podlasz *et al.*, 2018). In addition, enhancing the levels of *galn* led to an overall decrease in locomotor activity at the larval stage (Woods *et al.*, 2014; Podlasz *et al.*, 2018). However, it seems that the transgenic line *hsp70l:galanin* used in the mentioned studies leads to an ectopic expression of *galn* even without exposure to heat shock. Consequently, it cannot be excluded that the observed effects on locomotion are due to an increased expression of Galn in the whole-brain throughout the entire development. In zebrafish, Galn was also reported to be important for sleep homeostasis, ensuring proper rebound sleep (S. Chen *et al.*, 2017; Reichert, Pavón Arocas and Rihel, 2019). Interestingly, the same phenotype was reported after ablation of GAL-expressing neurons in the mouse POA (Ma *et al.*, 2019), suggesting that some neuronal functions of the peptide might be conserved across vertebrates.

Unlike mammals, in zebrafish four different receptors of Galn have been identified: GalnR1a, GalnR1b, GalnR2a, and GalnR2b (Liu *et al.*, 2010; Kim *et al.*, 2016). No data support the existence of a homologous of GALR3 in teleosts. Only a few studies have investigated the distribution of GalnRs and, except for RT-PCR analysis, these were limited to early developmental stages. *In situ* hybridization analysis conducted during embryogenesis, up to 3 dpf, showed that *galnR1a* mRNA is mainly expressed in the brain and intestine, while *galnR1b* was detected in all tissues by RT-PCR (Li *et al.*, 2013). No extensive information is available regarding the patterns of expression of *galnR2a* and *galnR2b*, which seem to be restricted to the CNS. At 3 dpf, *galnR2b* mRNA was detected by *in situ* hybridization in several brain regions, including the olfactory bulb, midbrain tegmentum, PoA, hindbrain, and spinal cord (Kim *et al.*, 2016). On the contrary, *galnR2a* expression at 3 dpf seems confined to a restricted area of the brain close to the anterior commisure, hypothesized to be the subpallium (Kim *et al.*, 2016). However, the lack of neuronal markers in most of these studies complicates the identification of the precise anatomical regions in which the receptors are expressed. Moreover, there are no conclusive data regarding the distinct functions of the GalnRs in zebrafish, except for a study indicating

the requirement of *galnR1a* for the proper development of color pigmentation in adult fish (Eskova *et al.*, 2020).

1.4 Stress in zebrafish

Zebrafish, *Danio rerio*, is a promising model to study the development, physiology, and genetics of stress as well as the neuronal circuits responsible for its modulation (Demin *et al.*, 2021). Importantly, most of the anatomical areas and neuronal populations responsible for mediating stress responses in mammals are conserved in zebrafish. The Hypothalamic Pituitary Interrenal (HPI) axis (Figure 6) is structurally and functionally homologous to the HPA axis, with cortisol being the main glucocorticoid both in humans and teleosts (Wendelaar Bonga, 1997; Mommsen, Vijayan and Moon, 1999; Flik *et al.*, 2006). The PVN is identified in zebrafish as part of the PoA, which contains several populations of peptidergic neurons (Figure 6), including parvocellular neurons expressing Crh and Avp (Herget and Ryu, 2015). In zebrafish, Crh^{+} neurons are responsible for activating the HPI axis and they release Crh directly to the pituitary gland, as fish lack the hypophyseal portal system (Herget *et al.*, 2014). Crh stimulates the release of Acth into the blood, which in turn induces the secretion of cortisol from the interrenal gland, homologous to the mammalian adrenal gland (Figure 6) (Alsop and Vijayan, 2008). In addition to cortisol, stress also triggers the release of catecholamine from the chromaffin cells of interrenal tissue and leads to a rapid release of epinephrine and noradrenaline (de Abreu et al., 2021).

The stress response system matures early in development. Crh^{+} neuronal projections innervating the pituitary are detectable as early as 3 dpf (Herget *et al.*, 2014). Zebrafish larvae begin *de novo* synthesis of cortisol at around 2 dpf, while cortisol increase after stress exposure is observed between 3 and 5 dpf, depending on the intensity and the type of the stressor (Alsop and Vijayan, 2008; Alderman and Bernier, 2009; Steenbergen, Richardson and Champagne, 2011).

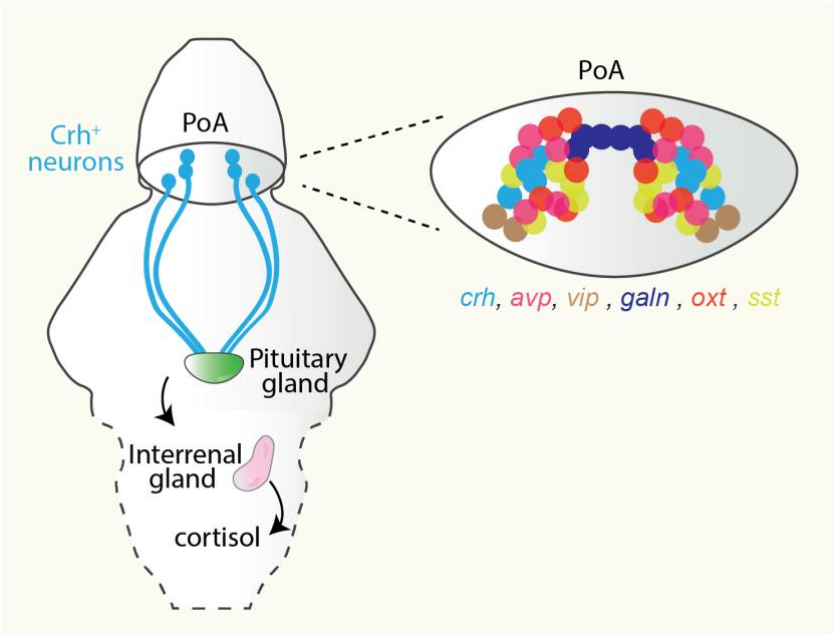

Figure 6: Organization of the zebrafish HPI axis and the neurosecretory region of the PoA. (left) Scheme showing a dorsal view of a larval zebrafish brain and the localization of the PoA containing Crh$^+$ neurons, which activate the HPI axis. In response to a stressor, Crh is directly secreted in the pituitary and stimulates the release of Acth, which induces the release of cortisol. The dashed line points out that the interrenal gland is located in a ventral region outside the brain. (right) Scheme showing the PoA with the main neuropeptides detected by *in situ* hybridization in the study of (Herget and Ryu, 2015). *crh* corticotropin releasing hormone, *avp* arginine vasopressin, *vip* vasoactive intestinal peptide, *galn* galanin, *oxt* oxytocin, *sst* somatostatin.

Like in mammals, cortisol exerts most of its functions through mineralocorticoid and glucocorticoid receptors (Mommsen, Vijayan and Moon, 1999), which translocate to the nucleus and bind to the promoter regions of target genes. In teleosts, cortisol affects many aspects of physiology, including reproduction, growth, metabolism, and immune functions. Interestingly, maternal cortisol is transferred into the offspring during oogenesis and it is crucial for the proper development of the stress axis (Eachus, Choi and Ryu, 2021). It was shown that manipulating maternal stress can alter HPI axis activity and affect the abundance of gene transcripts involved in the stress responses (Best, Kurrasch and Vijayan, 2017; van den Bos *et al.*, 2019).

After exposure to acute stress, cortisol rises within 10 minutes and returns to basal level after approximately 30 minutes (Yeh, Glöck and Ryu, 2013; Faught and Vijayan, 2018). As in mammals, the binding of cortisol to its receptors probably contributes to the termination of stress responses as in zebrafish the knockout of *gr* causes chronic elevation of cortisol and anxiety-like states (Griffiths *et al.*, 2012; Ziv *et al.*, 2012). However, a direct inhibitory effect

of cortisol on Crh^+ neuronal activity after stress has not been confirmed. As in mammals, the cortisol secretion in zebrafish larvae follows circadian rhythmicity and was shown to be dependent on light exposure (Yeh, 2015). Likewise, hypothalamic levels of *crhb,* encoding Crh*,* fluctuate during the day but do not correlate with cortisol concentrations (Yeh, 2015). Although there are many similarities between mammals and teleosts regarding the major components of the stress system, the neuronal circuits and the modulatory mechanisms controlling the HPI axis activity are still largely unknown in zebrafish.

1.4.1 Neuronal populations modulating stress

Most of the studies investigating stress in zebrafish have focused on the development of the stress axis, the signaling pathways affected by GCs receptors, and recently considerable attention has been paid to the consequences of early life stress exposure and social isolation (Shams, Khan and Gerlai, 2020; de Abreu et al., 2021; Eachus, Choi and Ryu, 2021; Fontana et al., 2021; Lara and Vasconcelos, 2021; Wee et al., 2022). Defensive behaviors elicited by certain types of stressful stimuli have also been studied in zebrafish larvae, with a particular focus on the neuronal mechanisms controlling locomotor responses (Corradi and Filosa, 2021). However, few studies focused on the neuronal mechanisms modulating behavioral and neuroendocrine responses to stress.

In zebrafish, Crh^+ neurons were shown to be the main activators of the stress axis. Lack of one of the Crh receptors, *crhr1*, disrupts cortisol synthesis and light-induced hyperactivity in zebrafish larvae (Faught and Vijayan, 2022). Ca^{2+} imaging analysis of Crh^+ neuronal activity demonstrated that these cells show a highly coordinated activation in response to acute stressors (vom Berg-Maurer *et al.*, 2016). Interestingly, a high synchronicity level was also detected in other unidentified peptidergic populations, suggesting crosstalk between Crh^+ neurons and the neighboring cells. In support of a role of other neurosecretory populations in the modulation of stress, genetic ablation of a cluster of peptidergic neurons including Avp, Crh, Oxt, and other not-identified neurons, led to reduced cortisol synthesis (Gutierrez-Triana *et al.*, 2014). In addition, it was shown that different types of stressors recruit multiple peptidergic neurons within the hypothalamus, including Crh^+ and Oxt^+ neurons, which seem indispensable to drive avoidance behavior in response to threats (Lovett-Barron *et al.*, 2020).

These studies highlight that in zebrafish, as in mammals, peptidergic signaling constitutes a crucial hypothalamic network regulating the stress response. However, the identity and the function of most peptidergic neurons modulating stress is still unknown. In addition, no studies report the intra-connectivity within the different classes of peptidergic neurons within the hypothalamus and whether their effect on the HPI axis activity is direct or mediated by Crh^{+} neurons. It is also unclear which regions in the zebrafish brain project to the PoA to communicate information about stressful stimuli and coordinate behavioral and neuroendocrine responses.

1.4.2 Stress-related behaviors in zebrafish

Several types of stressors have been reported to enhance the production of cortisol in zebrafish larvae, including hyperosmotic environment, pH change, light/dark transition, exposure to blue light, temperature fluctuations, visual predators-like stimuli, crowding, and turbulent water (Clark, Boczek and Ekker, 2011; Steenbergen, Richardson and Champagne, 2011; de Marco *et al.*, 2013; Yeh, Glöck and Ryu, 2013). Importantly, the established protocols to expose fish to stressful stimuli are shorter and less complex than those used for rodents, significantly reducing animal handling and avoiding invasive procedures, which ultimately could affect the outcome of the experiments.

The main physiological marker to assess the activation of the HPI axis in zebrafish is cortisol. However, the extraction of whole-body cortisol from zebrafish larvae requires the immediate sacrifice of the animals after stress exposure without the possibility of performing further analysis (Clark, Boczek and Ekker, 2011). In addition, the available techniques to detect hormone concentration in zebrafish larvae require pooling together multiple animals, limiting the detection of interindividual variability in stress responses. Therefore, behavioral assays are fundamental for investigating the neurobiology of stress in zebrafish larvae.

Zebrafish larvae display a rich repertoire of well-characterized behaviors in response to stressful stimuli. For example, an acoustic stimulus or a flash of light is detected by the animal as a threat and elicits the startle response, a fast unilateral C-bend of the tail which allows a rapid escape from the stimulus (Korn and Faber, 2005; Burgess and Granato, 2007). Another common readout of stress-related states is the measurement of locomotion. Zebrafish larvae respond to hyperosmotic stress, induced by administration of sodium chloride (NaCl), increasing their motility between three and 10 minutes after stress. This rapid change in

locomotion suggests the involvement of fast brain signaling in response to hyperosmotic stress rather than relatively slow hormone actions (Clark, Boczek and Ekker, 2011; de Marco *et al.*, 2014). Exposure to flashing blue light has the opposite effect on locomotion leading to decreased motor activity, which was reported to be dependent on corticotroph cells (de Marco *et al.*, 2016; Ryu and de Marco, 2017). Another measurement of a stress-like state, often correlated to anxiety, is thigmotactic behavior, which is the preference of an animal to spend more time near the borders of open spaces, most likely to avoid exposure to predators (Colwill and Creton, 2011).

Importantly, zebrafish are relatively easy to maintain, have a short generation cycle of approximately three months, and on average a female can lay around 100-500 eggs per week, allowing high-throughput behavioral analysis at larval stage. In addition, the development of automated tracking systems and custom-made software has simplified quantifying specific behavioral responses. Another great advantage of zebrafish is its transparency at early stages, which permits to visualize genetically-labeled neuronal populations and record their activity under different conditions, facilitating the elucidation of the neuronal mechanisms underlying behavioral responses.

1.4.3 Investigating neuronal circuits in zebrafish

Mutagenesis strategies are an essential tool to label and manipulate specific cell populations and investigate the neuronal circuits mediating stress responses. Genome editing tools, as clustered regularly interspaced short palindromic repeats/CRISPR-associated 9 (CRISPR/Cas9) system (Hwang *et al.*, 2013), are well established in zebrafish and permit the generation of specific mutant lines for reverse-genetic studies. CRISPR/Cas9 system is composed of a short single-stranded guide RNA (sgRNA) containing the target site which drives the Cas9 nuclease to the target genomic locus. The sequence recognition only requires a short sequence called protospacer-associated motif (PAM) at the 3′end of the target site. Cas9 creates double-strand breaks at the DNA target site complementary to the gRNA. The induced DNA double strand break is then repaired via DNA repair mechanisms as non-homologous end-joining or homology directed repair, which lead to mutations in the target gene or can be used to insert specific DNA sequences (Schmid and Haass, 2013).

Transgenesis systems such as Tol2 transposons can be used to integrate target genes into the zebrafish genome (Kawakami, 2005). Transposases catalyze the excision of the desired DNA sequence from a donor plasmid, leading to random integration of the excised DNA in the genome. These technologies have been used to generate a vast collection of transgenic fish and databases of tissue and cell-type-specific promoters (Sumbre and de Polavieja, 2014). For example, transgenic lines expressing GAL4 and the upstream activating sequences (UAS) constitute one of the most common inducible gene expression methodologies to label specific cell populations in zebrafish (Scott *et al.*, 2007; Asakawa *et al.*, 2008). In the Gal4/UAS combinatorial expression system, the transcriptional activator Gal4 drives the expression of transgenes downstream of its DNA binding motif, the UAS sequence. An effector gene, as a fluorescence reporter, is fused to the UAS sequence and can only be expressed in cells in which Gal4 is expressed.

Another crucial advance in zebrafish research is the generation of reporter lines expressing the genetically encoded Ca^{2+} indicator (GECI) GCaMP. GCaMP results from the fusion of the Ca^{2+}-binding protein calmodulin (CaM) with a green fluorescent protein (GFP) (Nakai, Ohkura and Imoto, 2001), whose fluorescence intensity changes depending on the Ca^{2+} concentration within the cell and can be used as a readout of neuronal activity (del Bene *et al.*, 2010). Specific promoters or the GAL4/UAS systems can be used to drive the expression of GCaMP in distinct cell populations or even in the whole-brain using pan-neuronal markers. The small size and transparency of zebrafish larvae, combined with advanced microscope techniques, allow to simultaneously record the neuronal activity in the whole-brain, including the most ventral brain regions of the hypothalamus.

Whole-brain imaging recordings can also be combined with immunohistochemistry and *in situ* hybridization techniques, as in the MultiMAP protocol (Lovett-Barron et al., 2017). This method combines *in vivo* Ca^{2+} imaging with *post mortem* staining of neuronal markers to label the neuronal population whose activity changed during the recording. Labeling and monitoring specific neuronal populations can also be combined with optogenetic tools and two-photon laser-mediated ablation strategies to manipulate the activity of single cells or entire neuronal populations (Wyart *et al.*, 2009; Ahrens *et al.*, 2012; Portugues *et al.*, 2013, 2014). All these methods are crucial in the effort of investigating the neuronal circuits modulating stress responses, as they provide the opportunity to study brain dynamics without invasive procedures to expose and image the brain.

2 Aims

The lack of a complete understanding of the neuronal mechanisms that control stress in humans, and the difficulties of analyzing neuronal responses *in vivo* in mammals, prompted us to investigate the neuronal circuits modulating stress in zebrafish. I chose to focus on a discrete population of hypothalamic neurons secreting the peptide Galn, whose function in stress-related behaviors has never been investigated in zebrafish and is still not fully understood in mammals. To achieve this, four main objectives were set:

- My first goal was to determine whether $Galn^+$ neurons are responsive to stress and whether aversive stimuli differentially modulate discrete populations of $Galn^+$ neurons localized in different regions of the hypothalamus. Taking advantage of the transparency of the zebrafish larval brain, I aimed to characterize the response dynamics of $Galn^+$ neurons *in vivo* to gain a first insight into their possible involvement in stress and in the modulation of the HPI axis.
- Second, I aimed to investigate whether the activation of $Galn^+$ neurons in response to stress insults influences the behavior of zebrafish larvae. To achieve this goal, I utilized different ablation procedures and behavioral assays to determine if the lack of $Galn^+$ neurons results in impaired stress-related responses.
- Third, I aimed to identify the signaling molecule transmitting stress-related information from $Galn^+$ neurons to downstream effectors to ultimately modulate the fish's behavior. Given the extensive, yet incomplete, literature advocating the involvement of Galn peptide in stress, I aimed to generate a Galn-mutant zebrafish line and asses its behavioral responses. The phenotype of *galn* mutants led me to analyze whether the peptide's absence or overexpression affects the neuronal activity of $Galn^+$ cells.
- Finally, I wanted to determine the downstream neuronal population regulated by $Galn^+$ neurons that affect behavioral and endocrine responses to stress. Considering the main function of Crh^+ neurons in activating the HPI axis, I aimed to assess whether these two neuronal populations are functionally connected.

3 Materials

3.1 Zebrafish lines

Zebrafish line	Reference	Identifier ZFIN
TgBAC[galn:GAL4-VP16,myl7:mCherry] ^{mpn213}	(Förster *et al.*, 2017)	ZDB-ALT-170908-13
Tg[5xUAS:EGFP]^{nkuasgfp1a}	(Asakawa *et al.*, 2008)	ZDB-ALT-080528-1
Tg[UAS-E1b:NTR-mCherry]^{c264}	(Davison *et al.*, 2007)	ZDB-ALT-070316-1
Tg[14xUAS:GCaMP6s]^{mpn101}	(Thiele, Donovan and Baier, 2014)	ZDB-ALT-140811-3
Tg[elavl3:H2B-GCaMP6s]^{jf5}	(Freeman *et al.*, 2014)	ZDB-ALT-141023-2
galn^{md76}	This study	N/A

3.2 Vectors and Plasmids

Vector	Insert	Reference
pTol2	*UAS:galn-T2A-tdTomato-CAAX*	This study
pTol2	*UAS:tdTomato-CAAX*	This study
pGEM-T-Easy	wild-type *galn* cDNA	(Podlasz *et al.*, 2012)

3.3 Oligonucleotides

Oligonucleotides were synthesized by Eurofins Genomics.

	Sequence 5'-3'
sgRNA	CGGACTCACGAGGACCGAGG
Galn_F	ACATTTTGTGTAAAACAGGCAAAAG
Galn_R	GTAGACCTGAGAGCAGCATGA
Galn_Kozak_F	CGGAATTCGCCGCCACATGCACAGGTGTGTC
Galn_SrfI_R	GGCCCGGGCGTCGCTGAGGCTCCT
T2A_Tom_F	GAGGGCAGAGGAAGTCTTCTAACATG
T2A_Tom_R	TCAAGACAGGACGCACTTACAGGACAT
UAS_F	AGGGTCGACTCTAGAGGGTA
UAS_Gln_R	ATCCCGAGTGTTTCTGTCAGAA

3.4 Bacteria

Name	Origin	Identifier
5-alpha Competent *E. coli*	NEB	Cat# C2987H

3.5 Antibodies

Primary Antibodies	Origin	Identifier
polyclonal chick Anti-GFP	Thermo Fisher	Cat# A10262 RRID: AB_2534023
monoclonal mouse Anti-p44/42 MAP Kinase	Cell Signaling	Cat# 4696 RRID: AB_390780
monoclonal rabbit Anti-p44/42 MAP Kinase (Thr202/Tyr204)	Cell Signaling	Cat#4370 RRID: AB_2315112
monoclonal rat anti-mCherry	Thermo Fisher	Cat# M11217 RRID: AB_2536611
polyclonal rabbit anti-Galanin	Millipore	Cat# AB5909 RRID:AB_2108517
Anti-DIG-AP	Roche	Cat# 11093274910 RRID: AB_514497

Secondary Antibodies	Origin	Identifier
Alexa Fluor 405 Anti-rabbit	Thermo Fisher	Cat# A-31556 RRID:AB_221605
Alexa Fluor 488 Anti-mouse	Cell Signaling	Cat# 4408 RRID: AB_10694704
Alexa Fluor 488 Anti-chicken	Thermo Fisher	Cat# A11039 RRID: AB_142924
Alexa Fluor 647 Anti-mouse	Cell Signaling	Cat# 4410S; RRID: AB_1904023
Alexa Fluor 647 Anti-rabbit	Thermo Fisher	Cat# A31573 RRID: AB_2536183
Alexa Fluor 555 Anti-rabbit	Cell Signaling	Cat# 4413 RRID: AB_10694110
Alexa Fluor 555 Anti-rat	Cell Signaling	Cat# 4417 RRID: AB_10696896

3.6 Chemicals and reagents

	Origin	Identifier
Agarose, Low Melting Point	Roboklon	E0303-50
Agarose NEEO Ultra Qualität	Carl Roth	2267.3
Ampicillin	Sigma	A9518
Bacterial LB Agar	Carl Roth	X969.2
Bacterial LB Medium	Carl Roth	X969.2
5-Brom-4-chlor-3-indoxylphosphat (BCIP)	Sigma	B5655
Bovine Serum Albumin	Serva	11943.02
BsaJI restriction enzyme	NEB	R0536
Calcium nitrate ($Ca(NO_3)_2$)	Honeywell	C1396
Cas9 protein	MDC facility	N/A
DIG-labeling mix	Roche	11277065910
Dimethyl sulfoxide (DMSO)	Th. Geyer	23419.3
DNaseI	Roche	10104159001
EcorI – HF restriction enzyme	NEB	R0101
Ethanol p.a	Carl Roth	9065.2
Ethyl Acetate	Sigma	270989
Ethylenediaminetetraacetic acid (EDTA)	Carl Roth	X986.2
Formamide	Thermo Fisher	17899
Gel red Nucleid Acid Stain	Linaris	41003
GeneRuler 1kb DNA ladder	Thermo Fisher	SM0311
Goat serum	Sigma	G6767
Heparin	Sigma	H3393-100KU
Hydrochloric acid (HCl)	Sigma	H1758
Hydrogen peroxide (H_2O_2) 30%	ChemCruz	sc-203336A
(4-(2-hydroxyethyl)-1-piperazineethanesulfonic acid) (HEPES)	Carl Roth	9105.4
Loading dye (Orange G)	Carl Roth	0318.2
Magnesium sulfate ($MgSO_4$)	ChemCruz	sc-211764
Master Mix Taq 2x	New England Biolabs	M0270
Methanol	Roth	4627.1
Nifurpirinol	Sigma	32439
Nitro blue tetrazolium chloride (NBT)	Sigma	B5655
NotI – restriction enzyme	New England Biolabs	R0189
Pancuronium bromide	Sigma	P1918
Paraformaldehyde (PFA)	Sigma	P6148

Penicillin-Streptomycin	Thermo Fisher	15140122
Phenol red	Sigma	P0290
Phosphate-buffered saline (PBS)	Sigma	P4417
Phusion High-Fidelity DNA Polymerase	Life Technologies	F530L
Potassium chloride (KCl)	ChemCruz	sc-203207
Potassium hydroxide (KOH)	Alfa Aesar	A16199
Proteinase K	Sigma	3115879001
Ribonucleic acid from torula yeast	Sigma	R6625-25G
RNase H	Life Technologies	EN0201
RNase inhibitor (40 U/µL)	Life Technologies	EO0381
Saline-sodium citrate (SSC) 20x	Sigma	S6639-1L
SOC-Medium	New England Biolabs	B9020S
Sodium Chloride (NaCl)	Serva	39781.02
SP6 polymerase	New England Biolabs	2706G
SpeI – HF restriction enzyme	New England Biolabs	3133
SrfI restriction enzyme	New England Biolabs	R0629S
T7 polymerase	New England Biolabs	M0255AAVIA
Tricaine (3-amino benzoic acidethylester)	MDC facility	N/A
Tris	Sigma	T1503
Trypsin-EDTA	Sigma	T4049
Triton X 100	Carl Roth	3051.3
Tween 20	Carl Roth	9127.2
Water H_2O RNase/DNase free	LIFE Technologies	R0581

3.7 Solutions and buffer

1xPBS

Reagent	Final concentration	Amount
PBS	1x	5 tablets
MilliQ H_2O	N/A	Add to 1 L
Total		1 L

1xPBT

Reagent	Final concentration	Amount
1xPBS	1x	Add to 500 mL
Triton X 100	0.3%	1.5 mL
Total		500 mL

4% PFA/PBT

Reagent	Final concentration	Amount
1xPBT	1x	30 mL
PFA 16%	4%	10 mL
Total		40 mL

30x Danieau's medium

Reagent	Final concentration	Amount
NaCl	1740 mM	101,7 g
KCl	21 mM	1,56 g
MgSO4	12 mM	2,96 g
Ca(NO3)2	18 mM	4,25 g
HEPES	150 mM	35,75 g
MilliQ H_2O	N/A	bring up to 1 L
Total		1 L

200 mM NaCl

Reagent	Final concentration	Amount
NaCl	200 mM	2,33 g
Danieau's medium 1x	N/A	Bring up to 200 mL
Total		200 mL

10% KOH

Reagent	Final concentration	Amount
KOH 10%	10 %	10 g
MilliQ H_2O		Bring up to 100 mL
Total		100 mL

Bleaching solution

Reagent	Final concentration	Amount
H_2O_2 30%	3%	100 µl
KOH 10%	0,5%	50 µl
PBT	1x	850 µl
Total		1 mL

Hybridization buffer (HB)

Reagent	Final concentration	Amount
Formamide	50%	25 mL
20x SSC	5x	12,5 mL

Tween 20 20%	0.1%	0,25 mL
Heparin 5 mg/ mL	50 µg/ mL	0,5 mL
tRNA 50 mg/mL	500 µg/ mL	0,5 mL
H_2O RNase/DNase free		Bring up to 50 mL
Total		50 mL

Immunostaining Blocking solution

Reagent	Final concentration	Amount
Goat serum	5%	500 µl
BSA	1%	0,1 g
DMSO	1%	100 µl
PBT	1x	Bring up to 10 mL
Total		10 mL

1,5 % LMP agarose

Reagent	Final concentration	Amount
Agarose, Low melting point	1,5%	1,5 g
1x Danieau's medium	1x	Bring up to 100 mL
Total		100 mL

2 % agarose

Reagent	Final concentration	Amount
Agarose, NEEO	2%	2 g
MilliQ H_2O	1x	Bring up to 100 mL
Total		100 mL

TE buffer ph 8

Reagent	Final concentration	Amount
Tris-Cl 1M	10 mM	1 mL
EDTA 0.5 M	1 mM	0.2 mL
MilliQ H_2O		Bring up to 100 mL

Tricaine

Reagent	Final concentration	Amount
Tricaine	4 mg/mL	2 g
1x Danieau's medium	1x	Bring up to 500 mL
Total		500 mL

3.8 Kits

	Origin	Identifier
Cortisol ELISA Kit	Biomol	500360-96
HCRv3 reagents	Molecular Instruments	https://www.molecularinstruments.com/
mMESSAGE mMACHINE	LIFE Technologies	AM1340
NucleoSpin Gel and PCR Clean-up	Macherey-Nagel	740609.25
NucleoSpin Plasmid	Macherey-Nagel	74058850S
Phusion High-Fidelity PCR Kit	Life Technologies	F553L
SuperScript III First Strand Kit	Life Technologies	18080051

3.9 Consumables

	Origin	Identifier
Bacterial culture tubes	TPP	352059
Centrifuge tubes 15 ml	TPP	91015
Centrifuge tubes 50 ml	TPP	91050
Glass Capillaries	Science Products	GB120F-8P
Microcentrifuge tubes 1.5 ml	Sarstedt	72.706.400
Microcentrifuge tubes 2 ml	Sarstedt	72.695.400
Multiwell plates (6, 12, 24, 48, 96)	Falcon, Greiner	
Pellet Pestle, 1.5 ml	Fisher Scientific	11872913
Petri dish (60 mm)	Sarstedt	83.3901
Petri dish (35 mm)	Sarstedt	82.1135.500
Plastic pipette 3 mL	Pastette	LW4111
PCR tubes	Sarstedt	72.991.002
Pipette tips 10 µl	Sarstedt	701130
Pipette tips 200 µl	Sarstedt	70.760.002
Pipette tips 1000 µl	Sarstedt	70.1186
Serological pipette tips 10 ml	Sarstedt	86.1254.001
Serological pipette tips 25 ml	Sarstedt	86.1685.001

3.10 Equipments

	Origin	Identifier
Agarose gel documentation device	Biozym	Azure 200
Agarose gel systems	Thermo Scientific	Owl Easycast B1
Bacteria incubator	Infors HT	n/a
Benchtop centrifuge	Eppendorf	5417R
Camera	XIMEA	MQ003MG-CM
Centrifuge	Eppendorf	5417R
Confocal Microscope LSM 800	Zeiss	LSM 800
Electro-Tunable Lens	ETL, Optotune	10-30-c-nir-ld-mvo
Fluorescence-Stereomicroscope	Olympus	SZX16
Incubator zebrafish 28°C	Velp Scientifica	FOC215L
Incubator 37°C	LLG Labware	uni INCU 20
Magnetic stirrer	WWR	VMS-C7
Multiphoton system	Thorlabs	Bergamo I series
Microinjector	World Precision I.	PV820
Microinjection molds	MDC, selfmade	N/A
Microwave	Exquisit	N/A
Microscale	Fisher Scientific	PAS214
Mini Vortex	Carl Roth	HXH6.1
Nano Drop / Photometer	Eppendorf	D30
Needle Puller	Narishige	PC-100
PCR machine	Eppendorf	6337000019
Pellet Pestle	Fisher Scientific	12-141-361
pH Meter	Mettler-Toledo	Five Easy
Pipette 10 µl, 100 µl, 200 µl and 1000 µl	Eppendorf	Research Plus
Pipetboy	Integra	Acu 2
Petri dish (60 mm)	Sarstedt	83.3901
Petri dish (35 mm)	Sarstedt	82.1135.500
Plastic pipette 3 mL	Pastette	LW4111
Power Meter Photodiode Sensor	Thorlabs	S170C
Rotor (rotator)	Stuart	SRT6
Scale	Kern	EW4200
Stereomicroscope	Leica	S6
Thermo block	Eppendorf	5382000015
UV Transilluminator	Alpha Imager HP	n/a
Waterbath	GFL	11347017J

Water-immersion Objective (W Plan-Apochromat 20x/1.0 DIC VIS-IR)	Zeiss	n/a

3.11 Softwares

	Origin	Identifier
ANTs (Anatomical Normalization Toolkits)	Deneux *et al.*, 2016	http://stnava.github.io/ANTs/
GraphPad Prism 7	GraphPad Software	https://www.graphpad.com/scientific-software/ prism/
EthoVision XT version 8.5	Noldus	https://www.noldus.com/ethovision-xt
Fiji/ImageJ	NIH	https://fiji.sc/
Matlab	The MathWorks	https://www.mathworks.com/products/ matlab.html
Python	Python	https://www.python.org/
Scipy.Signal (Pyhton library)	Python	https://docs.scipy.org/doc/scipy/reference/signal.html
ZEN software	Zeiss	N/A

4 Methods

4.1 Zebrafish general methods

4.1.1 Zebrafish husbandry

Zebrafish eggs were obtained by mating AB/TL mixed strain adult zebrafish. Fish were placed in the evening in breeding tanks. Fertilized eggs were collected the next morning and transferred to petri-dishes containing Danieau's medium. Zebrafish embryos and larvae were raised under standard conditions at 28.5°C on a 14 hr/10 hr light/dark cycle in Danieau's medium. All animal procedures were conducted in accordance with institutional (Max Delbrück Center for Molecular Medicine), State (LAGeSo Berlin), and German ethical and animal welfare guidelines and regulations. Experiments were performed in 5 dpf zebrafish larvae unless otherwise stated. At this developmental stage, the sex of the fish could not be determined.

4.1.2 Microinjections

Microinjections into zebrafish eggs were performed at one/two cell stage. Injection needles were generated with a needle puller device. Agar plates to perform the injections were prepared by placing microinjections molds into a petri dish containing 1.5% agarose in Danieau's medium. Eggs were sorted and carefully placed into the cavities of the injection plates prior to injection of approximately 5 pl of a solution containing 1x Phenol red together with sgRNA/Cas9 reagents (see section 4.1.3) or DNA construct (see section 4.2.4) into the cell.

4.1.3 Generation of CRISPR/Cas9 mutants

The *galn*^{md76} mutant line was generated using CRISPR/Cas9 technique. Cas9 protein was provided by the Protein Production & Characterization facility of the MDC institute and aliquots were stored at -20°C until use. Cas9 protein at a final concentration of 0.6 µg/µl was co-injected with a sgRNA (400 ng/µl) targeting the exon3 of the *galn* gene (see section 3.3). After injection, eggs were placed in a fish incubator and kept under standard conditions. At 3 dpf, approximately 20 injected embryos were used for genotyping to confirm the efficiency

of the mutagenesis (see section 4.2.2). At 5 dpf the remaining larvae were transferred into the zebrafish facility for raising. Adult zebrafish were genotyped using genomic DNA extracted by tail fin biopsies.

4.1.4 Fin biopsies of adult zebrafish

Adult zebrafish were anesthetized in water containing 0.168 mg/ml of Tricaine. Once anesthetized, single fish were placed on a plastic petri dish and a scissor was used to cut a small portion of the tail fin, which was placed in a PCR tube. The tissue was then used to extract genomic DNA and perform genotyping (see section 4.2.2). After the procedure, fish were rapidly transferred to a single fish tank labeled as the PCR tube and monitored until recovery.

4.2 Molecular biological methods

4.2.1 Isolation of genomic DNA

For the isolation of genomic DNA from fin biopsies and larvae, 50 µl or 30 µl of TE buffer containing 10% Proteinase K were added to the adult or larval tissue, respectively. Samples were lysed at 55˚C overnight and on the next day Proteinase K was inactivated by incubation at 95˚C for 10 minutes. The supernatant containing the genomic DNA was used for genotyping or stored at -4˚C until further use.

4.2.2 Genotyping *galn*^{md76} mutants

CRISPR/Cas9 mutants were identified using genomic DNA extracted from larvae or adult tissues. Polymerase chain reaction (PCR) was used to amplify the region of interest using Galn_F and Galn_R primers (see section 3.3) flanking the sgRNA target site on *galn* gene. Per reaction, 1.5 µl of genomic DNA was amplified with 12.5 µl of Taq 2X Master Mix and 0.5 µl of each forward and reverse primer (10 mM), and 10 µl of dH_2O. The following PCR program was used:

Cycle Step	Temperature	Time	No. of cycles
Initial Denaturation	94°C	2 min	1
Denaturation	94°C	30 s	32
Annealing	58°C	30 s	
Extension	72°C	5 min	
Final Extension	72°C	5 min	1

In the initial screening, the amplified genomic DNA was used to sequence the *galn* gene to identify the precise site and length of the mutations. Once the $galn^{md76}$ line was established, mutants were identified using restriction fragment length polymorphism analysis. 10 µl of each PCR amplicons were digested using 0.8 µl of BsaJI restriction enzyme, 2.5 µl of CutSmart Buffer, and 11.7 µl of dH_2O. After incubation at 60°C for 4 hours, restriction digest products were analyzed by agarose gel electrophoresis. The wild-type allele digestion results in two bands of 34 base pair (bp) and 104 bp, while in the $galn^{md76}$ mutant allele, missing the restriction site, the 177 bp PCR amplicon is intact.

4.2.3 *in situ* hybridization probe synthesis

Antisense probe for colorimetric in situ hybridization was generated using as DNA template a pGEM-T-Easy vector containing the galn target sequence kindly provided by Prof. Pertti Panula (Podlasz *et al.*, 2012). The construct was linearized using 2 µg of DNA template, 2 units of the restriction enzyme SpeI, and 1x of the enzyme buffer. After incubation at 37°C for two hours, the linearized DNA was purified using the NucleoSpin PCR Clean-up kit according to the manufacturer's instructions. For the generation of the labeled RNA, a solution containing 1µg of linearized DNA, 20 units of T7 RNA polymerase, 1x of DIG labeling mix, 2x of transcription buffer, and 30 units of RNAse inhibitor was incubated at 37°C for 2 hours. The DNA template was then digested by the addition of 1 unit of DNAse for 15 minutes at 37°C. The antisense probe was then precipitated using 2.5 µl LiCl 4M and 75 µl of prechilled 100 % Ethanol. After overnight incubation at -20°C, the solution was centrifuged for 30 min at 4°C at 13000 rpm. The supernatant was discarded and the pellet

was washed twice using 75% ethanol. The pellet was finally dried at room temperature and dissolved in 20 µl of ultrapure H_2O. After verifying the quality of the synthesized RNA by agarose gel electrophoresis and its concentration using a nano photometer, the antisense probe was stored at -20°C until usage.

4.2.4 Cloning

To generate the *UAS:galn-T2A-tdTomato-CAAX* plasmid, the *galn* coding sequence was amplified by PCR from a 5 dpf zebrafish cDNA library using the primers Galn_Kozak_F and Galn_SrfI_R (see section 3.3). The *T2A-tdTomato-CAAX* cassette was amplified by PCR from an existing pTol2 plasmid using the primers T2A_Tom_F and T2A_Tom_R (see section 3.3). Per reaction, 1 µl of cDNA was amplified with 4 µl of 5x GC buffer, 0.4 µl of 10 mM dNTPs, 0.5 µl of each forward and reverse primer (10 mM), each forward and reverse primer (10mM), 0.5 µl of DMSO, 0.2 µl of Phusion polymerase, up to 20 µl of dH_2O. The following PCR program was used:

Cycle Step	Temperature	Time	No. of cycles
Initial Denaturation	98°C	30 s	1
Denaturation	98°C	10 s	32
Annealing	55°C	30 s	
Extension	72°C	5 min	
Final Extension	72°C	5 min	1

The amplified *galn* and *T2A-tdTomato-CAAX* sequences were then purified using the NucleoSpin PCR Clean-up kit according to the manufacturer's instructions. Next, 1 µg of a pTol2 plasmid containing the 14*xUAS* cassette was cut using 0.5 µl of EcorI and 0.5 µl of NotI restriction enzymes, 2.5 µl of CutSmart Buffer, and dH_2O up to 25 µl. After incubation at 37°C for two hours, the linearized vector was purified using the NucleoSpin PCR Clean-up kit according to the manufacturer's instructions. To insert the *galn* sequence downstream of the linearized plasmid containing the 14*xUAS* cassette, a ligation reaction containing 2 µl of T4 DNA Ligase buffer, 1 µl of T4 DNA Ligase vector, the insert DNA, and dH_2O up to

20 µl was incubated overnight at 16°C. The mass of vector and insert was calculated considering a 6:1 insert:vector ratio. After heat inactivation, 5 µ of the ligation reaction was transformed in chemically competent E. coli cells (see section 4.2.5).

After selection of clones containing the correct insert, the resulting *14xUAS:galn* plasmid was linearized using 1 µl of SrfI restriction enzyme, 2.5 µl of CutSmart Buffer, and dH_2O up to 25 µl and incubated at 37°C for two hours. After purification, the plasmid was incubated with the *T2A-tdTomato-CAAX* sequence, and the ligation was performed as described above. The successful insertion of the *T2A-tdTomato-CAAX* downstream of the *galn* sequence was confirmed by colony PCR (see section 4.2.6) and then sequencing. To generate the *UAS:tdTomato-CAAX* plasmid, not containing the *galn* sequence, the *tdTomato-CAAX* cassette was cloned downstream of the *UAS* sequences of the pTol2 plasmid. The plasmid *UAS:tdTomato-CAAX* was cloned and donated by Margherita Zaupa.

4.2.5 Transformation of bacteria

To transform plasmid DNA, chemically competent *E. coli* cells were thawed on ice and 5 µl of the ligation reaction was added and incubated on ice for 30 minutes. After heat-shock at 42°C for 30 seconds, the cells were quickly incubated on ice for 2 minutes. After the addition of 200 µl SOC medium, the cells were incubated at 37°C, 400 rpm for 45 min. 50-100µl of the transformation was spread on pre-warmed LB agar plates containing the antibiotic ampicillin. After incubation overnight at 37°C, colonies on LB agar plates were selected and analyzed for the integration of the correct plasmid by colony PCR.

4.2.6 Colony PCR

Prior to sequencing, the correct insertion of single clones was assessed using colony PCR. Each colony was picked with pipette tips and inoculated in a PCR tube with 30 µl of LB medium containing the antibiotic ampicillin. After incubation at room temperature for approximately 30 minutes, the colony resuspension was mixed, and 1.5 µl was used as PCR template. UAS_F primer targeting the *14xUAS* cassette and UAS_Gln_R primers (see section 3.3) targeting the *galn* sequence were used to determine the correct insertion of *galn* downstream of the *UAS* sequence. UAS_F primer and T2A_Tom_R primer (see section 3.3) were used to verify the insertion of the *T2A-tdTomato-CAAX* sequence. The PCR reaction

contained 1.5 µl of colony resuspension and 0.5 µl of each forward and reverse primers (10 mM), together with 12.5 µl of Taq 2X Master Mix and 10 µl of dH2O. The following PCR program was used for both the colony's PCRs:

Cycle Step	Temperature	Time	No. of cycles
Initial Denaturation	94°C	2 min	1
Denaturation	94°C	30 s	32
Annealing	55°C	30 s	
Extension	72°C	5 min	
Final Extension	72°C	5 min	1

PCR products were analyzed by agarose gel electrophoresis and the colonies containing the correct insert were subjected to bacterial cultivation and DNA extraction prior to sequencing.

4.2.7 Bacterial cultivation and DNA extraction

After identification of the clones with the correct insert, 10 µl of clone resuspension were inoculated with 4 mL of LB medium containing ampicillin and incubated overnight at 37°C, 200 rpm. Next day, plasmid DNA was isolated using the commercial kit NucleoSpin Plasmid according to the manufacturer's protocol. After determining the DNA concentration using a nano photometer, plasmids were sequenced to confirm the correct insertion and stored at -20°C until further use.

4.3 Staining procedures

4.3.1 Fixation of zebrafish larvae

For immunofluorescence staining, anesthetized zebrafish larvae were transferred into 1.5 mL microcentrifuge tubes and fixed with 4% paraformaldehyde (PFA) in PBS with 0.3% Triton (PBT) overnight at 4°C. For *in situ* hybridization, samples were anesthetized and fixed with 4% PFA in PBS with 0.1% Tween-20 (PBST) overnight at 4°C. Next day, the solution

containing the PFA was removed and samples were washed three times for 15 minutes with PBT (for immunostaining) or PBST (for *in situ* hybridization) at room temperature under agitation. Samples used for colorimetric and fluorescent *in situ* hybridization were subjected to a series of washes for 5 minutes under agitation (25% methanol in PBST, 50% methanol in PBST, 75% methanol in PBST). After incubation in 100% methanol for 15 minutes, the samples were stored at -20°C until usage.

4.3.2 Clearing of zebrafish tissue

To remove melanin pigments prior to immunofluorescence or *in situ* hybridization, a clearing step of the tissues was performed after fixation. Samples were incubated for 15 minutes at room temperature in bleaching solution (see section 3.7). After verifying at the microscope that the brain tissue was efficiently cleared, the samples were rapidly rinsed with PBS.

4.3.3 Immunofluorescence staining

Immunostaining was performed using a previously described protocol (Filosa *et al.*, 2016). After fixation and bleaching, larvae were washed under agitation three times in PBT for 15 minutes. The samples were then incubated in 150 mM Tris-HCl (pH 9) for 5 minutes at room temperature and then transferred at 70°C for 15 minutes. After three washes washed under agitation in PBT for 15 minutes, larvae were incubated in Trypsin EDTA (diluted 1:50 in PBT) for 40 minutes on ice. After three washes under agitation in PBT for 15 minutes, the samples were incubated in immunostaining blocking solution (see section 3.7) for one hour at room temperature on a shaker. Primary antibodies were diluted 1:500 in blocking solution and added to the samples. After incubation at 4°C for 96 hours under agitation, the samples were washed at least three times for 15 minutes in PBT. Next, samples were incubated for 48 hours at 4°C under agitation with secondary antibodies diluted 1:300 in blocking solution. A list of the antibodies used is provided in section 3.5. After removing the secondary antibodies solution, samples were washed at least three times for 15 minutes with PBT under agitation. Samples were mounted in 1.5% low melting point agarose and then imaged using a Confocal Microscope.

4.3.4 Colorimetric *in situ* hybridization

The colorimetric *in situ* hybridization was performed based on a previously described protocol (Thisse and Thisse, 2008). Fixed samples were rehydrated by a series of washing steps with decreasing concentrations of methanol (75% methanol in PBST, 50% methanol in PBST, 25% methanol in PBST). After three washes in PBST for 15 minutes, the samples were permeabilized using 10 µg/ml Proteinase K for 40 minutes at room temperature. Afterward, larvae were rapidly rinsed with PBST and re-fixed with 4% PFA for 20 minutes at room temperature. Samples were washed three times in PBST for 15 minutes prior to pre-hybridization in hybridization buffer (HB) (see section 3.7) for four hours at 70°C in a water bath. The HB was removed and replaced with fresh HB containing 75 ng of the antisense digoxigenin RNA probe targeting the *galn* gene (see section 4.2.3), and the samples were incubated at 70°C overnight. Next day, probes were removed and the samples were washed for 10 minutes in a 70 °C thermoblock under gentle agitation with increasing concentrations of 2xSSC (75% HB in 2x SSC, 50% HB in 2x SSC, 25% HB in 2x SSC, 2x SSC). After two washes with 0.2x SSC for 10 minutes at 70 °C, the samples were transferred at room temperature on a shaker. The 0.2x SSC was gradually replaced with PBST washing the samples for 10 minutes with increasing concentrations of PBST (75% 0.2x SSC in PBST, 50% 0.2x SSC in PBST, 25% 0.2xSSC in PBST, PBST). Next, samples were incubated in the *in situ* hybridization blocking solution (see section 3.7) for two hours at room temperature on a shaker prior to overnight incubation at 4°C with an anti-digoxigenin antibody conjugated to alkaline phosphatase diluted 1:5000 in blocking solution. Next day, samples were washed three times for 10 minutes at room temperature with PBST and then transferred into a transparent glass 6-well plate. A staining buffer containing Nitro blue tetrazolium chloride (NBT) and 5-Brom-4-chlor-3-indoxylphosphat (BCIP) was added to the samples which were kept in the dark. The colorimetric reaction was monitored periodically and then stopped with several washes in PBST once the desired labeling intensity was reached. Samples were imaged using a Stereomicroscope.

4.3.5 Fluorescent *in situ* hybridization chain reaction

To label *crhb*, *gad2*, *galnR1a*, *galnR1b*, *galnR2a*, and *galnR2b* transcripts, the third generation *in situ* hybridization chain reaction (HCR) was used (Choi *et al.*, 2018). Fixed

samples were rehydrated by a series of washing steps with decreasing concentrations of methanol (75% methanol in PBST, 50% methanol in PBST, 25% methanol in PBST). After three washes in PBST for 15 minutes, larvae were permeabilized with 30 µg/mL proteinase K at room temperature for 45 minutes. Next, larvae were rapidly rinsed with PBST and re-fixed with 4% PFA for 20 minutes at room temperature and then washed five times for 5 minutes with PBST. The samples were pre-hybridized with the hybridization buffer provided by Molecular Instruments Inc. for 30 minutes at 37°C prior to incubation overnight at 37°C with fresh hybridization buffer containing 1 pmol of each probe. Probes were designed and purchased by Molecular Instrument Inc. Next day, the excess probe was removed by washing the samples four times for 15 minutes with wash buffer (provided by Molecular Instrument Inc) at 37°C prior to two washes of five minutes with 5× SSCT at room temperature. Samples were pre-amplified with amplification buffer for 30 minutes at room temperature. Prior to the amplification step, the hairpins (purchased by Molecular Instrument In.c) were snap-cooled at 95°C for 90 seconds and kept at room temperature in the dark for 30 minutes. Next, samples were incubated at room temperature in the dark overnight with fresh amplification buffer containing 30 pmol of each snap-cooled fluorescently labeled hairpin. Next day, the excess hairpins were removed by washing the samples with 5× SSCT at room temperature (2x 5 minutes, 2x 30 minutes, 1x 5 minutes). Samples were kept in the dark at 4°C until embedding in 1.5% low-melting-point agarose for confocal imaging. To perform immunostaining for pERK and tERK after *in situ* HCR, the samples were incubated for one hour at room temperature under agitation in immunostaining blocking solution and primary and secondary antibodies were added as described earlier (see section 4.3.3).

4.4 Neuronal ablation methods

4.4.1 Chemogenetic ablation

To perform chemogenetic ablation of $Galn^{+}$ neurons, *galn:Gal4; UAS:NTR-mCherry* adult fish were bred with wild-type AB/TL fish. The progeny was sorted at 3 dpf using a fluorescent microscope to distinguish larvae expressing NTR-mCherry in the PoA, where $Galn^{+}$ neurons are located, from control siblings lacking NTR-mCherry expression. At 3 dpf both groups were treated with 2.5 mM nifurpirinol plus 0.5% DMSO in Danieau's solution for ~24 hours in the dark. Next day, the solution was removed and the larvae were incubated

for ~20 hours in the dark with 5 mM nifurpirinol plus 0.5% DMSO. At 5 dpf, 5 hours prior to the experiment, the drug was removed and replaced with fresh Danieau's medium, and the larvae were left in the incubator under standard conditions. To not cause unwanted stress to the fish, the efficiency of ablation was verified after performing the stress-related assays using a fluorescent stereomicroscope or a confocal microscope.

4.4.2 Two-photon laser ablation

The two-photon-laser-mediated neuronal ablation was performed in 4 dpf *galn:Gal4; UAS:EGFP* larvae. The larvae were embedded in 1% low-melting-point agarose after being anesthetized with 0.016% tricaine. To ablate $Galn^+$ neurons, a confocal microscope equipped with a TiSa two-photon laser set at 880 nm was used. Each $Galn^+$ neuron in the PoA was irradiated by the laser for ~50 ms and the larva was rapidly transferred in a petri-dish containing fresh Danieau's medium. The behavioral assays were performed after ~24 hours to allow the fish to recover from the stress caused by the procedure. To confirm the efficiency of the ablation, the larvae were re-imaged using a confocal microscope after performing stress-related behavioral assays. If less than 90% of all the PoA-$Galn^+$ neurons were ablated, the larva was excluded by the behavioral analysis.

To test whether the laser pulse could damage other neurons than the ones of interests, the procedure was first optimized using 5 dpf *galn:Gal4; UAS:NTR-mCherry; elavl3:H2B-GCaMP6s* larvae. In this line $Galn^+$ neurons are labeled by mCherry while the pan-neuronal marker *elavl3* drives nuclear expression of GCaMP in the whole-brain. The day after the laser-mediated cell ablation, the larvae were re-imaged to verify that only $Galn^+$ neurons were efficiently ablated by the laser procedure and the surrounding neurons were intact.

4.5 Stress-related assays

4.5.1 Hyperosmotic stress in freely swimming larvae

The hyperosmotic stress exposure was performed in 5 dpf *galn:Gal4; UAS:EGFP, galn:Gal4; UAS:NTR-mCherry* after cell ablation (see section 4.4), or AB/TL wild-type larvae depending on the experiment. One hour before the assay, 20/25 larvae per experimental group were transferred into clean petri-dish (60 mm). The Danieau's medium

was gently removed and substituted with 15 mL of fresh Danieau's solution. The petri-dishes were then left at room temperature to recover from any potential stress. To induce hyperosmotic stress by exposure to a concentration of 100 mM NaCl (hypertonic solution), 15 mL of a 200 mM NaCl solution was added to the desired group.

To avoid unspecific stress-related differences caused by the flow of the water rather than the hyperosmotic stress itself, 15 mL of Danieau's solution was added to the control groups. Larvae were kept in the control or NaCl solution for 10 minutes for the experiments aiming at quantify $Galn^{+}$ neurons activity and two minutes for Crh^{+} neurons activity. Finally, larvae were anesthetized with tricaine and rapidly transferred to a solution containing PFA for staining procedures (see section 4.3.1) or frozen at -80°C for cortisol extraction.

4.5.2 Blue light exposure in freely swimming larvae

The exposure to flashing blue light to induce stress was performed in 5 dpf *galn:Gal4; UAS:EGFP larvae.* 40 minutes before the assay, 20/25 larvae per experimental group were transferred into a clean petri dish (60 mm) containing fresh Danieau's medium and left in the dark until the experiment. The experimental group was exposed to pulses of blue light (470 nm) at 30Hz, and dark, each lasting one second. After five minutes of flashing blue light, larvae were anesthetized and rapidly fixed with PFA for immunostaining (see section 4.3.1). After 40 minutes of dark adaptation (as the experimental group), the control group was transferred back to standard illumination conditions and kept in the dark for five minutes prior to anesthesia and fixation. To deliver the blue light, a custom-built array of LEDs was placed at a fixed distance below the petri dish to allow homogeneous illumination. A light power of 2.8 mW cm^{-2} was chosen based on a previous publication (De Marco *et al*, 2013) and measured using a Power Meter Photodiode Sensor.

4.5.3 Cortisol measurement

After hyperosmotic stress (see section 4.5.1), larvae were rapidly anesthetized with tricaine, pooled in 1.5 mL microcentrifuge tubes and frozen at -80°C until further usage. Cortisol extraction was performed following a previously described protocol (Yeh, Glöck and Ryu, 2013). Samples were thawed on ice and 150 µL of DNase/RNase-Free H_2O was added to each tube. The samples were thoroughly homogenized using a pellet pestle prior to

addition of 1 mL of ethyl acetate. After mixing the solution using a vortex at maximum speed, the samples were centrifuged at 9000x g at 4°C for 10 minutes to obtain solvent and aqueous phase separation. After this step, the aqueous phase was discarded as the solvent phase contained the cortisol. To let the ethyl acetate quickly evaporate, samples were placed in a vacuum centrifuge at 4000x g for 30 minutes at 30°C. After verifying that all the solvent was evaporated, 110 µL of ELISA buffer was added to each tube to resuspend the cortisol. Samples were kept on ice until proceeding with the ELISA assay.

Cortisol amounts were measured using an enzyme immunoassay detection kit (see section 3.8) according to the manufacturer's instructions. Briefly, for each sample 50 µL of cortisol dissolved in ELISA buffer was added in duplicate to a 96-well plate pre-coated with a goat anti-mouse IgG. After preparing the cortisol standards with a series of dilutions, 50 µL of each diluted standard was added to the plate in duplicate. Next, 50 µL of conjugate cortisol tracer and cortisol monoclonal antibody were added to each well containing the samples or the standards and the plate was covered in the dark and incubated overnight at 4°C. Next day, the plate was rinsed three times prior to the addition of the detection reagent. The well-plate was then incubated on a plate-reader under constant gentle orbital shaking in the dark. The absorbance (between 405-420 nm) was read every 15 minutes for a total duration of three hours, and the optimal time point of absorbance reading was then used for analysis.

4.6 Behavioral tests

4.6.1 Locomotion assay

The hyperosmotic stress-related behavioral assay was performed in 5 dpf *galn:Gal4; UAS:EGFP* and *galn:Gal4; UAS:NTR-mCherry* after cell ablation, in 5 dpf *galn*^{md76} mutants, and in 5 dpf *galn:Gal4* larvae injected with the *UAS:galn-T2A-tdTomato-CAAX* depending on the experiment. Experimental animals and control siblings were always handled in the same fashion and recorded simultaneously. To record the locomotion of zebrafish, a custom-made behavioral setup placed on a vibration isolation table was used. The setup consisted of a swimming chamber kept at a temperature of 28 ± 0.5°C. Illumination was provided using a white screen placed below the chamber. A high-speed camera positioned above was used to image at 40 frames per second (fps) the movements of the larvae.

One hour prior to the assay, larvae were placed in a multiwell plate with each well holding 100 µl of Danieau's solution. The multiwell plate was placed in the swimming chamber for 10-20 minutes before starting the experiment to leave the larvae to acclimatize to the behavioral setup. At first, larvae were imaged for 10 minutes without any stimulus to record the baseline locomotion. Afterward, a solution of 100 µl of NaCl 200 mM was added using a multiwell pipette to obtain a final concentration of NaCl 100 mM in each well and thus induce the hyperosmotic stress. Locomotion under stress was recorded for 10 minutes.

The videos were then converted in ImageJ/Fiji and analyzed with EthoVision XT to measure the distance moved by each larva before and during stress. The motility ratio was calculated by dividing the distance traveled by each larva during stress by the distance traveled by the same larva during the baseline recording. After behavioral experiments, *galn:Gal4; UAS:EGFP* larvae and *UAS:galn-T2A-tdTomato-CAAX* injected larvae were imaged using a confocal microscope to confirm cell ablation or expression of the construct, respectively.

4.6.2 Acoustic-induced startle response

The acoustic-induced startle response was measured in 5 dpf *galn:Gal4; UAS:NTR-mCherry* after chemogenetic cell ablation (see section 4.4.1). Experimental animals and control siblings were always handled in the same fashion and recorded simultaneously. To image the response of the larvae to a sound stimulus, the same custom-made behavioral setup described above was used. A 6-well plate was placed in the swimming chamber at a temperature of 28 ± 0.5°C 10 minutes before starting the experiment to leave the larvae to acclimatize to the behavioral setup.

Five loud sound stimuli of 3-ms duration and 13-dB intensity with an inter-stimulus time of 120 seconds were generated using a custom Python code. Two speakers positioned at the sides of the swimming chamber containing the multiwell delivered the sound stimuli. The movement of the larvae was imaged for one second before and one second after the sound stimulus onset with a high-speed camera at 500 fps. The movement of the larvae was classified as acoustic-induced startle responses if the typical C-turn escape was initiated no later than 50 ms from the end of the sound stimulus. Acoustic-induced responses were measured as a binary variable (1 for response and 0 for no response). Five repetitions were averaged to calculate the startle probability.

4.6.3 Thigmotactic behavior

Thigmotactic behavior was analyzed in 5 dpf *galn:Gal4; UAS:NTR-mCherry* after chemogenetic cell ablation. Experimental animals and control siblings were always handled in the same fashion and recorded simultaneously. Larvae were transferred in a 12-well plate, with each well containing 2.5 mL of Danieau's medium and placed in the same custom-made behavioral setup previously. The multiwell was placed in the swimming chamber 10 minutes before starting the experiment to leave the larvae to acclimatize to the behavioral setup. The locomotion of the fish was imaged using a high-speed camera at 40 fps. Thigmotaxis was calculated as the average ratio of time spent at the border zone versus the center of the well during 10 minutes of recording. EthoVision XT software was used to delineate border and center zones and to track the movements of the larvae.

4.7 Calcium imaging

4.7.1 Sample preparation

The activity of $Galn^+$ neurons was recorded using 5 dpf *galn:Gal4; UAS:GCaMP6s* larvae, while the imaging of $Galn^+$ neurons and of the entire PoA was performed in 5 dpf *galn:Gal4; UAS:NTR-mCherry; elavl3:H2BGCaMP6s* larvae. All the larvae used for calcium imaging experiments carried the homozygous *mitfa* mutation, which prevents the development of skin melanophores (Lister *et al.*, 1999). Prior to the experiment, larvae were paralyzed using 0.3 mg/mL pancuronium bromide and embedded in a 35 mm petri dish lid using 1% low-melting-point agarose. One larva was mounted on each petri dish lid. Once the agarose was solidified, 2.5 mL of Danieau's solution was added to each petri dish lid, and the larvae were acclimatized at room temperature in the microscope room for at least 20 min before imaging.

4.7.2 Exposure to stimuli

Spontaneous activity of $Galn^+$ neurons was recorded for 120 seconds prior to administration of the stimuli. To induce hyperosmotic stress, 50 mL of a 5 M NaCl solution was added manually to obtain a final 100 mM NaCl concentration inside the petri dish lid. The solution drop was always administrated in front of the larva's mouth to ensure an

immediate perception of the stressor. Variations in the precise timing of the administration of the solutions were corrected later during the analysis. After inducing hyperosmotic stress, the activity of $Galn^+$ neurons was recorded for five minutes.

For the control experiment assessing whether the response of $Galn^+$ neurons was specific to the stressor or to the movement of the solution, 50 mL of Danieau's solution was added to the Petri dish containing the larva.

For the experiments showing the response of $Galn^+$ neurons to two consecutive stimuli, the first exposure to stress was performed as described above. After the first trial, the petri dish lid containing the larva was rinsed twice using Danieau's solution to eliminate as much hypertonic solution as possible. After washing, 2.5 mL of Danieau's solution was added to the petri dish lid and the animal was left at room temperature for 30 minutes to recover. After that, the second stimulus was applied as described earlier.

4.7.3 Image acquisition

A Zeiss LSM880 NLO confocal microscope with a 20x water-immersion objective was used to record $Galn^+$ neuronal activity in 5 dpf *galn:Gal4; UAS:GCaMP6s* larvae. To perform a fast recording of GCaMP6s signal, a resolution of 256 x 256 pixels and a frame rate of 5 fps were set.

In the Ca^{2+} imaging experiments recording the activity of the entire PoA in 5 dpf *galn:Gal4; UAS:NTR-mCherry; elavl3:H2BGCaMP6s* larvae, a multiphoton microscope with an Electro-Tunable Lens for multiplane imaging was used. A volume of 400 x 200 x 180 mm^3 was acquired, which included 30 planes at one volume per second. The resolution per plane was set at 1024 x 512 pixels with a relative z-interval of 6 mm. After Ca^{2+} imaging, a stack of the whole-brain was acquired for the anatomical registration aimed at identifying the Crh^+ neurons after HCR *in situ* hybridization (see section 4.3.5). The imaging was performed by Prof. Marco dal Maschio and Matteo Bruzzone.

4.7.4 Image analysis

Acquired image time series were first corrected for motion artifacts in x and y thanks to a modified version of the algorithm NoRMCorre using Matlab (Pnevmatikakis and Giovannucci, 2017). Images showing a displacement in z were not considered for further

analysis. Corrected images were then processed using ImageJ to measure GCaMP6s fluorescence signal intensity. Each $Galn^+$ neuron was manually selected as region of interest, and the average baseline fluorescence intensity and the fluorescence intensity at different time points were measured to calculate the $\Delta F/F_0$. To identify and characterize the Ca^{2+} events the algorithm Mlspike (Deneux *et al*., 2016) implemented for Matlab was used. Each $Galn^+$ neuron recording was analyzed separately.

After detection of the Ca^{2+} events, a further analysis was performed to categorize $Galn^+$ neurons in different response types. The number of Ca^{2+} events during the first 120 seconds of recording (baseline) was compared with the total number of calcium events during the 120 seconds after administration of NaCl. Neurons were categorized as ‘‘increased activity’’ if the number of Ca^{2+} events increased at least by 5% after exposure to the stimulus, compared to the baseline, ‘‘decreased activity’’ if the number of events was decreased at least by 5% or ‘‘invariant’’ when the change of frequency of events was less than 5%. Neurons were defined as inactive when no Ca^{2+} events were detected.

For identifying Crh^+ neurons after *in situ* HCR (see section 4.3.5), the anatomical registration pipeline based on the Anatomical Normalization Toolkits (Avants, Tustison and Johnson, 2014) and the MultiMap method (Lovett-Barron et al., 2017) were used. The images acquired during the Ca^{2+} imaging were registered to a template zebrafish brain atlas and a previously defined transformation (Kunst *et al.*, 2019) was applied to identify the position of the *live* imaged $GCaMP^+$ neurons in the atlas. Second, the whole-brain z-stack acquired after *in situ* HCR and containing the GCaMP and the *crhb* fluorescent signals were aligned to the images resulting from the previous transformation. In this way, it was possible to identify the coordinates of every $Galn^+$ and Crh^+ neuron in the recording of the live Ca^{2+} imaging. This analysis was performed by Prof. Marco dal Maschio and Matteo Bruzzone. The analysis of the Ca^{2+} events from $Galn^+$ and Crh^+ neurons, used for the categorization of the response profiles, was performed as described earlier. For the cross-correlation analysis of the Crh^+ neurons, increased and decreased activity types with $Galn^+$ neurons increased activity type, the first 60 seconds after NaCl administration were averaged using the Python signal processing library ScipySigna. This analysis was performed by Prof. Marco dal Maschio and Matteo Bruzzone.

4.7.5 *Post mortem* analysis

In the experiments characterizing the activity of $Galn^+$ and Crh^+ cells, larvae were anesthetized with tricaine after Ca^{2+} imaging recording and fixed with 4% PFA in PBS overnight at 4°C. The fluorescence *in situ* HCR v.3.0 method was performed as described in section 4.3.5 to detect *crhb* transcripts and thus identify Crh^+ neurons.

To assess whether different response profile categories of $Galn^+$ neurons were distributed in specific clusters in the PoA, *galn:Gal4; UAS:GCaMP6s* larvae used to record $Galn^+$ neuronal activity were anesthetized and fixed with 4% PFA in PBT overnight at 4°C. Immunostaining for GFP and tERK was performed as described in section 4.3.3. Acquired whole-brain z- stack were analyzed in ImageJ to map the position of the $Galn^+$ neurons within the PoA. The anterior commisure and the midline, identifiable thanks to the tERK staining, were used as reference to measure the distances of each $Galn^+$ neuron. The antero-posterior location was measured from the posterior edge of the anterior commissure, the left-right position from the midline, and the dorsal-ventral location from the dorsal edge of the anterior commissure.

4.8 Statistical analysis

Means and standard error of the mean (mean ± SEM) were calculated using GraphPad Prism and Microsoft Excel. Statistical analysis was performed using two-tailed Student's t tests in Microsoft Excel and GraphPad Prism. The two-sample Kolmogorov-Smirnov test was performed using Python. The tests used are reported in the figure legends. In the graphs, the level of significance is indicated by asterisks: * $p < 0.05$; ** $p < 0.01$; *** $p < 0.001$, and the exact p values are indicated in the graphs. If no significant difference was detected, the abbreviation n.s. is used. Outliers in behavioral analyses were removed using Rosner's Extreme Studentized Deviate test. A maximum of three outliers was removed from each behavioral dataset. When performing multiple comparisons, p values were corrected using the Benjamin-Hochberg Procedure. The number of animals and/or the number of neurons considered for each analysis are reported in the figure legends.

5 Results

5.1 Localization of Galn$^+$ neurons in the larval zebrafish brain

To investigate the role of Galn$^+$ neurons in stress, I used the transgenic zebrafish line *galn:Gal4* expressing the transcription factor Gal4 under the control of the *galn* promoter sequence (Förster *et al.*, 2017). In 5 dpf *galn:Gal4; UAS:NTR-mCherry* larvae, I observed two main populations of Galn$^+$ neurons at 5 dpf (Figure 7A): one group of neurons in the PoA and a second cluster positioned more caudally in the posterior part of the hypothalamus (pHyp), with few cells located close to a region identifiable as the post optic commissure (PoC).

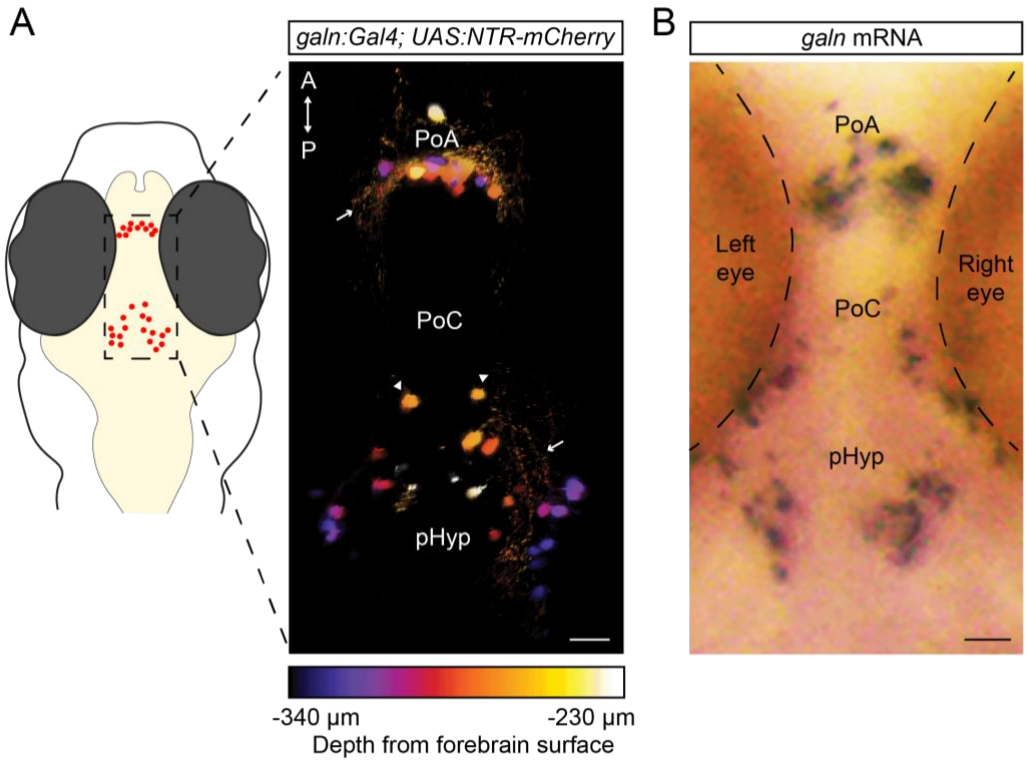

Figure 7: Localization of Galn$^+$ neurons and endogenous *galn* expression. (A). (left) Scheme of the dorsal view of a zebrafish larva showing the location of Galn$^+$ neurons. (right) Maximum projection of a confocal stack image showing Galn$^+$ neurons in a 5 dpf *galn:Gal4; UAS:NTR-mCherry* larva. Neurons are color-coded according to their dorsoventral location (darker, more ventral; lighter, more dorsal). A anterior, P posterior. Arrowheads point to two Galn$^+$ neurons located close to the PoC. Arrows indicate Galn$^+$ nerve fibers. **(B).** *In situ* hybridization in a 5 dpf wild-type larva showing *galn* mRNA expression (purple). PoA preoptic area, pHyp posterior hypothalamus, PoC post optic commisure. Scale bars = 25 µm.

I also observed several Galn$^+$ nerve fibers descending from the PoA to the pHyp (Figure 7A). However, it is difficult to distinguish the origin and the direction of the single projections and thus define if the fibers only pass close to the neurons or if the two populations are connected.

To confirm that the transgenic line *galn:Gal4* recapitulates the endogenous expression of *galn* gene, I labeled *galn* transcripts in wild-type larvae at 5 dpf using *in situ* hybridization. As shown in Figure 7B, *galn* mRNA was detected in the same brain regions where Galn$^+$ neurons are labeled by the Gal4-driven reporter expression, confirming that the transgenic line can be used to genetically label and eventually manipulate Galn$^+$ cells.

5.2 Activity of Galn$^+$ neurons in response to stress

5.2.1 Galn$^+$ neurons in the PoA are activated by hyperosmotic stress

To investigate whether Galn$^+$ neurons are recruited during physiological responses to stress, I exposed 5 dpf *galn:Gal4; UAS:EGFP* larvae for 10 minutes to a hypertonic solution (100 mM NaCl). Administration of NaCl is a well-characterized aversive stimulus for zebrafish larvae, which induces within minutes an immediate stress-related behavioral response along with an increase in cortisol secretion (de Marco *et al.*, 2014). After stress treatment, I performed immunostaining for phosphorylated extracellular signal-regulated kinase (pERK) and total ERK (tERK) to measure the activity of Galn$^+$ neurons in larvae treated with NaCl or with a control solution (Figure 8A). ERK is phosphorylated after neuronal depolarization and has been widely used in zebrafish as a reporter of neuronal activity (Randlett *et al.*, 2015). After measuring the fluorescence intensity of pERK normalized to tERK (pERK/tERK) in each Galn$^+$ neuron, I plotted the activity ratios in the form of cumulative distributions (Figures 8B and C).

The exposure to the NaCl solution led to a shift of PoA-Galn$^+$ neurons toward increased pERK/tERK values, indicating that this neuronal population is, on average, activated in response to hyperosmotic stress (Figure 8B). On the contrary, Galn$^+$ neurons located in the pHyp displayed lower pERK/tERK values in larvae exposed to the hypertonic solution compared to controls (Figure 8C), suggesting a different response of the two Galn$^+$ populations to stress exposure.

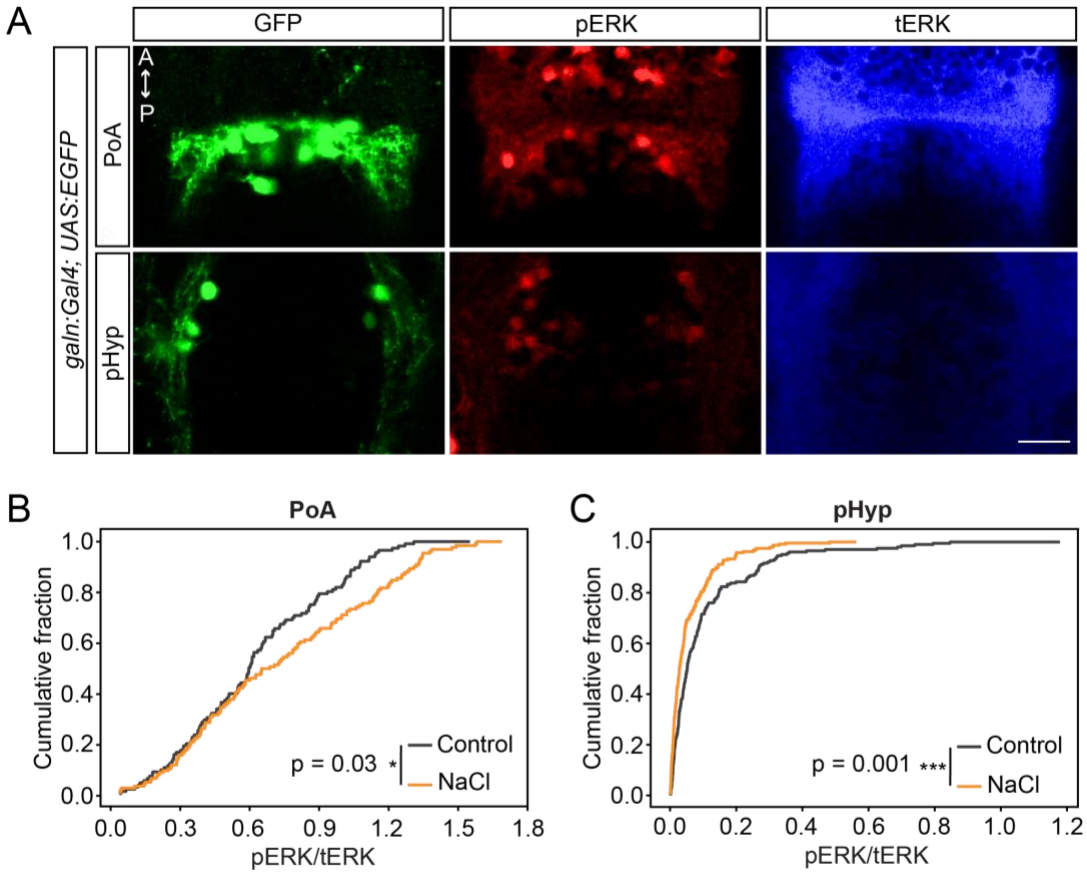

Figure 8: Responsiveness of Galn$^+$ neurons to hyperosmotic stress. (A). Confocal images showing immunostaining for GFP, pERK, and tERK in the PoA and pHyp of a 5 dpf *galn:Gal4, UAS:EGFP* larva. A anterior, P posterior. Scale bar = 25 µm. **(B, C).** Cumulative fractions of pERK/tERK values in Galn$^+$ neurons in the PoA (B) or pHyp (C), after exposure to the hypertonic solution (NaCl) or a control solution in freely swimming larvae. In (B) $n_{control}$ = 117 neurons (7 larvae), n_{NaCl} = 132 neurons (7 larvae). In (C) $n_{control}$ = 204 neurons (7 larvae), n_{NaCl} = 239 neurons (7 larvae). *p <0.05, ***p < 0.001, two-sample Kolmogorov-Smirnov test.

To verify the specificity of the response of Galn$^+$ cells to hyperosmotic stress, I analyzed pERK/tERK values of randomly selected Galn-negative neurons in the telencephalon. In this brain region, control and stressed larvae did not differ in terms of neuronal activity, showing that the response of Galn$^+$ neurons to the NaCl solution is specific and not due to a general alteration of the brain activity (Figure 9).

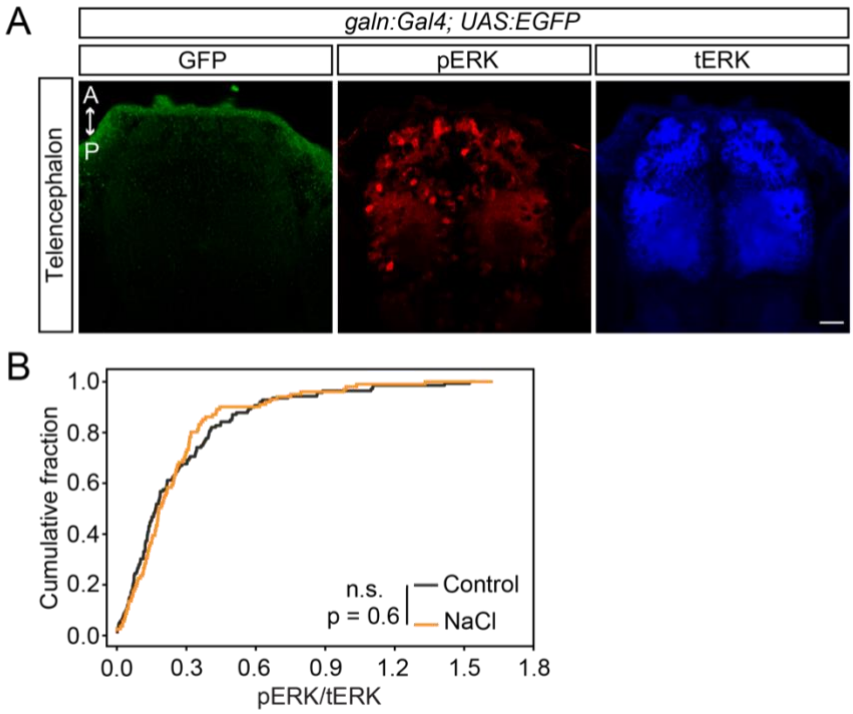

Figure 9: Activity of Galn-negative neurons in the telencephalon. (A). Confocal images showing the telencephalon of a 5 dpf *galn:Gal4; UAS:EGFP* larva immunostained with antibodies against GFP, pERK, and tERK. A anterior, P posterior. Scale bar = 25 µm. **(B).** Cumulative fraction of pERK/tERK values in Galn-negative telencephalic neurons after exposure to the hypertonic solution (NaCl) or a control solution in freely swimming larvae. $n_{control}$ = 138 neurons (7 larvae), n_{NaCl} = 100 neurons (7 larvae). n.s. = not significant, two-sample Kolmogorov-Smirnov test.

5.2.2 Galn$^+$ neurons in the PoA are activated by blue light stress

Since different types of stressors can engage different brain circuits (Herman and Cullinan, 1997; Godoy et al., 2018), which ultimately lead to the activation of the HPI axis, I tested whether Galn$^+$ neurons respond to stressful stimuli in general or exclusively to hyperosmotic stress. To this end, I exposed 5 dpf *galn:Gal4; UAS:EGFP* larvae for five minutes to intermittent blue light (λ = 470 nm) (Figures 10A and B), a type of aversive stimulus documented to activate zebrafish stress responses (de Marco *et al.*, 2016).

Galn$^+$ neurons in the PoA of light-stressed larvae displayed higher pERK/tERK ratios compared to control siblings (Figure 10C). This result, together with the increased activity of PoA-Galn$^+$ neurons after hyperosmotic stress (see Figure 8B), indicate that this neuronal population is, on average, activated in response to different stress conditions. On the contrary, the neuronal activity of Galn$^+$ neurons in the pHyp did not differ between controls and blue

light-stressed larvae (Figure 10D), suggesting that this subpopulation might respond to changes in osmolarity (see Figure 8C) but not to general aversive stimuli.

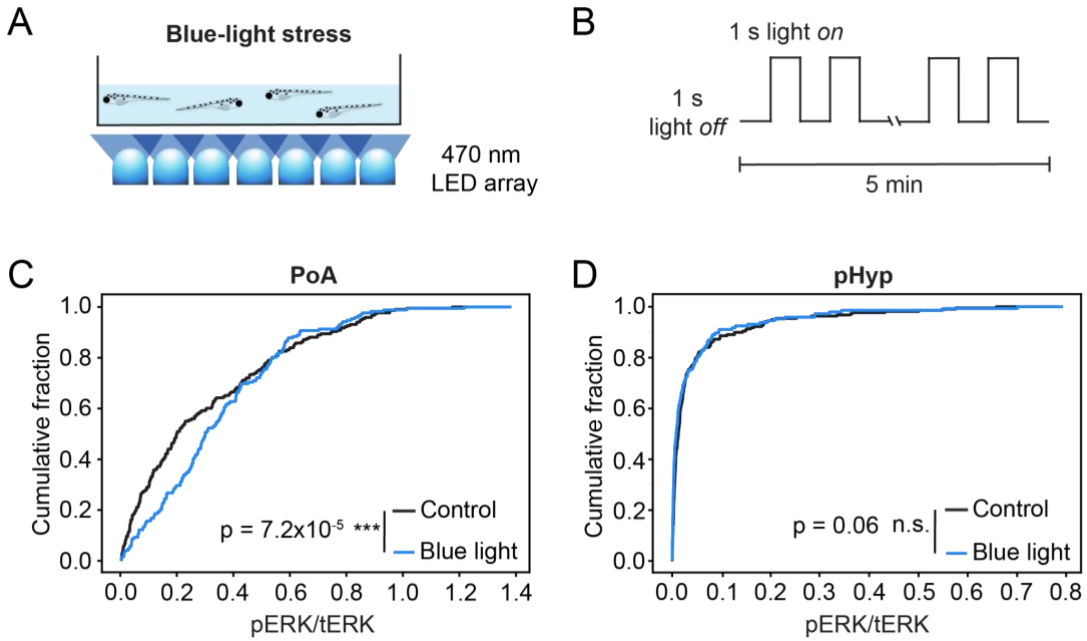

Figure 10: Responsiveness of Galn$^+$ neurons to blue light-induced stress. (A). Drawing showing the custom-made LED array used to expose 5 dpf *galn:Gal4; UAS:EGFP* freely swimming larvae to blue light. **(B).** Scheme of the intermittent light exposure protocol consisting of short pulses of light and dark, each lasting one second. **(C, D).** Cumulative fractions of pERK/tERK values in Galn$^+$ neurons in the PoA (C) and pHyp (D) of larvae exposed to blue light and control siblings. In (C) $n_{control}$ = 218 neurons (10 larvae), $n_{blue\ light}$ = 172 neurons (9 larvae). In (D) $n_{control}$ = 219 neurons (7 larvae), $n_{blue\ light}$ = 146 neurons (6 larvae). *** $p < 0.001$, n.s. = not significant, two-sample Kolmogorov-Smirnov test.

5.2.3 Galn$^+$ neurons display different response profiles during stress

To investigate the dynamics of response of Galn$^+$ neurons to hyperosmotic stress, I performed *live* Ca^{2+} imaging using the double transgenic line *galn:Gal4; UAS:GCaMP6s,* expressing the Ca^{2+} indicator GCaMP6s specifically in Galn$^+$ neurons (Figure 11A). Using a confocal microscope equipped with a water immersion objective, I imaged the activity of Galn$^+$ neurons in 5 dpf *galn:Gal4; UAS:GCaMP6s* larvae before and after administration of a small volume of a 5 M NaCl solution to obtain a final concentration of 100 mM NaCl (Figure 11B).

Galn$^+$ neurons showed various types of response to the administration of NaCl, which I classified based on the comparison between the number of Ca^{2+} events during baseline and

after stress (Figure 11C): increased activity (1) or decreased activity (2) if the hypertonic solution administration led to an increase or decrease in the neuronal response respectively; non-responsive (3) if the frequency of Ca^{2+} transients was similar before and during stress; inactive (4) if no Ca^{2+} events were detected.

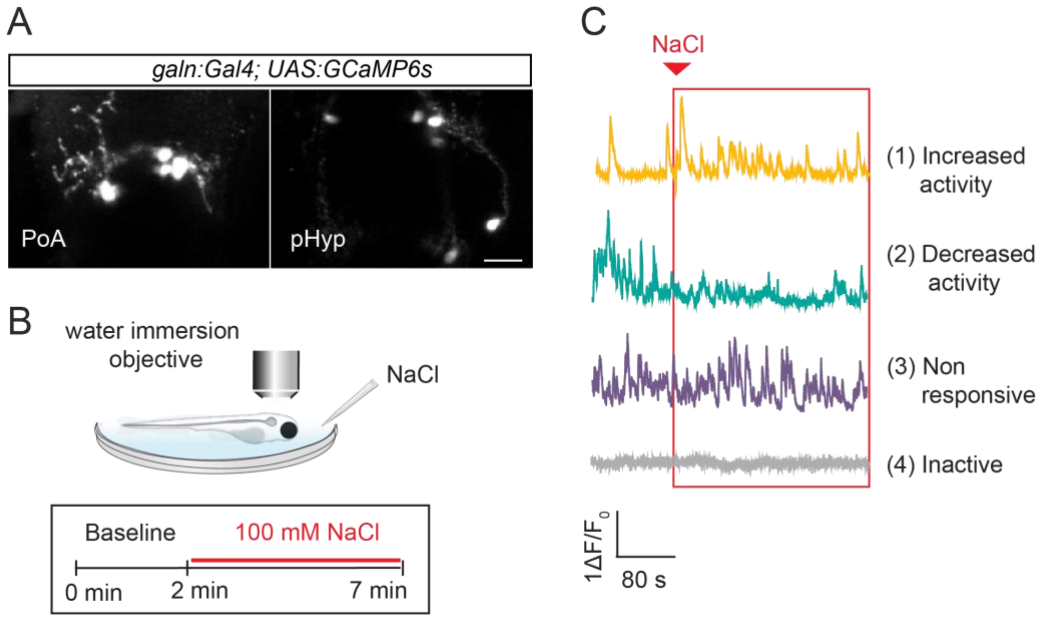

Figure 11: Ca^{2+} imaging of $Galn^{+}$ neurons during hyperosmotic stress. (A). Confocal images showing $Galn^{+}$ neurons in the PoA and pHyp of a 5 dpf *galn:Gal4; UAS:GCaMP6s* larva. Scale bar = 25 µm. **(B).** Scheme of the setup and the timeline of the experiment. $Galn^{+}$ neurons were imaged before (baseline) and after exposure to the hypertonic solution. The NaCl solution was manually added to the petri dish containing the embedded larvae to obtain a final concentration of 100 mM NaCl. **(C).** Representative $\Delta F/F_0$ traces of four different $Galn^{+}$ neurons exemplifying the different types of responses observed. The red rectangle indicates the administration of the hypertonic solution.

5.2.4 PoA-$Galn^{+}$ neurons increase their activity in response to hyperosmotic stress

Ca^{2+} imaging analysis revealed that the majority of $Galn^{+}$ cells (69%) in the PoA increased their activity, measured as frequency of Ca^{2+} events, after administration of the hypertonic solution (Figures 12A and B). This result is congruent with the pERK/tERK analysis showing an increased activation of PoA-$Galn^{+}$ neurons in response to hyperosmotic stress (see Figure 8B). In addition, I observed a minority of $Galn^{+}$ cells decreasing their activity (17%) or not responding (14%) to the administration of NaCl (Figures 12A and B). To investigate whether the amplitude of Ca^{2+} events, and not only their frequency, was affected by administration of the hypertonic solution, I compared the normalized levels of fluorescence intensity ($\Delta F/F_0$)

of GCaMP6s before and after exposure to NaCl (Figures 12C and D). A significant difference in the amplitude of Ca^{2+} events was detected in both $Galn^{+}$ neurons "increase activity" and "decrease activity" types (Figure 12D), in line with the categorization of the different types of neuronal responses.

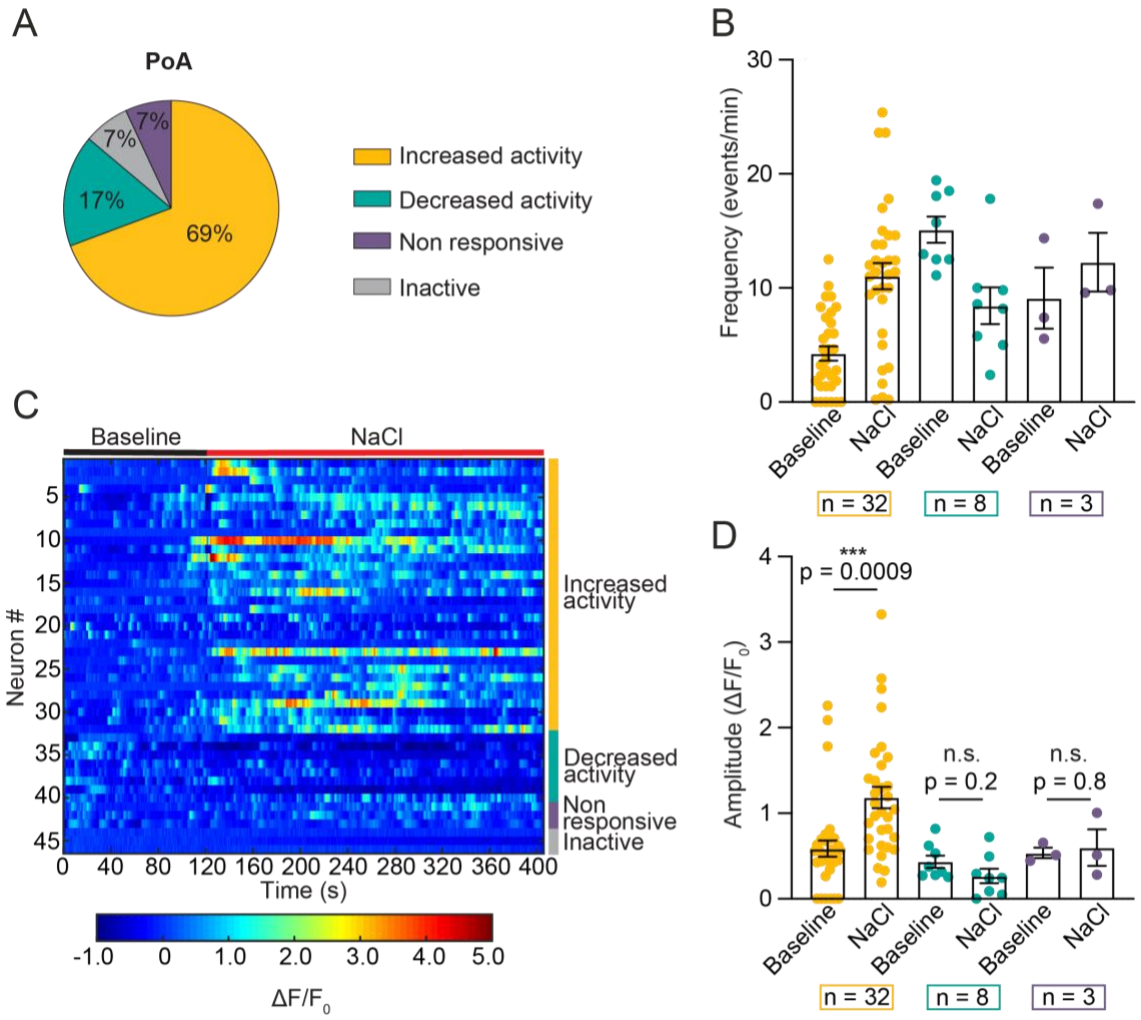

Figure 12: Ca^{2+} imaging of $Galn^{+}$ neurons in the PoA during hyperosmotic stress. (A). Pie chart showing percentages of response types of $Galn^{+}$ neurons in the PoA of 5 dpf *galn:Gal4; UAS:GCaMP6s* larvae. **(B).** Graph displaying average frequency of Ca^{2+} transients in $Galn^{+}$ neurons in the PoA before (baseline) and after (NaCl) exposure to the hypertonic solution. **(C).** Raster plot showing $\Delta F/F_0$ values of each $Galn^{+}$ neuron in the PoA during the recording. **(D).** Graph showing average amplitude of Ca^{2+} events of $Galn^{+}$ neurons in the PoA during baseline and upon stress. Data in (B) and (D) are shown as mean ± SEM. n = number of neurons. *** $p < 0.001$, n.s. = not significant, two-tailed t-test. Statistical tests were not performed in (B) as the frequency was used as parameter for the classification of the neuronal response types.

To verify that $Galn^{+}$ neurons response is specific to hyperosmotic stress and not to the water flow caused by the addition of NaCl, I repeated the Ca^{2+} imaging experiment

administrating a control solution to the larvae. Only a small percentage of PoA-Galn$^+$ neurons increased their activity after stress (11%), and most of the neurons did not respond (49%) or were inactive during the recording (9%) (Figure 13). This result strongly indicates that the water flow did not cause the increased activation of Galn$^+$ neurons in response to the hypertonic solution. On the other hand, a considerable percentage of neurons (31%) fell within the "decreased activity" category (Figure 13), suggesting that this subpopulation of PoA-Galn$^+$ neurons might respond to changes in the water flow.

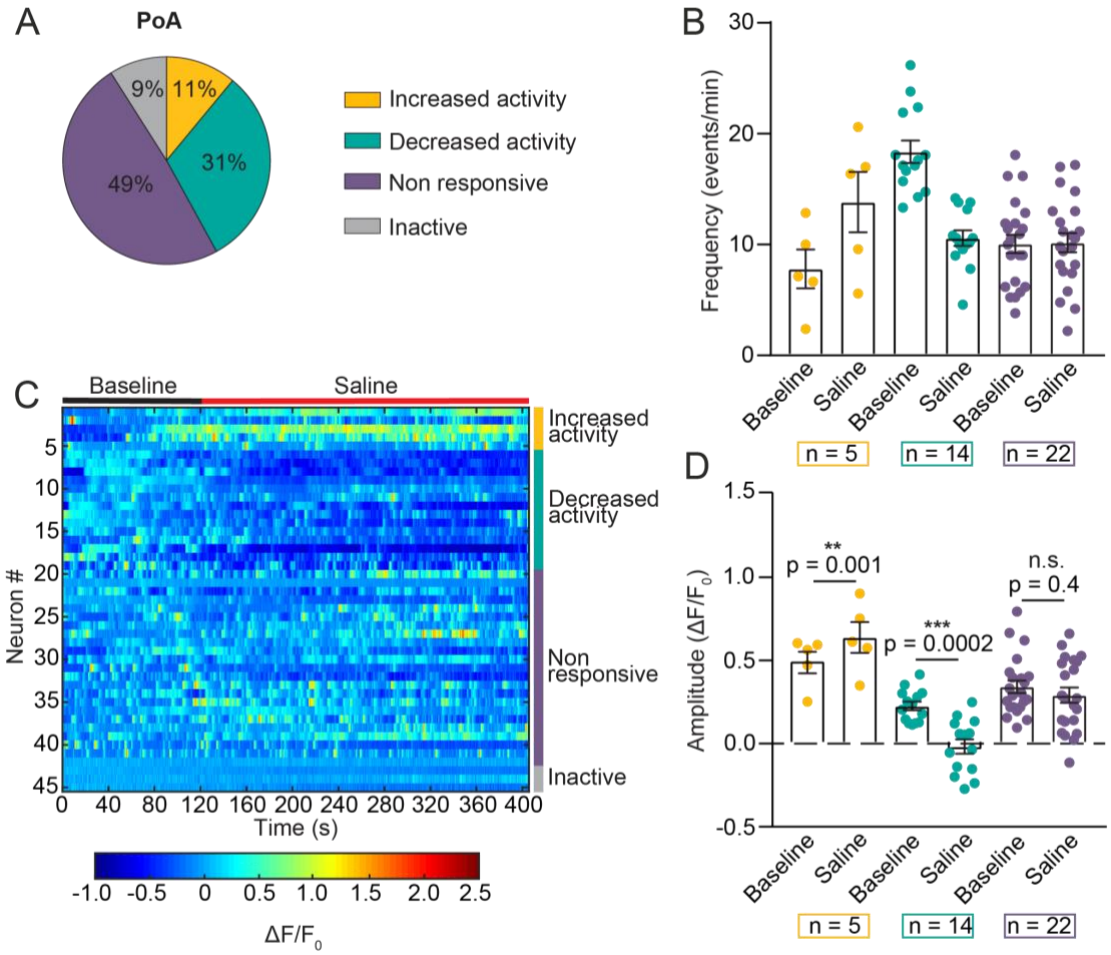

Figure 13: Ca^{2+} imaging of PoA-Galn$^+$ neurons after administration of a control solution. (A). Pie chart showing percentages of Galn$^+$ neurons in the PoA of 5 dpf *galn:Gal4; UAS:GCaMP6s* larvae. **(B).** Bar graph showing average frequency of Ca^{2+} events in PoA-Galn$^+$ neurons before (baseline) and after (saline) exposure to the control solution. **(C).** Raster plot of $\Delta F/F_0$ values of PoA-Galn$^+$ neurons during the recording. **(D).** Graph showing average amplitude of Ca^{2+} transients in PoA-Galn$^+$ neurons during baseline and after administration of the control solution. Data in (B) and (D) are shown as mean ± SEM. n = number of neurons. ** p< 0.01, *** p < 0.001, n.s. = not significant, two-tailed t-test. Statistical tests were not performed in (B) as the frequency was used as parameter for the classification of the neuronal response types.

5.2.5 Galn$^+$ neurons in the pHyp show a heterogeneous response to stress

While the majority of PoA-Galn$^+$ neurons were activated by hyperosmotic stress, Galn$^+$ neurons in the pHyp showed a more heterogeneous response (Figure 14). Most pHyp-Galn$^+$ neurons (38%) decreased their activity in response to the hypertonic solution, in line with the pERK/tERK analysis showing lower pERK values in this subpopulation of neurons after stress (see Figure 8C).

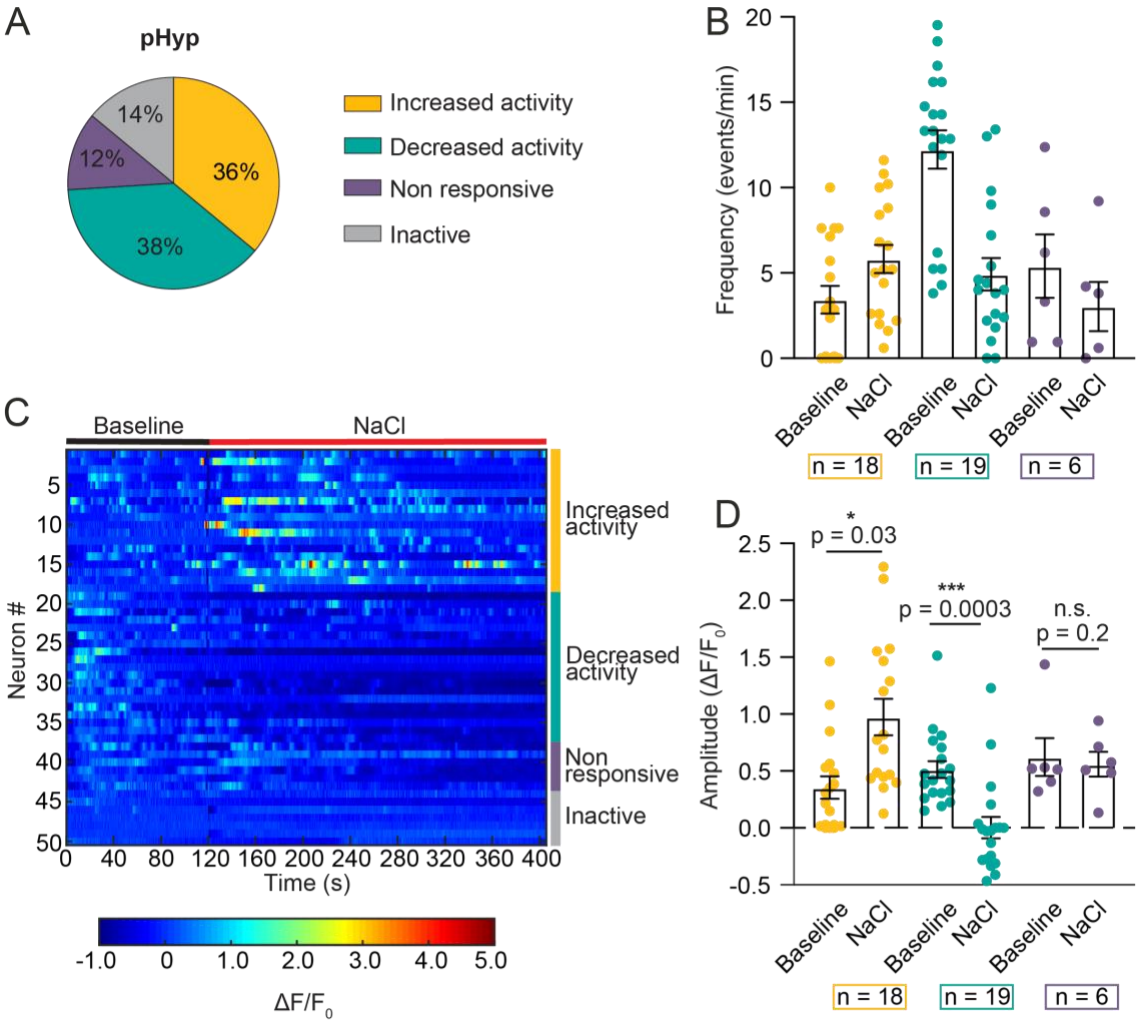

Figure 14: Ca^{2+} imaging of Galn$^+$ neurons in the pHyp during hyperosmotic stress. (A). Pie chart showing percentages of response profiles in pHyp-Galn$^+$ neurons of 5 dpf *galn:Gal4; UAS:GCaMP6s* larvae. **(B).** Bar graph showing average frequency of Ca^{2+} events in Galn$^+$ neurons before (baseline) and after (NaCl) exposure to the hypertonic solution. **(C).** Raster plot displaying $\Delta F/F_0$ values of pHyp-Galn$^+$ neurons during the recording. **(D).** Bar graph showing average amplitude of Ca^{2+} transients in pHyp-Galn$^+$ neurons before (baseline) and after stress (NaCl). Data in (B) and (D) are shown as mean ± SEM. n = number of neurons. * $p < 0.05$, *** $p < 0.001$, n.s. = not significant, two-tailed t-test. Statistical tests were not performed in (B) as the frequency was used as parameter for the classification of the neuronal response types.

A smaller fraction (36%) of Galn$^+$ neurons in the pHyp fell within the "increased activity" category, and the percentage of pHyp-Galn$^+$ neurons "inactive" or "not responsive" was almost doubled (26%) compared to PoA-Galn$^+$ neurons (see Figure 12A). The heterogeneous response of Galn$^+$ neurons in the pHyp to the hypertonic solution, together with the absence of response to blue-light stress (see Figure 10D), suggest that the main Galn$^+$ neuronal population responding to stressful stimuli resides in the PoA. Therefore, I concentrated my attention on these neurons for the remaining experiments.

5.2.6 The activity of PoA-Galn$^+$ neurons is not correlated with their anatomical localization

The identification of different subpopulations of Galn$^+$ neurons raised the question if Galn$^+$ neurons belonging to different response categories are distributed in distinct subregions of the PoA. To assess whether this is the case, I performed immunostaining on the *galn:Gal4; UAS:GCaMP6s* larvae utilized for the Ca^{2+} imaging experiment. Using an antibody against tERK, expressed in all neuronal cells, I could identify the main anatomical regions of the larval zebrafish brain and map the location of Galn$^+$ neurons in the PoA (Figure 15).

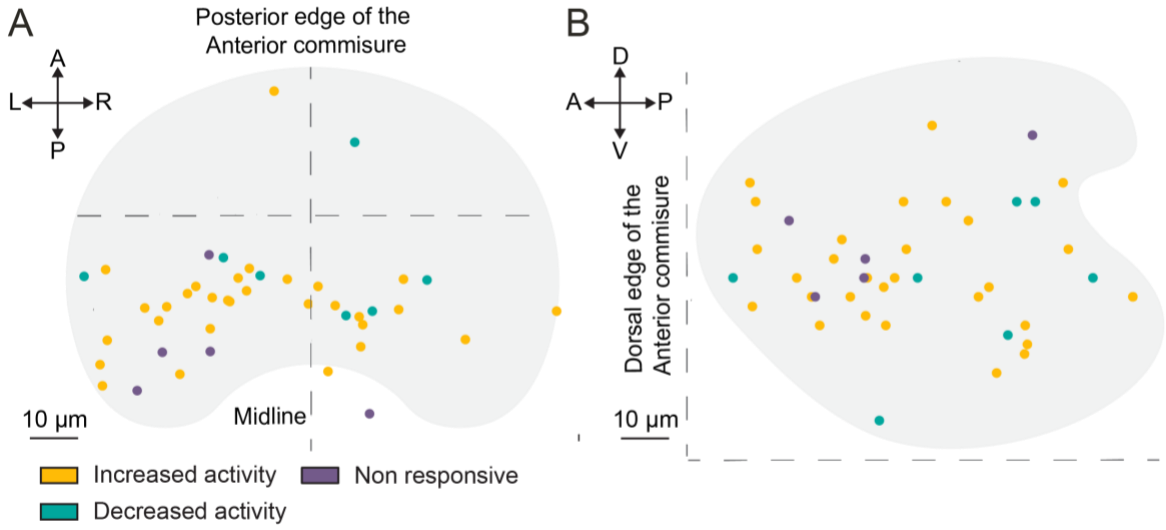

Figure 15: Analysis of the anatomical location of Galn$^+$ neurons within the PoA. (A, B). Scatter plots showing the location of Galn$^+$ neurons belonging to different response types in the PoA, displayed as top (A) and lateral (B) views. Each dot represents a Galn$^+$ neuron color-coded according to its response category. A anterior, D dorsal, L left, P posterior, R right, V ventral. Data were obtained from 20 larvae.

.

Specifically, I measured the anatomical positions of $Galn^+$ neurons from the posterior perimeter of the anterior commissure (for anterior-posterior distance), from the midline (for left-right positioning), and from the most dorsal edge of the anterior commissure (for dorsal-ventral measurement). The different subpopulations of $Galn^+$ did not appear to segregate in distinct subregions but were instead uniformly distributed within the PoA (Figure 15).

5.2.7 PoA-$Galn^+$ neurons respond to multiple applications of the hypertonic solution

To further confirm the specificity of the response of PoA-$Galn^+$ neurons to hyperosmotic stress, I repeated the Ca^{2+} imaging experiment administrating the hypertonic solution two consecutive times, with an interval between trials of 30 minutes. $Galn^+$ neurons responded similarly to the two stimuli as the percentages of $Galn^+$ neurons response types were almost identical between trials (Figure 16A), confirming the reproducibility of the analysis and the specificity of the activation of $Galn^+$ neurons to hyperosmotic stress. It is highly improbable that these similar percentages were due to a random redistribution of the neurons within different categories. Indeed, I compared the response of each $Galn^+$ neuron in the two trials, and most of them did not change their response profile (Figure 16B).

Although $Galn^+$ neurons displayed a similar frequency of Ca^{2+} events in the two experiments, which is the parameter used for the categorization, a change in the response dynamics of the neurons may still have occurred. Therefore, I compared the $\Delta F/F_0$ level of each $Galn^+$ neuron across trials. The average Pearson's correlation coefficient of each neuron was positive and significantly higher than the coefficient of neurons randomly matched across trials (Figure 16C), confirming the conserved response of $Galn^+$ neurons to the hypertonic solution.

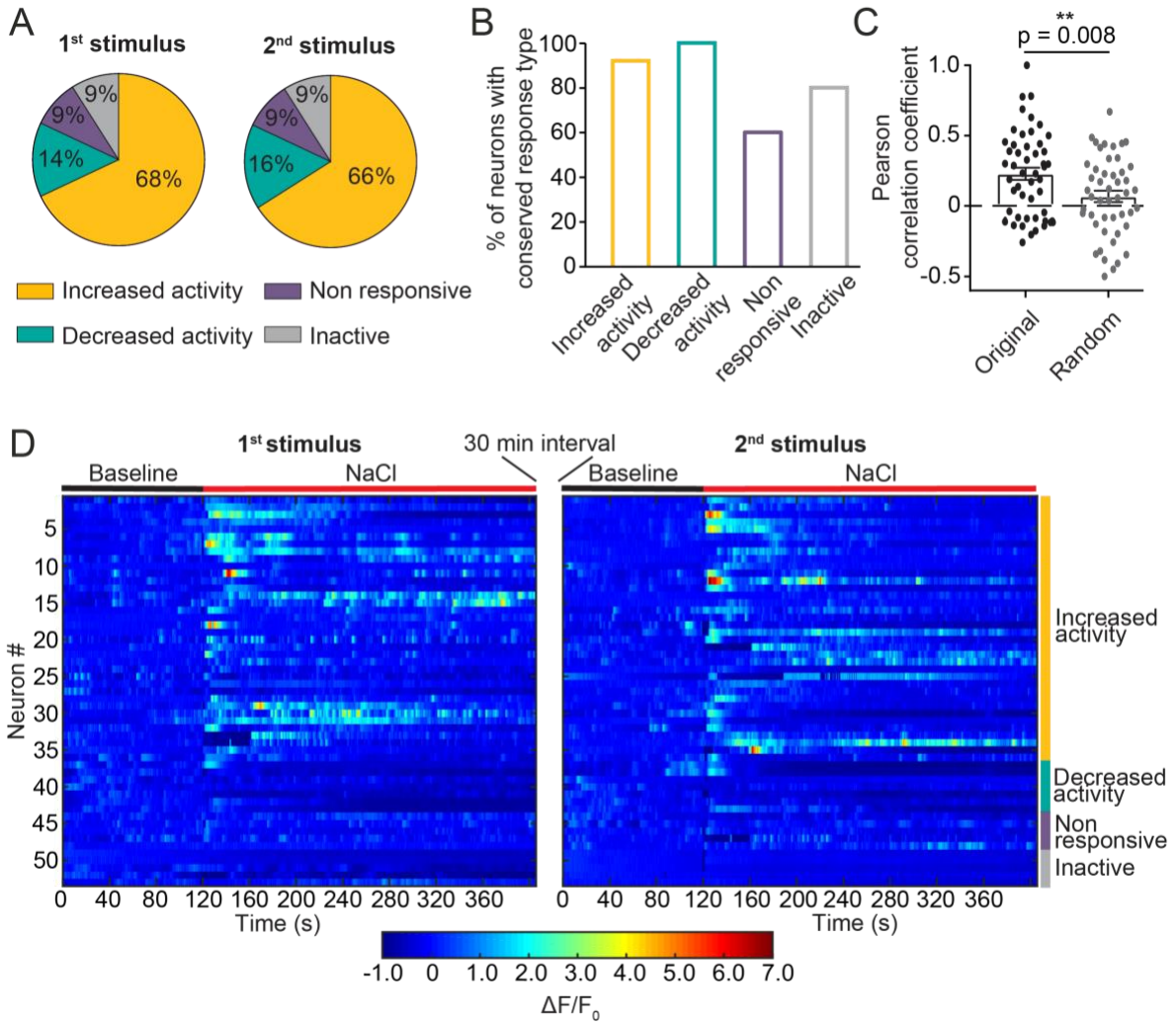

Figure 16: Ca^{2+} imaging of $Galn^{+}$ neurons during two consecutive exposures to the hypertonic solution. (A). Pie charts showing percentages of the four response categories of $Galn^{+}$ neurons in the PoA after the first and the second trial. **(B).** Bar graph showing the percentage of neurons that in the second trial displayed the same response profile observed in the first one. **(C).** Pearson's correlation coefficients of neuronal activity of each $Galn^{+}$ neuron during the first and second stimulation (original), or of neurons randomly selected and paired across the two trials (random). **(D).** Raster plots displaying $\Delta F/F_0$ values of $Galn^{+}$ neurons in the PoA of 5 dpf *galn:Gal4; UAS:GCaMP6s* larvae during the two applications of the hypertonic solution, with a time interval of 30 minutes.

5.3 Galn$^+$ neurons in the modulation of behavioral responses

5.3.1 Chemo-genetic ablation of Galn$^+$ neurons enhances locomotor response to stress

The responsiveness of Galn$^+$ neurons to stressful stimuli raised the question whether these neurons are required for behavioral responses to stress. To this end, I ablated Galn$^+$ cells using an established chemo-genetic approach that takes advantage of the *Escherichia coli* bacterial enzyme nitroreductase (NTR). NTR catalyzes the conversion of the non-toxic compound nifurpirinol into a cytotoxic agent that ultimately causes cell death (Bergemann *et al.*, 2018). In *galn:Gal4; UAS:NTR-mCherry* larvae, the expression of NTR is regulated by the *galn* promoter, allowing to genetically ablate Galn$^+$ cells in a specific and inducible manner.

To ensure that the drug treatment alone would not cause any unspecific behavioral effect, I treated both *galn:Gal4; UAS:NTR-mCherry* larvae and control siblings, lacking the *galn:Gal4* cassette, with nifurpirinol for 48 hours, from 3 dpf to 5 dpf. To investigate whether the ablation of Galn$^+$ cells affects stress-related behavioral responses, I recorded freely swimming Galn$^+$ neurons-ablated larvae and control siblings before and after administration of 100 mM NaCl (Figure 17A). It was previously shown that hyperosmotic stress increases the locomotor activity of zebrafish larvae, which positively correlates with the intensity of stress (Clark, Boczek and Ekker, 2011; de Marco *et al.*, 2014).

In absence of hyperosmotic stress, larvae in which Galn$^+$ neurons were ablated did not show any impairment in the spontaneous locomotion compared to control siblings (Figure 17B). This result indicates that the ablation of Galn$^+$ neurons did not cause any significant motor deficit. On the other hand, Galn$^+$ neurons-ablated larvae showed increased responsiveness to the administration of the hypertonic solution compared to controls. Such hyperactive phenotype of Galn$^+$ neurons-ablated larvae is indicated by the increase in their motility ratio, which was measured as the ratio between the distance moved by each fish after and before stress (Figure 17C).

Furthermore, chemo-genetic ablation of Galn$^+$ neurons led to an increase in whole-body cortisol levels after exposure to the hypertonic solution (Figure 17D), suggesting that the hyperactivity phenotype of Galn$^+$ neurons-ablated larvae is linked to an increased activity of the HPI stress axis.

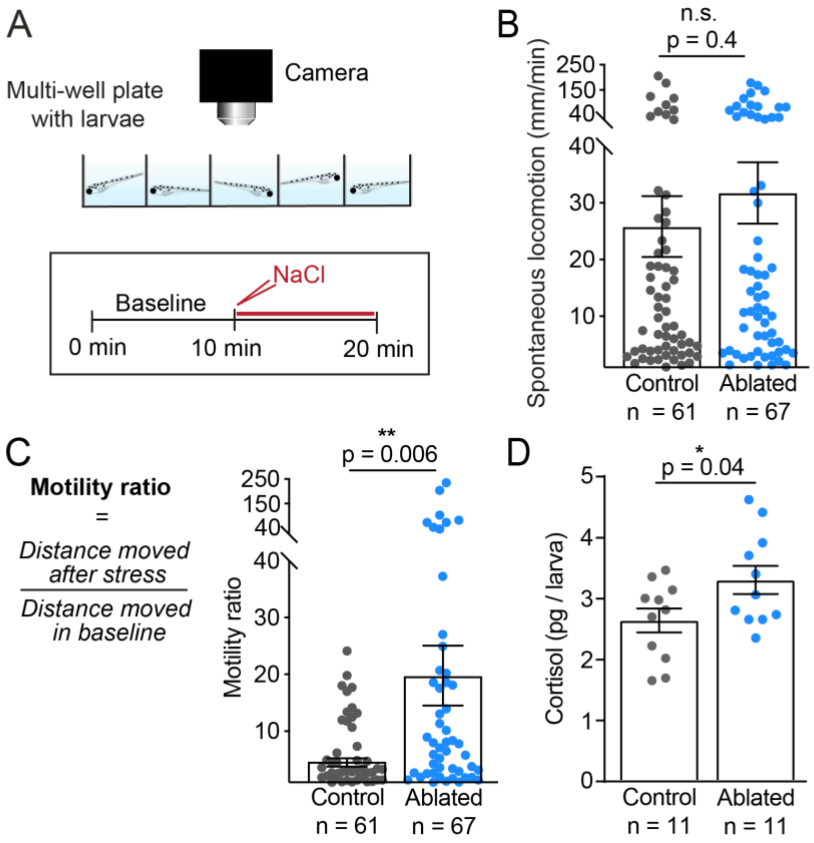

Figure 17: Hyperosmotic-behavioral assay and cortisol levels in Galn$^+$-neurons ablated larvae. **(A).** Scheme of the experimental setup and timeline of application of the hypertonic solution. Larvae were recorded for 10 minutes before and after administration of a 200 mM NaCl solution to obtain a final concentration of 100 mM NaCl. **(B).** Graph showing average spontaneous locomotion in 5 dpf larvae with (control) or without (ablated) Galn$^+$ neurons. **(C).** Formula used for calculating motility ratio and average motility ratio in control and ablated larvae after application of the hypertonic solution. **(D).** Graph displaying average whole-body cortisol level in 5 dpf control and Galn$^+$-neurons-ablated larvae after exposure to the hypertonic solution for 10 minutes. Data are shown as mean ± SEM. In (B) and (C) n indicates the number of larvae used for the experiment, while in (D) it indicates the number of biological replicates obtained by pooling 20 – 25 larvae. * $p < 0.05$, ** $p < 0.01$, n.s. = not significant, two-tailed t-test.

5.3.2 Ablation of Galn$^+$ neurons leads to increased anxiety-like states

To assess whether Galn$^+$ neurons mediate behavioral responses to different types of threats or exclusively to the hypertonic solution, I exposed Galn$^+$ neurons-ablated and control larvae to a sudden loud noise, which elicits an acoustic startle response (ASR) (Orger *et al.*, 2004). The ASR is an autonomous reflex consisting of a fast unilateral C-bend of the tail that allows the fish to escape threats and was previously shown to correlate with stress and anxiety states

(Grillon and Baas, 2003; Ray *et al.*, 2009; Griffiths *et al.*, 2012). Galn^{+} neurons-ablated larvae displayed elevated ASR probability (Figure 18A), suggesting the role of Galn^{+} neurons in modulating behavioral responses to different types of stressful stimuli.

To investigate whether ablation of Galn^{+} neurons leads to an increased stress state in absence of any aversive stimulus, I assessed the thigmotactic behavior of zebrafish larvae upon Galn^{+} neuronal ablation. Thigmotaxis is the natural tendency of an animal to spend more time on the edges of an open area to avoid exposure to predators and has been used as an indicator of anxiety in zebrafish (Champagne et al., 2010; Colwill and Creton, 2011). Galn^{+} neurons-ablated larvae spent significantly more time at the edges of the well plate, indicating an increased anxiety-related state compared to the control not-ablated siblings (Figure 18B).

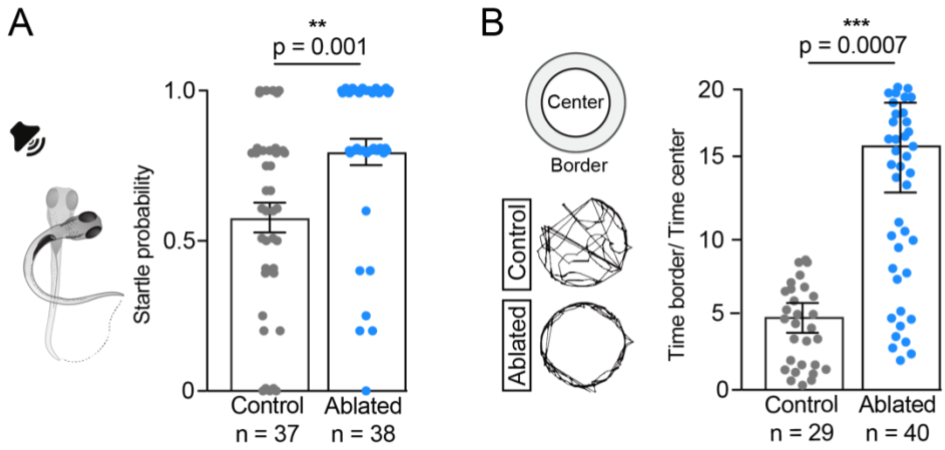

Figure 18: Startle response and thigmotactic behavior in Galn^{+}-neurons ablated larvae. (A). Drawing representing the typical startle response induced by a loud noise in young zebrafish larvae. On the right, the graph shows the average probability of the ASR response calculated in 5 dpf larvae with (control) or without (ablated) Galn^{+} neurons. **(B).** Example of the tracking of the movements of a zebrafish larvae in which Galn^{+} neurons were ablated and a control sibling and the subdivision of the well into center and border used for the analysis. On the right, the graph shows the average time spent by 5 dpf control and ablated larvae in the border of the well compared to the center. n indicates the number of larvae used for the experiment. ** $p < 0.01$, *** $p < 0.01$, two-tailed t-test.

5.3.3 PoA-Galn$^+$ neurons are required for behavioral responses to stress

Although these results point out the importance of Galn$^+$ neurons in the modulation of stress-related behaviors, the use of the NTR-mediated chemogenetic approach leads to the ablation of all the Galn-producing cells, both in the PoA and in the pHyp. The main population of Galn$^+$ neurons increasing its activity upon stressful stimuli resides in the PoA, as indicated by Ca^{2+} imaging and pERK data (see Figures 8, 10, and 12). To test whether this population alone is required to modulate behavioral responses to stress, I utilized a two-photon laser (λ = 880 nm) to ablate Galn$^+$ neurons in the PoA of agar-embedded 4 dpf *galn:Gal4; UAS:EGFP* larvae (Figure 19A). I left the fish recovering from the potential stress caused by the procedure for 24 hours and then I measured the locomotor activity before and after exposure to the hypertonic solution, as described earlier. Zebrafish larvae in which PoA-Galn$^+$ neurons were ablated displayed increased responsiveness to the administration of the hypertonic solution (Figure 19C), similar to the result obtained using the chemogenetic approach (see Figure 17C). General motor deficits could not cause this hyperactivity phenotype as the spontaneous locomotion did not differ between Galn$^+$-neurons ablated larvae and control siblings (Figure 19B).

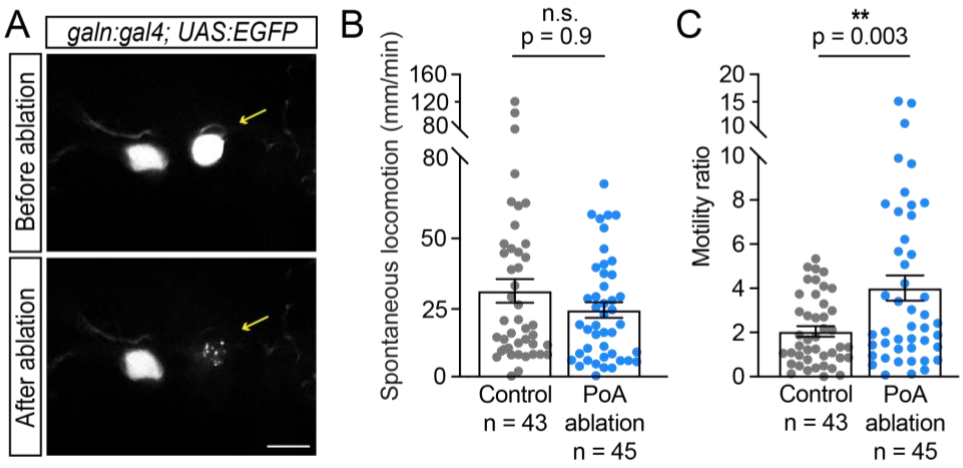

Figure 19: Hyperosmotic-behavioral assay after ablation of PoA-Galn$^+$ neurons. (A). Images exemplifying the targeted two-photon-laser-mediated ablation of a Galn$^+$ neuron (arrow). Scale bar = 10 µm. **(B, C)**. Graphs showing spontaneous locomotor activity (B) and average motility ratio upon hyperosmotic stress (C) in two-photon- laser-ablated larvae (PoA ablation) and not ablated control siblings. Data are shown as mean ± SEM. n = number of larvae. ** $p < 0.01$, n.s. = not significant, two-tailed t-test.

The hyperactivity phenotype displayed by PoA-Galn^{+}-neurons ablated larvae resembled the behavior observed after the chemo-genetic ablation of the Galn^{+} neurons. This result strongly suggests that the neuronal population residing in the PoA participates in the modulation of behavioral responses to stress.

To further confirm the role of PoA-Galn^{+} neurons in the modulation of stress responses, I repeated the two-photon laser procedure targeting only the population in the pHyp. As most pHyp-Galn^{+} neurons reside in the most ventral part of the hypothalamus (see Figure 7A), I could not efficiently perform the ablation without damaging the brain regions above the pHyp and thus I could not assess the behavioral consequences of the ablation of this neuronal population.

5.3.4 Lack of Galn decreases behavioral responses to stress

The increased responsiveness to stressful stimuli in larvae in which Galn^{+} neurons were ablated and the increased cortisol levels suggested that this neuronal population inhibits the activation of the HPI axis, possibly acting on downstream excitatory neurons. Galn peptide has inhibitory effects on neuronal activity (Zini *et al.*, 1993; Pieribone *et al.*, 1995; Kinney, Emmerson and Miller, 1998; Kozoriz *et al.*, 2006) and has been implicated in stress-related psychiatric conditions (Wrenn and Holmes, 2006; Tillage *et al.*, 2020; Rachel P Tillage *et al.*, 2021). Thus, we hypothesized that Galn might be the neuromodulator secreted by Galn^{+} neurons to mediate their function on stress-related responses.

To test this hypothesis, I used the CRISPR/Cas9 technique to generate a *galn* mutant (*galn*^{md76}) that harbors an 11 base pair deletion in the exon 3 of *galn* gene, leading to a frameshift mutation in the amino acids sequence and the creation of a premature stop codon (Figures 20A and B). The mutated *galn*^{md76} allele is predicted to encode two truncated isoforms of Galn missing most of the mature peptide, including the Galn receptor binding site. Immunostaining with an anti-Galn antibody confirmed the absence of the mature Galn peptide in *galn*$^{md76/md76}$ larvae (Figure 20C).

To assess the effect of lack of Galn on stress-related behaviors, I measured the locomotor activity of 5 dpf *galn*^{md76} mutants and wild-type larvae in response to hyperosmotic stress. Spontaneous locomotion was not altered in *galn*$^{+/md76}$ and *galn*$^{md76/md76}$ fish (Figure 20D), indicating that the mutation does not cause generalized motor deficits. In contrast,

homozygous *galn*$^{md76/md76}$ mutant larvae displayed a reduced motility ratio in response to the administration of NaCl compared to *galn*$^{+/+}$ and *galn*$^{+/md76}$ siblings (Figure 20E). This result indicates that Galn is required for proper behavioral response to hyperosmotic stress. However, the decreased activity observed in homozygous *galn*$^{md76/md76}$ mutants is opposite to the hyperactivity phenotype detected in Galn^{+}-ablated larvae (see Figures 17-19).

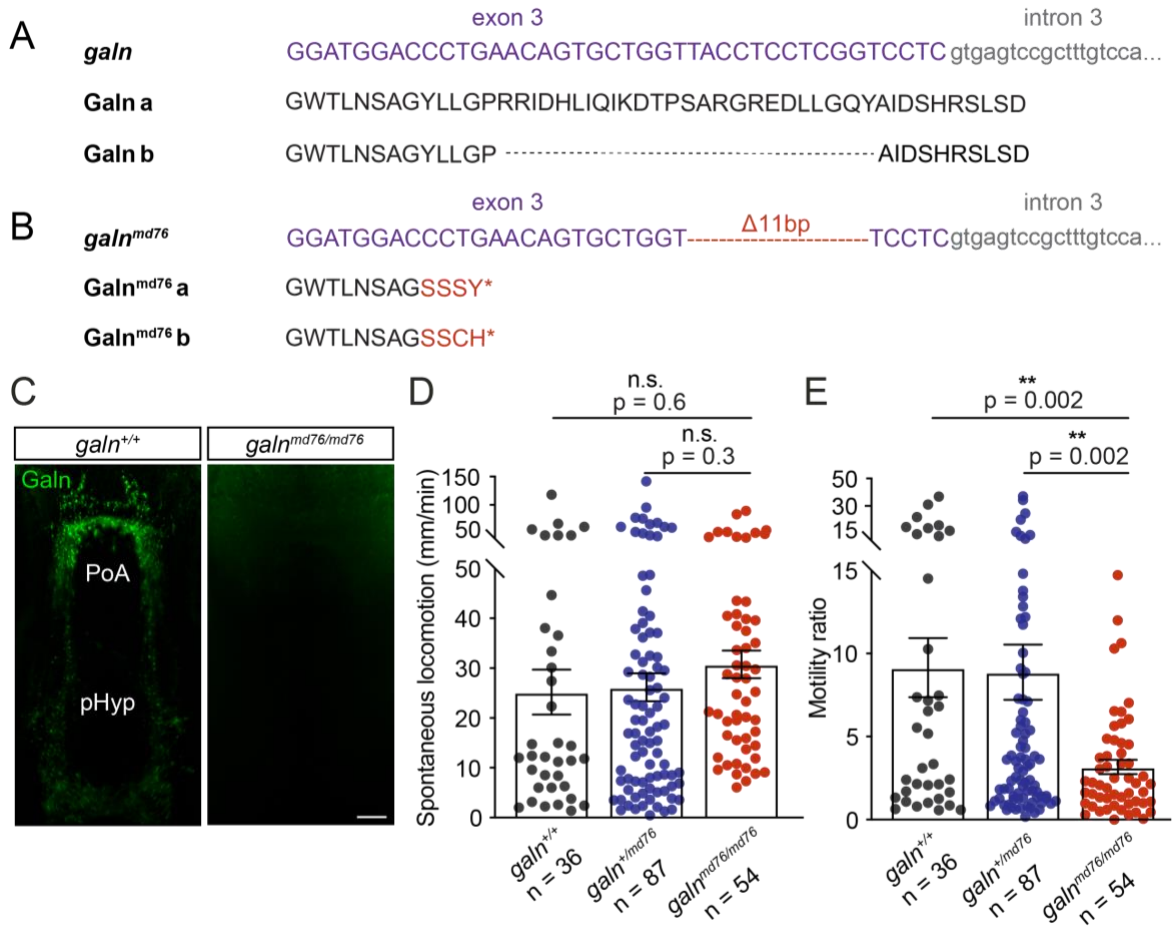

Figure 20: Hyperosmotic-behavioral assay in mutant *galn*^{md76} larvae lacking Galn. (A). Scheme of part of the exon 3 and intron 3 of the wild-type *galn* gene used to design the CRISPR/Cas9 mutagenesis strategy. In wild-type fish, the *galn* gene undergoes alternative splicing, resulting in two Galn isoforms, Galn a and Galn b. **(B)**. Scheme of the mutated *galn*^{md76} allele harboring a deletion of 11 base pairs (bp). The mutated sequence is predicted to encode two truncated isoforms of Galn, lacking the region required for Galn receptors-binding. Red letters indicate the mutated amino acids and the premature stop codon (*). **(C).** Immunostaining with an anti-Galn antibody showing lack of mature Galn peptide in 5 dpf *galn*$^{md76/md76}$ larvae compared to wild-type *galn*$^{+/+}$ siblings. Scale bar = 25 µm. **(D, E)**. Graphs showing average spontaneous locomotion (D) and motility ratio (E) after application of the hypertonic solution in 5 dpf *galn*$^{+/+}$, *galn*$^{+/md76}$, and *galn*$^{md76/md76}$ larvae. Data are shown as mean ± SEM. n = number of larvae. **p < 0.01, n.s. = not significant, two-tailed t-test.

5.3.5 Overexpression of *galn* enhances behavioral responses to stress

Taken together, the data obtained so far indicated that the absence of the Galn and ablation of Galn$^+$ neurons have different effects on stress-related behavioral responses. To understand whether the opposites phenotypes are due to a modulatory effect of Galn on Galn$^+$ neurons, I overexpressed *galn* specifically in Galn$^+$ neurons. To overcome the relatively long time required to generate a stable transgenic line, I cloned and injected a construct containing *UAS:galn-T2A-tdTomato-CAAX* sequence in *galn:Gal4* embryos at single-cell-stage and measured their stress-related behavioral response at 5 dpf. Expression of the construct was verified by tdTomato fluorescence signal (Figure 21A), and the presence of the self-cleaving T2A peptide ensured that the structure of Galn was not disrupted and thus its ability to bind to GPCRs.

Spontaneous locomotion was similar between larvae overexpressing *galn* and control siblings injected with the *UAS:galn-T2A-tdTomato-CAAX* construct but lacking the *galn:Gal4* transgene (Figure 21B). In the hyperosmotic behavioral assay, *galn* overexpression led to an increase in the motility ratio after exposure to the 100 mM NaCl solution (Figure 21C), indicative of an elevated stress state.

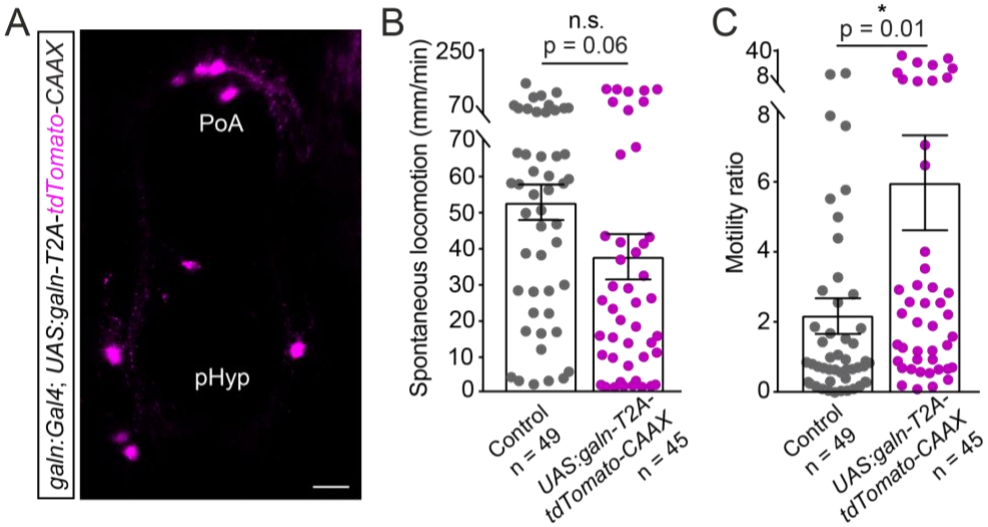

Figure 21: Hyperosmotic-behavioral assay in larvae overexpressing *galn*. (A). Image showing tdTomato expression in 5 dpf *galn:Gal4* larvae injected with *UAS:galn-T2A-tdTomato-CAAX*. **(B, C).** Graphs showing spontaneous locomotion (B) and motility ratio (C) after application of the hypertonic solution in 5 dpf *galn:gal4* larvae expressing tdTomato and control larvae injected with the construct but lacking *galn:gal4* transgene. Data are shown as mean ± SEM. n = number of larvae. *p < 0.05, n.s. = not significant, two-tailed t-test.

This result is in line with the phenotype of *galn*$^{md76/md76}$ mutants, in which the lack of Galn resulted in decreased motility in response to the hypertonic solution (see Figure 20E) and further indicates that Galn plays an important role in modulating behavioral responses to stress. However, these data contradict the hyperactive phenotype of Galn^{+} neurons-ablated larvae (see Figures 17-19), suggesting that Galn^{+} neurons most likely release another neuromodulator that mediates their inhibitory effect on stress-related responses.

5.4 Molecular mechanisms underlying the function of Galn^{+} neurons

5.4.1 An autocrine inhibitory model explains Galn and Galn^{+} neurons effect on stress-related behaviors

Since in mice hypothalamic GAL^{+} neurons co-release GAL and the inhibitory neurotransmitter GABA (Wu *et al.*, 2014), the neurotransmitter phenotype might be conserved in the zebrafish PoA-Galn^{+} neurons. In addition, in noradrenergic LC neurons, GAL was shown to affect neuronal activity binding to autoreceptors in GAL^{+} neurons (Wrenn and Holmes, 2006; Tillage *et al.*, 2020; Rachel P Tillage *et al.*, 2021). These previous studies led us to hypothesize that Galn peptide might negatively modulate the activity of Galn^{+} neurons in the PoA, thus affecting the release of GABA and ultimately the stress axis activation (Figure 22A).

The existence of a such autocrine inhibitory mechanism mediated by Galn would explain the stress-related phenotypes observed in this study. Indeed, in absence of the inhibitory effect of Galn in *galn*$^{md76/md76}$ fish, Galn^{+} neurons would increase their activity and thus inhibit downstream stress-promoting neurons through GABA. This would result in a decreased activation of the HPI axis and reduced behavioral responses to stress (Figure 22B). On the other hand, overexpression of *galn* in Galn^{+} neurons would enhance the inhibitory effect of Galn, causing a decreased activation of Galn^{+} neurons. This would cause increased activation of downstream excitatory neurons and increased responsiveness to stress (Figure 22C). Finally, in Galn^{+} neurons-ablated larvae, the absence of Galn^{+} neurons and their inhibitory GABAergic projections to downstream stress-promoting neurons would cause overactivation of the stress axis and a hyperactivity phenotype (Figure 22D).

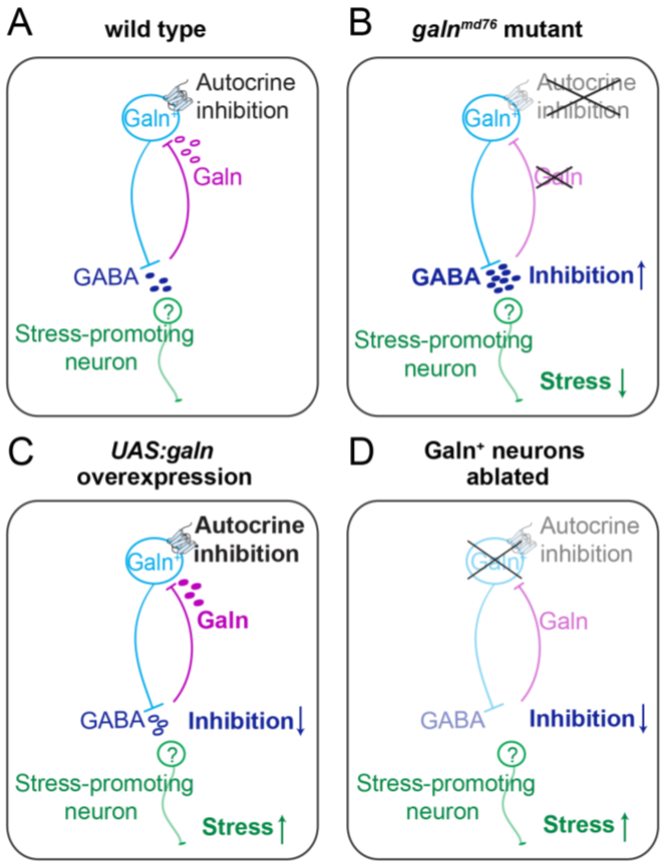

Figure 22: Hypothesized actions of Galn$^+$ neurons and Galn on stress. (A). Galn$^+$ neurons send GABAergic inhibitory inputs to a population of stress-promoting neurons. Release of Galn, which binds to autoreceptors on Galn$^+$ neurons, reduces their activity. **(B).** In *galn*$^{md76/md76}$ larvae, Galn is absent and cannot negatively modulate the activity of Galn$^+$ cells. Thus, Galn$^+$ neurons release more GABA to an unidentified downstream neuronal population, ultimately resulting in decreased stress responses. **(C).** In larvae overexpressing *galn,* the autocrine inhibition is enhanced, resulting in decreased GABA release and increased stress state. **(D).** In Galn$^+$ neurons-ablated larvae the absence of GABA inputs to downstream neurons leads to an increased stress state.

5.4.2 Galn$^+$ neurons in the PoA are GABAergic and express Galn receptors

To validate the existence of such autocrine inhibitory mechanism, I first investigated whether zebrafish PoA-Galn$^+$ neurons are GABAergic. To this end, I used fluorescent *in situ* hybridization HCR (Choi *et al.*, 2018) to label the transcripts of the gene *glutamate decarboxylase 2* (*gad2*), encoding an enzyme required for the synthesis of GABA. As shown in Figure 23A, in the PoA of 5 dpf *galn:Gal4; UAS:EGFP* the majority of Galn$^+$ neurons are GABAergic, as 95% of them co-localized with *gad2*.

Next, I performed *in situ* HCR in 5 dpf *galn:Gal4; UAS:EGFP* larvae to assess whether Galn receptors are expressed in Galn$^+$ cells. As shown in Figures 23B and C, PoA-Galn$^+$ neurons co-localize with *galnR1a, galnR1b,* and *galnR2b* transcripts, while I did not observe *galnR2a* expression in Galn$^+$ cells. The findings that PoA-Galn$^+$ neurons are GABAergic and *galnRs* are expressed on Galn$^+$ neurons, reinforced the possibility that Galn might have an autocrine effect on Galn$^+$ neurons, modulating their inhibitory functions on stress.

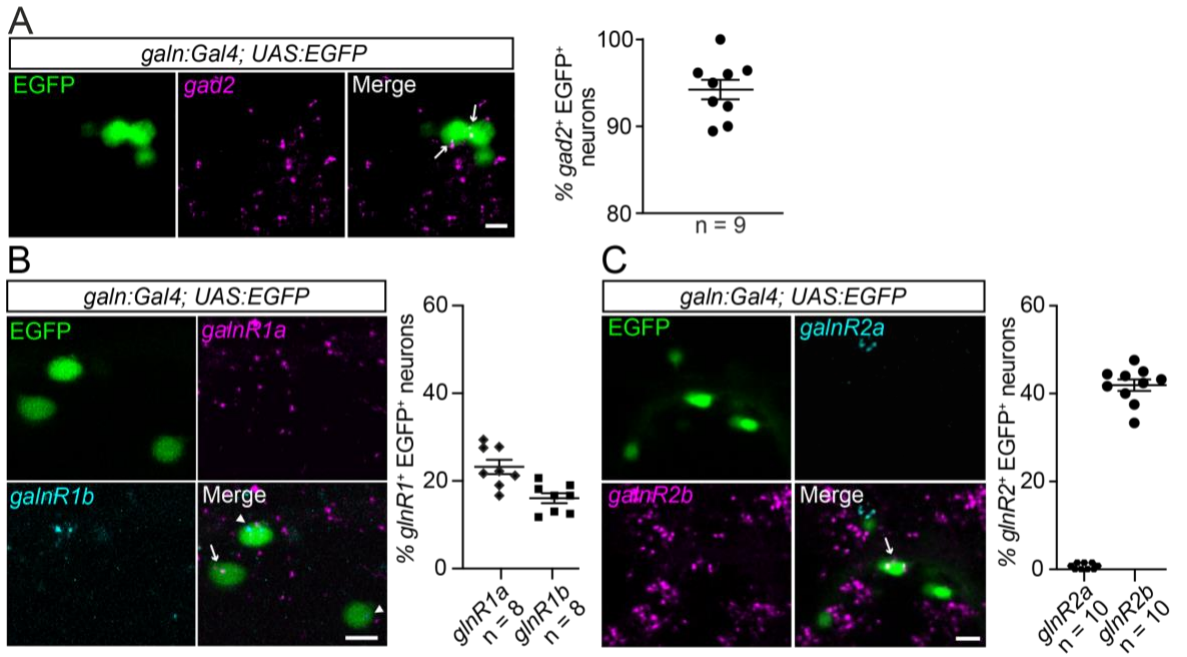

Figure 23: Co-localization of *gad2* and *galnRs* transcripts in PoA-Galn$^+$ neurons. (A). (left) Images showing localization of *gad2* transcripts (magenta) in PoA-Galn$^+$ neurons of a 5 dpf *galn:Gal4; UAS:EGFP* larva. The arrows indicate co-localization. (right) Percentages of Galn$^+$ neurons expressing *gad2* mRNA. **(B).** (left) Images of *galnR1A* (magenta) and *galnR1B* (cyan) transcripts. The arrow and arrowheads indicate localization of *galnR1A* and *galnR1B* mRNAs in Galn$^+$ neurons, respectively. (right) Percentages of Galn$^+$ neurons expressing *galnR1a* and *galnR1b*. **(C).** (left) Images showing *galnR2a* (cyan) and *galnR2b* (magenta). The arrow indicates *galnR2b* mRNA in a Galn$^+$ neuron. (right) Percentage of Galn$^+$ neurons expressing *galnR2b*. Data are shown as mean ± SEM. n indicates number of fish. Scale bars = 5 µm.

5.4.3 PoA-Galn$^+$ neurons are more active in absence of Galn

According to the hypothesized autocrine inhibitory mechanism, Galn peptide has an inhibitory effect on the activity of Galn$^+$ neurons. Consequently, the absence of Galn in *galn$^{md76/md76}$* larvae should cause increased activation of Galn$^+$ neurons. To test whether this is the case, I performed Ca^{2+} imaging of PoA-Galn$^+$ neurons in 5 dpf *galn:Gal4; UAS:GCaMP6s; galn$^{md76/md76}$* larvae and *galn$^{+/+}$* siblings during hyperosmotic stress.

Lack of Galn did not alter substantially the percentages of response categories of Galn$^+$ neurons in *galn$^{md76/md76}$* larvae compared to *galn$^{+/+}$* wild-type siblings (Figure 24A). On the other hand, in homozygous mutants *galn$^{md76/md76}$* larvae, Galn$^+$ neurons categorized as "increased response" type displayed a significant increase in the frequency of Ca^{2+} events both during the baseline recording and after administration of the hypertonic solution (Figure

24B). In contrast, the activity of Galn^{+} neurons classified as "decreased activity" was not significantly altered in *galn$^{md76/md76}$* larvae (Figure 24C), indicating that this subpopulation of neurons is not affected by the lack of Galn. These results not only confirmed the hypothesis that Galn has an inhibitory effect on the activity of PoA-Galn^{+} neurons, but also indicated that the modulatory function of Galn is specific to the "increased activity" PoA-population.

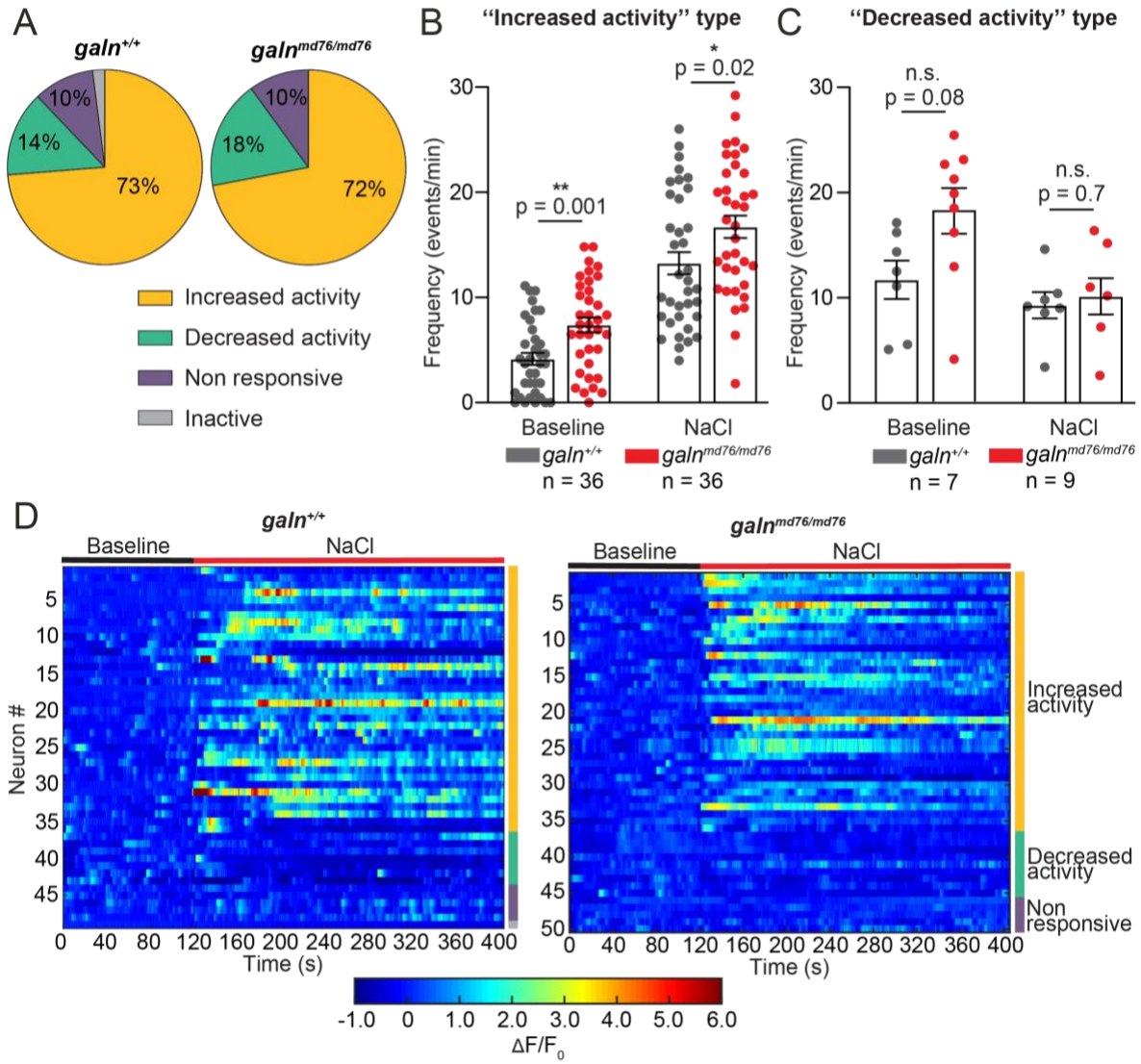

Figure 24: Ca^{2+} imaging of PoA-Galn^{+} neurons in *galn$^{md76/md76}$* mutants during hyperosmotic stress. (A). Pie charts showing percentages of response categories of PoA-Galn^{+} neurons in 5 dpf *galn:Gal4; UAS:GCaMP6s; galn$^{+/+}$* and *galn$^{md76/md76}$* larvae. **(B, C).** Bar graphs displaying frequency of Ca^{2+} events of Galn^{+} neurons "increased activity" (B) and "decreased activity (C) types in *galn$^{+/+}$* and *galn$^{md76/md76}$* larvae. **(D).** Raster plots showing $\Delta F/F_0$ values of PoA-Galn^{+} neurons in *galn$^{+/+}$* and *galn$^{md76/md76}$* larvae. Data in the bar graphs are shown as mean ± SEM. n indicates number of neurons. * $p < 0.05$, ** $p < 0.001$, n.s. = not significant, two-tailed t-test.

5.4.4 Overexpression of *galn* reduces the activity of Galn^{+} neurons

To further prove the inhibitory effect of Galn on Galn^{+} neurons, I analyzed the neuronal activity of PoA-Galn^{+} neurons in 5 dpf *galn:Gal4; UAS:GCaMP6s* embryos injected at one-cell stage with the construct containing the *UAS:galn-T2A-tdTomato-CAAX* sequence. According to the proposed autocrine inhibitory mechanism, Galn^{+} neurons overexpressing Galn should display a decrease in their activity. This would ultimately lead to the hyperactivity phenotype observed in the hyperosmotic-behavioral assay.

The percentages of the four response profile categories of neurons were similar in fish overexpressing *galn* and control siblings injected with a *UAS:tdTomato-CAAX* construct (Figure 25A).

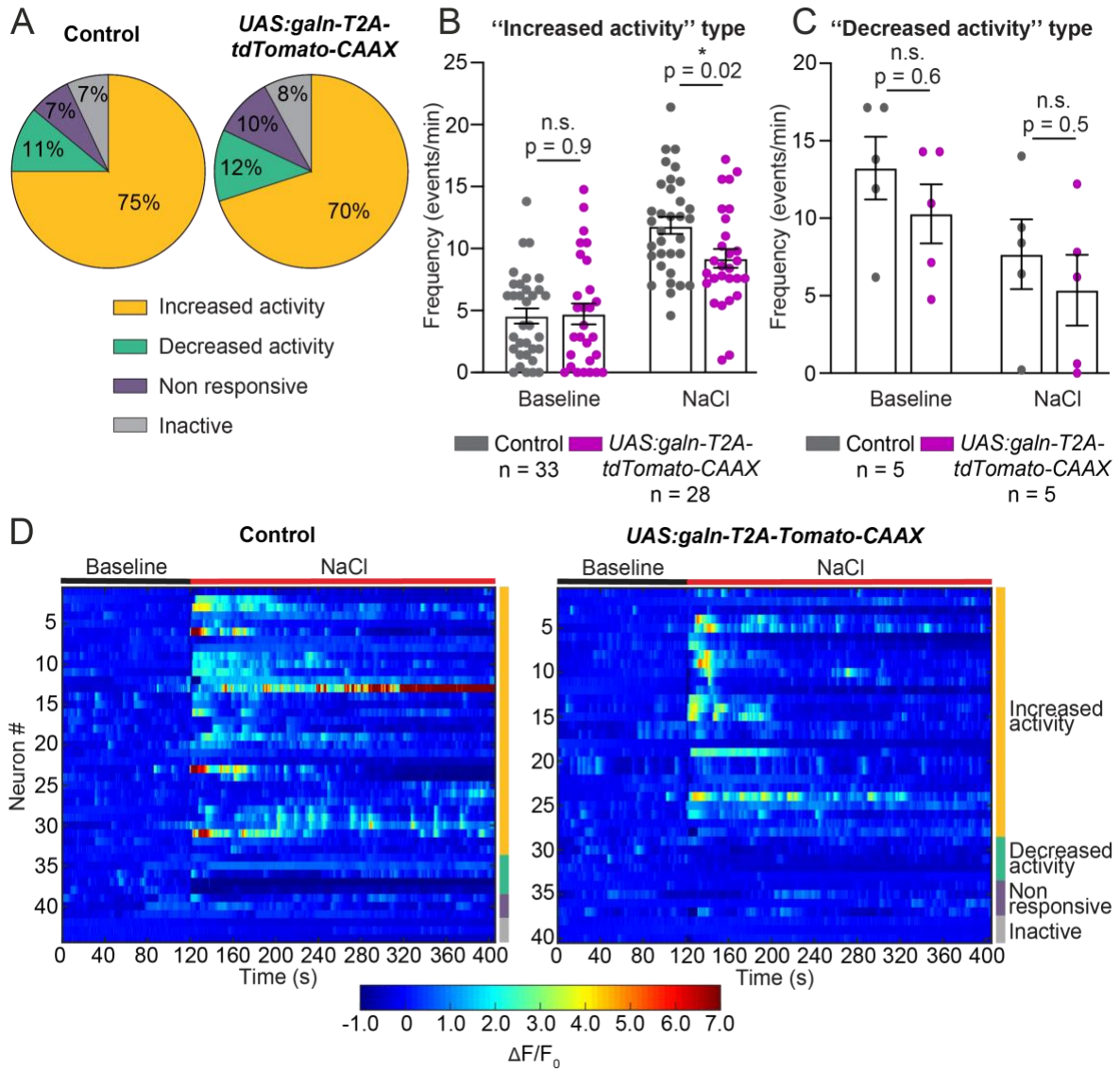

Figure 25: (from previous page): Ca^{2+} imaging of PoA-$Galn^{+}$ neurons overexpressing *galn* during hyperosmotic stress. (A). Pie charts showing percentages of PoA-$Galn^{+}$ neurons in 5 dpf *galn:Gal4; UAS:GCaMP6s* larvae injected with the control construct *UAS:tdTomato-CAAX* or the *UAS:galn-T2A-tdTomato-CAAX* plasmid. **(B, C).** Graphs showing frequency of Ca^{2+} events in the "increased activity" (B) and "decreased activity" (C) types of PoA-$Galn^{+}$ neurons in larvae overexpressing *galn* (*UAS:galn-T2A-tdTomato-CAAX*) or siblings injected with the control plasmid. **(D).** Raster plots showing $\Delta F/F_0$ values of PoA-$Galn^{+}$ neurons in the PoA in larvae overexpressing *galn* (*UAS:galn-T2A-tdTomato-CAAX*) or siblings injected with the control plasmid. Data in (B) and (C) are shown as mean ± SEM. n indicates number of neurons. *$p < 0.05$, n.s. = not significant, two-tailed t-test.

As expected, *galn* overexpression in $Galn^{+}$ cells reduced the frequency of Ca^{2+} events of "increased activity" neurons after application of the hypertonic solution (Figure 25B), while the activity of the neurons categorized as "decreased activity" was unchanged (Figure 25C). These results mirror the changes in neuronal activity detected in $galn^{md76/md76}$ mutant larvae (see Figure 24) and constitute a further confirmation that Galn inhibits the "increased activity" subpopulation of $Galn^{+}$ neurons, which in turn modulate stress-related responses likely through GABA.

5.5 Stress-promoting neuronal populations affected by $Galn^{+}$ neurons

5.5.1 Activation of $Galn^{+}$ neurons correlates with a decreased activity of Crh^{+} neurons

The results reported so far indicate that $Galn^{+}$ neurons negatively modulate stress-related responses, possibly sending GABAergic inputs to a downstream unidentified neuronal population that activates the HPI axis. As Crh^{+} neurons in the PoA of zebrafish are known to be the main activators of the stress response (vom Berg-Maurer *et al.*, 2016), we hypothesized that their activity might be directly or indirectly affected by PoA-$Galn^{+}$ neurons.

To measure Crh^{+} and $Galn^{+}$ neuronal responses during stress, I first tried to generate a *chrb:Gal4* transgenic line to genetically label Crh^{+} neurons. Unfortunately, no labeled cells were observed in the PoA (data not shown). Likewise, injecting a *chrb:EGFP* plasmid led to the same issue, most probably due to the low transgene expression driven by the *crhb* regulatory sequence used to generate the constructs. To overcome this technical impediment and record the activity of PoA-Crh^{+} neurons in the absence of any specific marker, we decided to use *galn:Gal4; UAS:NTR-mCherry; elavl3:H2B-GCaMP6s* larvae in which the

regulatory region of *elavl3,* a pan-neuronal marker (Park *et al.*, 2000), drives nuclear expression of GCaMP in the whole-brain. To perform these experiments, we collaborated with Prof. Marco dal Maschio and PhD candidate Matteo Bruzzone from the University of Padua. They performed multiplane Ca^{2+} imaging using a multiphoton system equipped with an Electro-Tunable Lens, which enabled the recording of the neuronal activity of the entire PoA during the administration of the hypertonic solution (Figure 26). To identify after the Ca^{2+} imaging which $GCaMP^{+}$ cell corresponded to a Crh^{+} neuron, I performed *in situ* HCR labeling *crhb* transcripts on the same larvae used for the *live* imaging experiment (Figure 26). Next, I imaged the PoA of the stained larvae acquiring both *crhb* and GCaMP fluorescent signals. Using a pipeline similar to the MultiMAP method (Lovett-Barron et al., 2017), Prof. M. dal Maschio and M. Bruzzone aligned the confocal stacks of the fixed samples and those obtained during live imaging (Figure 26) and analyzed the activity of *crhb*$^{+}$/$GCaMP^{+}$ cells and $Galn^{+}$/ $GCaMP^{+}$ neurons, which were identifiable by mCherry expression.

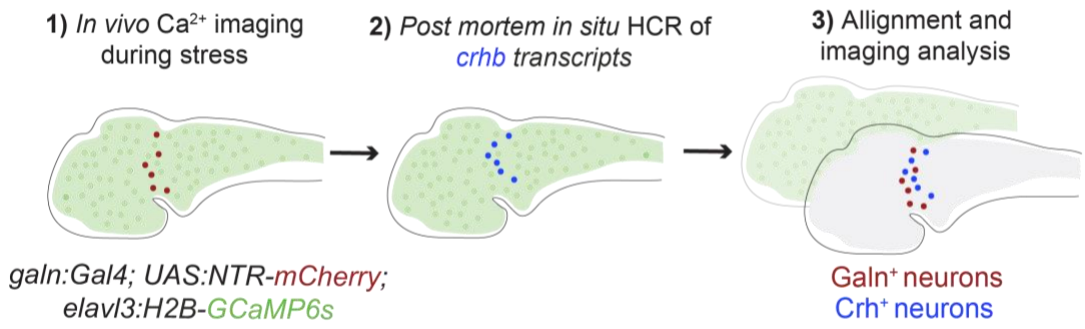

Figure 26: Scheme of the experimental approach used to investigate the correlation between the activity of $Galn^{+}$ neurons and Crh^{+} neurons. 1) The neurons in the PoA of 5 dpf *galn:Gal4; UAS:NTR-mCherry; elavl3:H2B-GCaMP6s* larvae were imaged before and during hyperosmotic stress. 2) *Post mortem in situ* HCR was used to identify Crh^{+} neurons. 3) Confocal stack images of the stained larvae were aligned with those acquired during the Ca^{2+} imaging recording to analyze the neuronal activity of Crh^{+} and $Galn^{+}$ neurons in the PoA.

Most Crh^{+} neurons increased or decreased their activity after administration of 100 mM NaCl solution (Figure 27A) and were classified according to the comparison between the number of Ca^{2+} events before and during hyperosmotic stress, as previously described for $Galn^{+}$ neurons (see section 5.2.3). Since the results obtained so far indicated that PoA-$Galn^{+}$ neurons of the "increased activity" type are activated during stress and inhibit their downstream targets, we analyzed the correlation between $Galn^{+}$ neurons of the "increased

activity" and Crh$^+$ neurons of the "decrease activity" types. The two populations initially showed a similar response to the administration of the hypertonic solution, as indicated by the positive value in the cross-correlation analysis (Figure 27B). Importantly, this trend was reversed once the Galn$^+$ neurons reached their peak activity, with a correlation coefficient turning to negative values (Figure 27B). This analysis shows that Crh$^+$ neurons decrease their activity once Galn$^+$ neurons are activated, supporting the hypothesis that Galn$^+$ neurons have an inhibitory effect on Crh$^+$ neuronal activity.

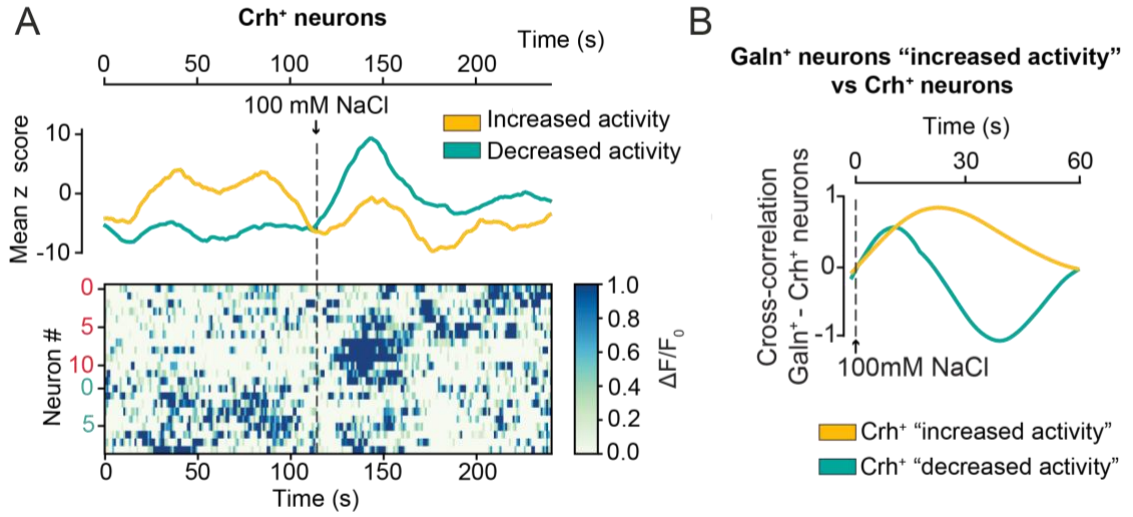

Figure 27: Correlation between increased activity Galn$^+$ neurons and Crh$^+$ neurons. (A). Graph showing mean activity (z score) of "increased activity" and "decreased activity" types of Crh$^+$ neurons before and after exposure to 100 mM NaCl. (Bottom) Raster plot displaying $\Delta F/F_0$ values of each Crh$^+$ neuron. **(B).** Cross-correlation analysis between "increased activity" type Galn$^+$ cells and Crh$^+$ neurons belonging to "increased activity" and "decreased activity" categories after exposure to 100 mM NaCl.

5.5.2 Galn$^+$ neurons negatively modulate Crh$^+$ cells activity in the PoA

The correlation between the activity of PoA-Crh$^+$ neurons and PoA-Galn$^+$ neurons suggested the existence of a functional connection between these two neuronal populations. To confirm this hypothesis, I analyzed the activity of Crh$^+$ neurons after chemo-genetic ablation of Galn$^+$ cells. I treated *galn:Gal4; UAS:NTR-mCherry* larvae and control siblings, lacking *galn:Gal4* cassette, with nifurpirinol for 48 hours. After hyperosmotic stress treatment, I performed *in situ* HCR to detect *crhb* mRNA and immunostaining for pERK and tERK to analyze Crh$^+$ neuronal activity (Figure 28A).

Ablation of Galn$^+$ cells resulted in increased activation of Crh$^+$ neurons after administration of both control and NaCl solution (Figures 28B and C), demonstrating a functional connection between the two populations. This result suggests that Galn$^+$ neurons are upstream modulators of Crh$^+$ neurons, negatively controlling their activation under both physiological and stress conditions. However, it cannot be excluded that Galn$^+$ neurons might affect the activity of a different neuronal population, which in turn modulates the activity of Crh$^+$ neurons.

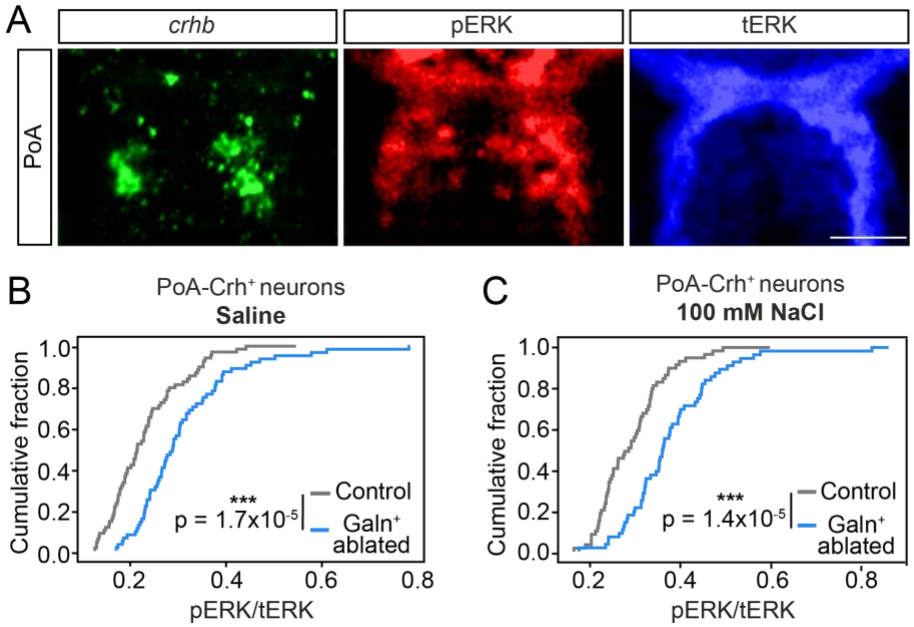

Figure 28: Activity of PoA-Crh$^+$ neurons after chemo-genetic ablation of Galn$^+$ neurons. (A). Images showing *in situ* HCR labeling *crhb* transcripts, pERK, and tERK staining in the PoA of a 5 dpf wild-type larva. Scale bar = 25 µm. **(B, C).** Cumulative fractions of pERK/tERK values in Crh$^+$ neurons in the PoA of 5 dpf Galn$^+$ neurons-ablated larvae and control siblings after exposure to a control solution (B) or 100 mM NaCl (C). In (B) $n_{control}$ = 70 neurons (11 larvae), $n_{ablated}$= 65 neurons (14 larvae). In (C) $n_{control}$= 60 neurons (11 larvae), $n_{ablated}$= 57 neurons (12 larvae). *** $p < 0.001$, two-sample Kolmogorov-Smirnov test.

6 Discussion

The perception and integration of stressful stimuli is followed by the activation of the HPA axis. Although this neuroendocrine pathway is essential to initiate physiological alterations in the brain and peripheral organs to allow proper responses to stressors, its activity must be continuously regulated. Chronic activation of the HPA axis can lead to several pathological conditions, including mental health disorders, such as anxiety and depression, and even cardiovascular diseases, early aging, immunosuppression, metabolic disorders, and many others (de Kloet, Joëls and Holsboer, 2005; Godoy *et al.*, 2018). In recent years, the incidence of stress-related diseases has dramatically increased, highlighting the risks of continuous exposure to stress and the urge to identify the underlying neuronal mechanisms.

The investigation of neuronal circuits modulating stress in rodent models is limited by several factors, including the absence of non-invasive techniques to access hypothalamic regions and the complexity of a brain that in mice contains approximately 70 million neurons. The transparent and small larval zebrafish brain, containing roughly 100 thousand cells, overcome these limitations and is now widely used for studying the neurobiology of stress. Importantly, the HPA axis is greatly conserved between teleosts and mammals and the hypothalamic region controlling its activation has a high level of similarity with the PoA of zebrafish (Herget and Ryu, 2015). As in mammals, Crh^{+} neurons are the main activator of the HPI axis and modulate cortisol secretion in zebrafish (vom Berg-Maurer *et al.*, 2016). However, the neuronal network and the molecular mechanisms rapidly modulating the activity of Crh^{+} neurons and the HPI axis during stress have not yet been identified.

The main aim of this study was to take advantage of zebrafish larvae to identify and eventually characterize the hypothalamic circuits modulating the activity of the HPI axis and behavioral responses to stress. Specifically, I investigated a population of hypothalamic cells secreting the peptide Galn. The function of Galn in zebrafish has been connected to sleep, epilepsy, and blood glucose regulation (Podlasz *et al.*, 2016, 2018; S. Chen *et al.*, 2017; Reichert, Pavón Arocas and Rihel, 2019) but no previous studies have characterized the neuronal populations secreting the peptide. In rodents, hypothalamic $Galn^{+}$ neurons were reported to regulate parental behavior and food reward (Wu *et al.*, 2014; Qualls-Creekmore *et al.*, 2017; Kohl *et al.*, 2018). However, the role of this neuronal population in modulating stress-related mechanisms has never been investigated, either in zebrafish or mammals.

In this work, I described for the first time how Galn$^+$ neurons in the hypothalamus of zebrafish respond to stressful stimuli. Most Galn$^+$ neurons in the PoA were activated in response to different types of acute stress, in agreement with previous studies showing that the PoA of zebrafish brain is an important region for processing stress-inducing stimuli (de Marco *et al.*, 2016; vom Berg-Maurer *et al.*, 2016; Lovett-Barron *et al.*, 2020). I further characterized these neurons and showed that Galn$^+$ neurons in the PoA are GABAergic, as in mice (Qualls-Creekmore *et al.*, 2017), indicating co-transmission of Galn and GABA in this neuronal population. The results reported in this study also reveal that Galn$^+$ neurons negatively modulate stress-related behavioral responses, as ablation of this neuronal population led to an over-responsiveness to acute stressors. In addition, the increased activation of Crh$^+$ neurons upon ablation of Galn$^+$ neurons indicates that these two neuronal populations are functionally connected. Finally, I investigated the function of Galn within this hypothalamic circuit. Previous *in vitro* studies showed that Galn is an inhibitory peptide and diminishes neuronal activity in LC neurons (Picciotto et al., 2010; Hökfelt et al., 2018), but its actions in the hypothalamus *in vivo* during stress have never been revealed. This work suggests that Galn inhibits the activity of hypothalamic Galn$^+$ neurons, most likely by binding to autoreceptors, and thus affects the activity of the HPI axis. It is likely that the inhibitory effect of Galn on Galn$^+$ neurons serves to modulate the release of GABA to downstream Crh$^+$ neurons or another intermediate cell-population. According to this hypothesis, the increased neuronal activity of Galn$^+$ cells observed in *galn* mutants led to an enhanced release of GABA from Galn$^+$ neurons and an over-inhibitory effect on stress-related responses. On the other hand, overexpression of *galn* in Galn$^+$ cells increased stress-related responses decreasing the activity of Galn$^+$ neurons and their inhibition on downstream neuronal cells.

Taken together, the results reported in this study suggest the existence of a novel hypothalamic circuit controlling neuroendocrine and behavioral responses to stress (Figure 29). Galn$^+$ neurons in the PoA inhibit directly or indirectly Crh$^+$ neurons to negatively modulate stress-related behavioral responses. In addition, the neuropeptide Galn has a modulatory function within this hypothalamic circuit, regulating the activation of Galn$^+$ neurons through an autocrine inhibitory mechanism, and thus affecting the inhibition of their downstream targets.

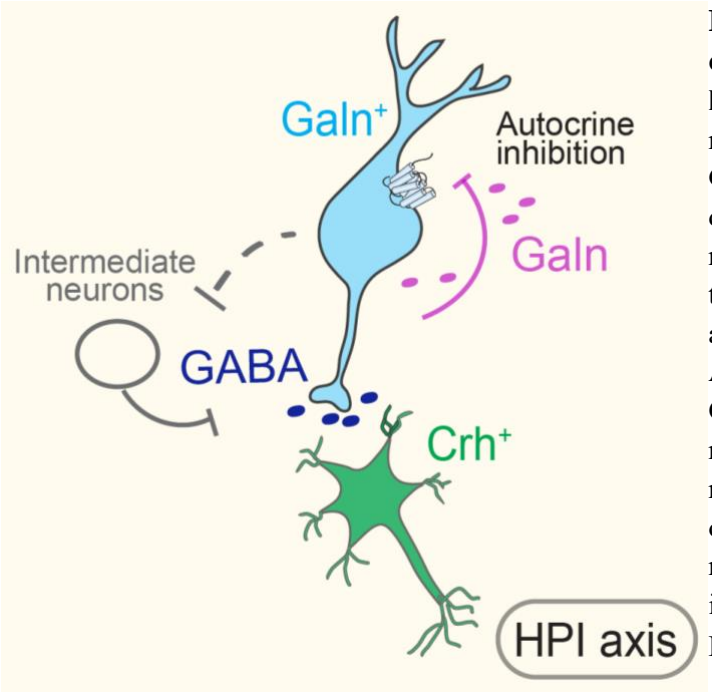

Figure 29: A novel hypothalamic circuit modulating stress in zebrafish larvae. Schematic drawing of the model that emerged from this study. Galn$^+$ neurons negatively modulate downstream stress-promoting Crh$^+$ neurons, possibly through GABAergic transmission, and thus influence the activation of the HPI axis. Alternatively, Galn$^+$ neurons modulate Crh$^+$ neurons through an intermediate neuronal population (dashed line). The neuropeptide Galn inhibits the activity of Galn$^+$ neurons through an autocrine mechanism, thus regulating the inhibition over Crh$^+$ neurons and the HPI axis.

6.1 Galn$^+$ neurons "increased activity" type is the main population modulating stress

Galn$^+$ neurons in the PoA responded to two different types of aversive stimuli: hyperosmotic stress and blue light. Further analysis revealed the presence of different subpopulations of PoA-Galn$^+$ neurons with different stress-induced response profiles. Most of them increased their activity in the presence of hyperosmotic stress and were the only category of Galn$^+$ cells affected by the lack of *galn* or its overexpression. These results indicate that this group of Galn$^+$ neurons is probably the main population acting on the proposed hypothalamic circuit modulating stress.

Why do Galn$^+$ cells increase their activity in response to a stressor? Most likely to allow activation of the stress axis. According to the results, Galn$^+$ neurons prevent the activation of the HPI axis inhibiting directly or indirectly the activity of Crh$^+$ cells. Once a stressor is perceived, this inhibitory control must be reduced to allow activation of Crh$^+$ neurons. Thus, Galn$^+$ neurons increase their activity and release Galn, which in turn inhibits the activity of Galn$^+$ neurons, resulting in a reduced inhibition over Crh$^+$ stress-promoting neurons. This hypothesis is supported by the general notion that neuropeptides are mostly secreted when neurons fire at high frequency, as after detection of a stressful stimulus (Nusbaum, Blitz and

Marder, 2017), which is indeed the type of response of this subpopulation of $Galn^+$ neurons to the administration of the hypertonic solution.

Is Galn being released by $Galn^+$ neurons of the "increased activity" type specifically in response to stress? The results indicate that there is a release of Galn also in basal conditions. Using Ca^{2+} imaging, I showed that in *galn* mutants the activity of $Galn^+$ neurons of the "increased activity" type is significantly higher during both stress and in the baseline recording, indicating that there is a basal release of Galn in absence of stressful stimuli. Ablation of $Galn^+$-cell caused increased activation of Crh^+ neurons, as indicated by their pERK/tERK values, both after administration of a control solution and after hyperosmotic stress. In addition, in the thigmotaxis assay, not involving any exposure to stressful stimuli, the larvae in which $Galn^+$ neurons were ablated displayed an increased anxiety-like state. All these results indicate that $Galn^+$ neurons of the "increased activity" type release Galn both during stress and in physiological states. The combined release of GABA and Galn probably provides a homeostatic balance over the activation and inhibition of Crh^+ neurons and of the HPI axis. Both in zebrafish and in mammals, the activation of Crh^+ neurons is regulated by circadian and ultradiurnal rhythmicity (Yeh, 2015; Julia K. Gjerstad, Lightman and Spiga, 2018). Consequently, there must be a continuous control over their activation and inhibition throughout the day. I hypothesize that $Galn^+$ neurons secrete both GABA and Galn in physiological states to maintain this balance over the HPI axis activity. Once a stressor is perceived, the increased firing of $Galn^+$ neurons results in an increased release of Galn, which reduces the activity of $Galn^+$ neurons to allow the activation of Crh^+ neurons in response to stress.

6.2 Are the other populations of PoA-$Galn^+$ neurons involved in stress?

The Ca^{2+} imaging analysis revealed the existence of subpopulations of PoA-$Galn^+$ neurons reducing their activity or not responding to the administration of the hypertonic solution. Unresponsive and inactive $Galn^+$ neurons are almost certainly not involved in stress mechanisms and might be involved in other types of behavior. In rodents, hypothalamic $Galn^+$ neurons affect parental behavior and food reward (Wu *et al.*, 2014; Qualls-Creekmore *et al.*, 2017; Kohl *et al.*, 2018) and in zebrafish Galn affects sleep (S. Chen *et al.*, 2017; Reichert, Pavón Arocas and Rihel, 2019). Given that zebrafish do not display parental behavior, I hypothesize that these $Galn^+$ cells might be involved in feeding and sleep

behaviors, which are known to be modulated by hypothalamic circuits and strongly influenced by peptidergic signaling (Corradi and Filosa, 2021).

Are PoA-Galn^{+} neurons decreasing their activity involved in the response to hyperosmotic stress? The role of this subpopulation in stress-related responses was not well characterized in this study. However, according to the results, it might be probable that these neurons are responding to the movement of the water caused by administration of the NaCl solution during Ca^{2+} imaging rather than the stress itself. Indeed, the percentages of Galn^{+} neurons falling within the decreased response category were similar after administration of a control or of a hypertonic solution. In addition, these neurons did not change their activity upon lack or overexpression of *galn*. It is also true that the larvae were embedded in agarose during the Ca^{2+} imaging experiment, which is surely a stressful condition for the animal and thus I cannot exclude that the "decreased activity" type Galn^{+} neurons are involved to some extent in the modulation of the HPI axis.

It is possible that the various subpopulations of PoA-Galn^{+} neurons, as the "non-responsive" or "decrease activity" types, are involved in other types of behaviors that can be affected by stress. In line with this view, Galn^{+} neurons would be part of a hypothalamic circuit integrating external and internal information to mediate proper behavioral and physiological responses. For instance, some populations of Galn^{+} neurons might process stress-inducing stimuli while others might affect feeding and sleep, which are two behaviors greatly affected by stress states. In rodents, hypothalamic NPY-producing neurons modulate both feeding and stress depending on the brain regions receiving their projections (Reichmann and Holzer, 2016). In zebrafish, stress was shown to affect feeding, as exposure to hyperosmotic stress led to suppression of food consumption at larval stages (de Marco *et al.*, 2014). A recent study showed that in zebrafish hypothalamic Oxt neurons integrate external social clue information to modulate nociceptive and feeding-related behaviors (Wee *et al.*, 2022). Further work would be necessary to investigate whether different subtypes of Galn^{+} neurons project to brain regions involved in other types of behavior and correlate their activity with downstream effectors. An informative experiment to investigate the function of the different subpopulations of Galn^{+} cells would be to ablate Galn^{+} neurons displaying different response profiles using a two-photon laser and analyze the behavioral consequences. However, this approach might be challenging, as I showed that Galn^{+} neurons with different response profiles do not segregate in distinct anatomical regions of the PoA.

6.3 Response of pHyp-Galn$^+$ neurons to hyperosmotic stress

While the majority of PoA-Galn$^+$ neurons responded to stressful stimuli, the population of Galn$^+$ cells located in the pHyp showed a less evident trend. This population did not change its activity upon exposure to blue light and decreased it in response to the hypertonic solution. One possibility is that the change in their activity in response to NaCl is caused by the water flow rather than by the exposure to hyperosmotic stress. Thus, the pHyp-Galn$^+$ neurons might not be responsive to stress in general but to other types of stimuli, as it was hypothesized for the PoA-Galn$^+$ neurons "decreased activity" type. I did not record the activity of pHyp-Galn$^+$ neurons during administration of a control solution, which would be a crucial experiment to assess this hypothesis.

On the other hand, the response of pHyp-Galn$^+$ neurons might also be specific to hyperosmotic stress. In mammals, it is well documented that different types of threats are processed in distinct brain regions, which ultimately convey into the activation of the peptidergic neurons of the PVN (Godoy et al., 2018). In addition, most monosynaptic projections modulating the PVN derive from hypothalamic nuclei (Myers, Jessica M McKlveen and Herman, 2012). In zebrafish, different homeostatic threats were shown to ultimately recruit several neurons producing peptides in the PoA (Lovett-Barron *et al.*, 2020), but their afferents have not been elucidated. The pHyp region of the larva's brain might be connected to the PoA region and communicate information about distinct types of external stimuli. In line with this hypothesis, pHyp-Galn$^+$ neurons might be responsive to only certain stimuli and ultimately transmit the information to the peptidergic populations located in the PoA, as the PoA-Galn$^+$ neurons increasing their activity.

This hypothesis leads to another unanswered question, which is whether the two main hypothalamic populations of Galn$^+$ neurons are functionally and/or structurally connected. I observed several galaninergic fibers descending from the PoA to the pHyp, but I could not distinguish single projections and define whether the two populations are structurally connected. I also did not investigate whether the modulatory mechanisms controlling the activation of PoA-Galn$^+$ neurons overlap with the ones modulating the activity of pHyp-Galn$^+$ neurons. While I observed that most pHyp-Galn$^+$ neurons are GABAergic (data not shown), I did not test whether the activity of pHyp-Galn$^+$ neurons is affected by the lack or overexpression of Galn. Consequently, it might be possible that Galn, secreted by pHyp-Galn$^+$ neurons, participates in the inhibitory control of PoA-Galn$^+$ neurons.

Do pHyp-Galn$^+$ neurons contribute to the behavioral responses to stress described in this study? In most of the behavioral assays, I ablated Galn$^+$ neurons using a chemogenetic approach, which led to the cell death of all the cells producing Galn, including the population located in the pHyp. Ablating only the PoA population with a two-photon laser recapitulated the hyperresponsive-stress phenotype observed using the nifurpirinol-mediated cell ablation. Although I cannot exclude the involvement of pHyp-Galn$^+$ neurons in the behavior observed, the consequences of the laser-mediated ablation of PoA-Galn$^+$ neurons strongly indicate that this population is the one required for behavioral responses to hyperosmotic stress.

Further experiments using different types of stressors, Ca^{2+} imaging recording, and tracing studies are required to gain a deeper understanding of the importance of the pHyp neuronal population and its possible involvement in stress-related responses.

6.4 Galn$^+$ neurons circuitry

Which are the upstream neuronal circuits modulating PoA-Galn$^+$ neurons activation? While this study revealed that hypothalamic Galn$^+$ neurons mediate behavioral responses to stress, it is unclear how the information about different external stimuli is transmitted to the Galn$^+$ cells. The stressors used in this study (hyperosmotic stress, blue light, and sound) require the activation of different sensory modalities that identify the type and intensity of the stimulus. It was shown that vibrational and acoustic stimuli lead to the activation of neuronal populations in the hindbrain (Korn and Faber, 2005) while changes in light intensity are processed in the optic tectum (Dunn *et al.*, 2016) and hyperosmotic stress was recently shown to be detected primarily in the olfactory system (Herrera *et al.*, 2021). Thus, different sensory circuits might directly modulate PoA-Galn$^+$ cells or alternatively modulate intermediate neuronal populations such as pHyp-Galn$^+$ neurons. While in mammals the brain regions sending monosynaptic inputs to the PVN have been identified, in zebrafish this is still largely unknown. It will be important for future studies to identify the upstream circuits connecting the sensory system and the HPI axis. This would likely require the development of new approaches for studying connectivity in zebrafish, as retrograde tracing techniques are not well established in zebrafish larvae and require both the generation of transgenic lines and the use of viruses, whose injection might be a source of stress for the fish.

Another unanswered question is the downstream connection between hypothalamic peptidergic neurons and motor centers. I showed that Galn$^+$ neurons and Crh$^+$ neurons are

functionally connected, but I did not investigate how their response affects downstream circuits or the spinal cord. Ablation of Galn$^+$ neurons led to increased motility in response to the hyperosmotic stress but did not affect spontaneous locomotion. In addition, in the transgenic line used in this study to genetically label Galn$^+$ neurons, I did not observe any galaninergic fiber in the spinal cord of 5 dpf larvae. Although these results suggest that Galn$^+$ neurons are not directly required for locomotion under physiological conditions, they could modulate avoidance responses through intermediate circuits. A recent study showed that ablation of Crh$^+$ neurons using a chemogenetic approach did not abolish avoidance behavior to physiological threats such as heat, salinity, and acidity (Lovett-Barron *et al.*, 2020). However, the combined ablation of Crh$^+$ neurons and Oxt$^+$ neurons reduced avoidance responses to the stimuli. The connection between the motor centers and the PoA might occur via glutamatergic synapses between the preoptic peptidergic neurons and brainstem spinal-projecting neurons (Lovett-Barron et al., 2017, 2020). A study conducted in mice showed that stimulation of glutamatergic neurons in the PVN induces escape responses, probably through projections to the ventral midbrain area (Mangieri *et al.*, 2019). Future studies using zebrafish and rodents will be important to elucidate the neuronal network responsible to process stressful stimuli, elicit proper behavioral responses, and clarify the relevance of peptidergic neurons, including PoA-Galn$^+$ cells, in this network.

6.5 Galn receptors

The data presented in this study provide a better understanding of the function of Galn peptide in stress-related responses. I hypothesize that Galn has an autocrine inhibitory function on Galn$^+$ neurons, causing their hyperpolarization and reducing their inhibitory effect on downstream targets. Previous studies suggested that GAL might be released by soma/dendrites in LC neurons and induce the opening of K^+ channels through GALR1, thus reducing the release of noradrenaline (Pieribone *et al.*, 1995; Vila-Porcile *et al.*, 2009; Bai *et al.*, 2018). According to the data reported in this study, a similar mechanism might occur in PoA-Galn$^+$ neurons, with Galn modulating the activity of Galn$^+$ neurons “increased activity” type to reduce the release of GABA to their postsynaptic targets. In zebrafish, ectopic overexpression of Galn was shown to have an antiepileptic effect, supporting an inhibitory action of the peptide on neuronal activity (Podlasz *et al.*, 2018).

In mammals, GALR1 and GALR3 are coupled with GIRK channels, while GALR2 can affect the intracellular Ca^{2+} levels and the opening of Cl^- channels (Lang *et al.*, 2014). Therefore, while GALR1 and GALR3 mediate the inhibitory effects of GAL, GALR2 is generally considered excitatory. Although in zebrafish the GalnRs have not been characterized and their signaling pathways are unknown, it is reasonable to suppose that in zebrafish GalnR1a/b mediate the hyperpolarization of $Galn^+$ neurons. Then why do the majority of PoA-$Galn^+$ neurons express *galnR2b* if their activity is modulated by GalnR1a/b? I did not investigate whether *galnR1a* and *galnR1b* are co-expressed in the same $Galn^+$ neurons or on distinct cells. Thus, it cannot be excluded that the total amount of $Galn^+$ neurons expressing at least one of the two *galnR1* transcripts is comparable to the percentage of cells expressing *galnR2b.* Alternatively, *galnR2b* downstream signaling pathway might not be conserved between zebrafish and rodents and might mediate the inhibitory effects of Galn.

A further hypothesis is that *galnR2a*, not expressed on $Galn^+$ neurons, is functionally homologous to GALR2, which in mammals is considered excitatory. In fact, synteny analysis showed that GALR2 can be classified as the same class of *galnR2a* in non-mammalian vertebrates (Kim et al., 2014). *galnR2b,* highly expressed on $Galn^+$ neurons, might be functionally equivalent to GALR3, which was shown to be coupled with GIRK channels and mediate the inhibitory effect of GAL (Hökfelt et al., 2018). Although a homologous for GALR3 has not been identified in teleost genome, GalnR2b shares the highest degree of amino acid sequence similarity (55%) with GALR3 among all the zebrafish GalnRs.

In absence of studies describing the pharmacological properties of GalnRs in zebrafish, these hypotheses are purely speculative, and I cannot conclude which GalnRs mediate the inhibitory effect of Galn. Future studies should characterize which GalnRs are coupled with K^+ channels in zebrafish and their distribution on the different subtypes of PoA-$Galn^+$ neurons. The development of selective GalnRs agonists and antagonists, as well as *galnRs* mutant lines, would be fundamental to elucidate which GalnRs modulate the activity of $Galn^+$ neurons and their function on stress-related behaviors.

Another unanswered question is whether Galn is preferentially released from the soma/dendrites or by the nerve terminals. Somatodentriditic release of neuropeptides has been extensively reported, as in the magnocellular neurons of the hypothalamus, in which OXT and AVP bind to their autoreceptors to modulate their own release (Brown *et al.*, 2020).

Importantly, it was suggested that GAL might be released from the soma/dendrites of LC neurons and exerts an inhibitory effect through GALR1/3 (Hökfelt et al., 2018). Future studies should assess whether in the hypothalamus Galn is released by the soma/dendrites and investigate whether a differential site of release affects the binding of Galn to its autoreceptors and eventually the modulation of stress-related responses.

6.6 Co-transmission of Galn and GABA

In mammals, the majority of GAL-producing neurons in the hypothalamus are GABAergic (R. Chen *et al.*, 2017). In this study, I showed that the neurotransmitter phenotype of $Galn^+$ cells is conserved in zebrafish, as the majority of PoA-$Galn^+$ neurons express *gad2*. Most neuropeptides coexist with classic neurotransmitters (Nusbaum, Blitz and Marder, 2017), so it is not surprising that GABA and Galn are co-transmitted. But what is the significance of Galn and GABA co-transmission? According to the hypothesized model, the release of Galn reduces the neuronal excitability of $Galn^+$ cells and thus affects the release of GABA to downstream cell populations in the hypothalamus, most probably Crh^+ neurons. In mice, it was shown that the PVN is highly enriched with GABAergic cell populations and more than half of all CRH neurons in the PVN express GABA receptors (Cullinan, 2000).

Only a few studies indicate that GAL might affect the release of GABA. For instance, in serotonergic neurons of the dorsal raphe, application of GAL was shown to reduce presynaptic GABA release likely through GALR1 (Sharkey *et al.*, 2008). On the other hand, other neuropeptides have been shown to co-localize with GABA and affect its release. For instance, OXT facilitates or inhibits presynaptic GABA release binding to autoreceptors localized in OXT-producing neurons in a dose-dependent mechanism (Israel, Poulain, and Oliet, 2008). Similar to OXT, somatodendritic released AVP was shown to bind to autoreceptors and induces the release of endocannabinoids to inhibit presynaptic GABA release (Wang and Armstrong, 2012).

Although few evidence indicate that Galn might influence the release of GABA, the effect of Galn on the release of noradrenaline has been observed. Bath application of GAL in rat brain slices was shown to hyperpolarize noradrenaline-containing LC neurons through GALR1 coupled with GIRK channels (Bai *et al.*, 2018), causing a decreased release of noradrenaline. As in the noradrenergic neurons, exogenous administration of GAL was found

to inhibit the firing rate of serotonergic neurons, probably via GALR1/3 and activation of GIRK channels (Mazarati *et al.*, 2005). According to the model proposed in this study, Galn might affect the release of GABA *in vivo* in the hypothalamus through a mechanism similar to the one hypothesized in LC and serotonergic neurons. Importantly, in the PVN, GALR1 constitutes approximately 90% of all GAL-binding sites, with the remaining 10% being occupied by GALR2 or GALR3 (Zorrilla *et al.*, 2007), supporting the hypothesis of a autocrine inhibitory mechanism in hypothalamic neurons.

However, the decreased release of GABA to downstream targets is only a hypothesis and further studies should assess whether manipulating Galn causes a differential release of the neurotransmitter. GABA signaling is traditionally analyzed by pharmacology intervention and electrophysiological measurements. While electrophysiological techniques in zebrafish have been previously described (Baraban *et al.*, 2005; Baraban, 2013), these are not well established and involve invasive procedures which are most likely to cause distress to the animal. A promising alternative would be to use a genetically encoded fluorescent sensor to monitor GABAergic signaling, which was recently developed and used to monitor GABA release in the cerebellum of zebrafish (Marvin *et al.*, 2019). The advancement of new techniques to investigate neuronal communication *in vivo* in zebrafish larvae might shed new light on the functional effects of co-transmission of neurotransmitters and neuropeptides, which is an exciting, yet understudied, area of research.

6.7 Galn and Crh

Are $Galn^+$ neurons and Crh^+ neurons connected? I cannot conclude that these two populations are synaptically connected as $Galn^+$ neurons might regulate the activity of Crh^+ neurons through intermediate not-identified cell populations. However, the results of this study suggest a functional connection between these neuronal populations, with $Galn^+$ neurons negatively modulating the activation of Crh^+ neurons. The Ca^{2+} imaging data showed an anti-correlation between $Galn^+$ neurons “increased activity” type and Crh^+ neurons “decreased activity” type. In addition, the ablation of $Galn^+$ neurons led to increased activity of Crh^+ neurons after administration of both a control solution and exposure to hyperosmotic stress.

While the connectivity between $Galn^+$ neurons and Crh^+ neurons has not been addressed in previous studies, a link between the two neuropeptides has been reported. Administration

of GAL in the absence of stress was shown to increase the levels of CRH and ACTH (Picciotto *et al.*, 2010). In cultured hypothalamic neurons, GAL stimulated CRH secretion (Bergonzelli *et al.*, 2001). In rats, injection of GAL was shown to induce increased blood levels of ACTH (Tortorella, Neri, and Nussdorfer, 2007). While these studies did not address the precise mechanism by which GAL affects CRH, they lead to another unanswered question: is Galn binding to Crh^+ neurons? According to the data reported in this study, the effect of Galn on Crh is probably indirect. Most likely, Galn affects the release of Crh modulating the activity of $Galn^+$ neurons, which in turn inhibits directly or indirectly the Crh^+ neuronal population. On the other hand, I cannot exclude that Galn might also have a modulatory effect on Crh^+ neurons and this possibility should be investigated in the future.

6.8 Translational implications of Galn signaling

Dysfunctions in galaninergic signaling have been correlated with increased vulnerability to psychosocial stress and the risk of developing major depressive disorders (Juhasz et al., 2014; Barde et al., 2016; Hökfelt et al., 2018). In rodents, GAL and its receptors were connected to various types of stress-induced behavioral responses, even though with contradicting results (Karlsson and Holmes, 2006; Hökfelt et al., 2018). In recent years, several studies focused on the co-existence of GAL and noradrenaline in LC neurons and serotonergic neurons, suggesting that the interaction between GAL and monoaminergic signaling might be a key component in stress-related disorders (Borodovitsyna, Joshi, and Chandler, 2018; Morales et al., 2018; Rachel P. Tillage et al., 2021). For instance, it was hypothesized that GAL might prevent the overactivation of LC neurons during stress, acting on its autoreceptors GALR1/3 and thus conferring resilience to stress (Hökfelt et al., 2018). Notably, an antagonist for GALR3 was shown to exhibit antidepressant effects in rodent models, but the drug showed *in vitro* toxicity in pre-clinical studies (Koller *et al.*, 2016).

The results of this study provide a new modulatory effect of GAL on hypothalamic neurons and on the regulation of the stress axis, which might be relevant considering that GAL and its receptors are of great interest in pre-clinical investigations for novel antidepressants (Demsie et al., 2020). It is important to note that I evaluated the role of $Galn^+$ neurons in the modulation of stress exclusively in response to acute stressors. As depression-related disorders are linked to prolonged exposure to stress, it would be fundamental in the future to investigate the function of $Galn^+$ neurons during chronic stress conditions. Future

studies should also assess whether the hypothalamic circuit and the underlying modulatory mechanisms described in this study are conserved between zebrafish and rodents.

7 References

de Abreu, M.S., Demin, K.A., Giacomini, A.C.V.V., Amstislavskaya, T.G., Strekalova, T., Maslov, G.O., Kositsin, Y., Petersen, E. v. and Kalueff, A. v. (2021) 'Understanding how stress responses and stress-related behaviors have evolved in zebrafish and mammals', *Neurobiology of Stress*, 15, p. 100405. Available at: https://doi.org/10.1016/j.ynstr.2021.100405.

Aguilera, G. (1994) 'Regulation of pituitary ACTH secretion during chronic stress', *Frontiers in neuroendocrinology*, 15(4), pp. 321–350. Available at: https://doi.org/10.1006/frne.1994.1013.

Ahrens, M.B., Li, J.M., Orger, M.B., Robson, D.N., Schier, A.F., Engert, F. and Portugues, R. (2012) 'Brain-wide neuronal dynamics during motor adaptation in zebrafish', *Nature*, 485(7399), pp. 471–477. Available at: https://doi.org/10.1038/nature11057.

Alderman, S.L. and Bernier, N.J. (2009) 'Ontogeny of the corticotropin-releasing factor system in zebrafish.', *General and comparative endocrinology*, 164(1), pp. 61–69. Available at: https://doi.org/10.1016/j.ygcen.2009.04.007.

Alsop, D. and Vijayan, M.M. (2009) 'Molecular programming of the corticosteroid stress axis during zebrafish development', *Comparative biochemistry and physiology. Part A, Molecular & integrative physiology*, 153(1), pp. 49–54. Available at: https://doi.org/10.1016/j.cbpa.2008.12.008.

Anselmi, L., Stella, S.L., Brecha, N.C. and Sternini, C. (2009) 'Galanin Inhibition Of Voltage Dependent Ca2+ Influx In Rat Cultured Myenteric Neurons Is Mediated By Galanin Receptor 1', *Journal of neuroscience research*, 87(5), p. 1107. Available at: https://doi.org/10.1002/jnr.21923.

Antoni, F.A. (1986) 'Hypothalamic Control of Adrenocorticotropin Secretion: Advances since the Discovery of 41-Residue Corticotropin-Releasing Factor', *Endocrine Reviews*, 7(4), pp. 351–378. Available at: https://doi.org/10.1210/edrv-7-4-351.

Asakawa, K., Suster, M.L., Mizusawa, K., Nagayoshi, S., Kotani, T., Urasaki, A., Kishimoto, Y., Hibi, M. and Kawakami, K. (2008) 'Genetic dissection of neural circuits by Tol2 transposon-mediated Gal4 gene and enhancer trapping in zebrafish', *Proceedings of the National Academy of Sciences*, 105(4), pp. 1255 LP – 1260. Available at: https://doi.org/10.1073/pnas.0704963105.

Avants, B.B., Tustison, N. and Johnson, H. (2014) 'Advanced Normalization Tools (ANTS) Release 2.x'. Available at: https://brianavants.wordpress.com/2012/04/13/updated-ants-compile-instructions-april-12-2012/

Bai, Y.F., Ma, H.T., Liu, L.N., Li, H., Li, X.X., Yang, Y.T., Xue, B., Wang, D. and Xu, Z.Q.D. (2018) 'Activation of galanin receptor 1 inhibits locus coeruleus neurons via GIRK channels', *Biochemical and Biophysical Research Communications*, 503(1), pp. 79–85. Available at: https://doi.org/10.1016/j.bbrc.2018.05.181.

Baraban, S.C. (2013) ‘Forebrain electrophysiological recording in larval zebrafish’, *Journal of visualized experiments : JoVE*, (71). Available at: https://doi.org/10.3791/50104.

Baraban, S.C., Taylor, M.R., Castro, P.A. and Baier, H. (2005) ‘Pentylenetetrazole induced changes in zebrafish behavior, neural activity and c-fos expression’, *Neuroscience*, 131(3), pp. 759–768. Available at: https://doi.org/10.1016/j.neuroscience.2004.11.031.

Barde, S., Rüegg, J., Prud’homme, J., Ekström, T.J., Palkovits, M., Turecki, G., Bagdy, G., Ihnatko, R., Theodorsson, E., Juhasz, G., Diaz-Heijtz, R., Mechawar, N. and Hökfelt, T.G.M. (2016) ‘Alterations in the neuropeptide galanin system in major depressive disorder involve levels of transcripts, methylation, and peptide’, *Proceedings of the National Academy of Sciences*, 113(52), pp. E8472–E8481. Available at: https://doi.org/10.1073/pnas.1617824113.

Baribeau, D.A. and Anagnostou, E. (2015) ‘Oxytocin and vasopressin: Linking pituitary neuropeptides and their receptors to social neurocircuits’, *Frontiers in Neuroscience*, 9, p. 335. Available at: https://doi.org/10.3389/fnins.2015.00335/bibtex.

Bartfai, T., Lu, X., Badie-Mahdavi, H., Barr, A.M., Mazaratit, A., Hua, X.Y., Yaksh, T., Haberhauer, G., Ceide, S.C., Trembleau, L., Somogyi, L., Kröck, L. and Rebek, J. (2004) ‘Galmic, a nonpeptide galanin receptor agonist, affects behaviors in seizure, pain, and forced-swim tests’, *Proceedings of the National Academy of Sciences of the United States of America*, 101(28), pp. 10470–10475. Available at: https://doi.org/10.1073/pnas.0403802101.

Bedecs, K., Langel, Ü. and Bartfai, T. (1995) ‘Metabolism of galanin and galanin (1–16) in isolated cerebrospinal fluid and spinal cord membranes from rat’, *Neuropeptides*, 29(3), pp. 137–143. Available at: https://doi.org/10.1016/0143-4179(95)90015-2.

Beinfeld, M.C. (1998) ‘Prohormone and proneuropeptide processing. Recent progress and future challenges’, *Endocrine*, 8(1), pp. 1–5. Available at: https://doi.org/10.1385/endo:8:1:1.

del Bene, F., Wyart, C., Robles, E., Tran, A., Looger, L., Scott, E.K., Isacoff, E.Y. and Baier, H. (2010) ‘Filtering of Visual Information in the Tectum by an Identified Neural Circuit’, *Science*, 330(6004), p. 669. Available at: https://doi.org/10.1126/science.1192949.

Bergemann, D., Massoz, L., Bourdouxhe, J., Carril Pardo, C.A., Voz, M.L., Peers, B. and Manfroid, I. (2018) ‘Nifurpirinol: A more potent and reliable substrate compared to metronidazole for nitroreductase-mediated cell ablations.’, *Wound repair and regeneration : official publication of the Wound Healing Society [and] the European Tissue Repair Society*, 26(2), pp. 238–244. Available at: https://doi.org/10.1111/wrr.12633.

Berger, A., Lang, R., Moritz, K., Santic, R., Hermann, A., Sperl, W. and Kofler, B. (2004) ‘Galanin receptor subtype GalR2 mediates apoptosis in SH-SY5Y neuroblastoma cells’, *Endocrinology*, 145(2), pp. 500–507. Available at: https://doi.org/10.1210/en.2003-0649.

vom Berg-Maurer, C.M., Trivedi, C.A., Bollmann, J.H., de Marco, R.J. and Ryu, S. (2016) ‘The severity of acute stress is represented by increased synchronous activity and recruitment of hypothalamic CRH neurons’, *Journal of Neuroscience*, 36(11), pp. 3350–3362. Available at: https://doi.org/10.1523/jneurosci.3390-15.2016.

Bergonzelli, G.E., Pralong, F.P., Glauser, M., Cavadas, C., Grouzmann, E. and Gaillard, R.C. (2001) 'Interplay Between Galanin and Leptin in the Hypothalamic Control of Feeding via Corticotropin-Releasing Hormone and Neuropeptide Y', *Diabetes*, 50(12), pp. 2666–2672. Available at: https://doi.org/10.2337/diabetes.50.12.2666.

Bernard, C. (1865) *Introduction à l'étude de la médecine expérimentale*. Available at: http://dx.doi.org/doi:10.1522/cla.bec.int

Best, C., Kurrasch, D.M. and Vijayan, M.M. (2017) 'Maternal cortisol stimulates neurogenesis and affects larval behaviour in zebrafish', *Scientific reports*, 7. Available at: https://doi.org/10.1038/srep40905.

Beurel, E. and Nemeroff, C.B. (2014) 'Interaction of stress, corticotropin-releasing factor, arginine vasopressin and behaviour', *Current topics in behavioral neurosciences*, 18, p. 67. Available at: https://doi.org/10.1007/7854_2014_306.

Borodovitsyna, O., Joshi, N. and Chandler, D. (2018) 'Persistent stress-induced neuroplastic changes in the locus coeruleus/norepinephrine system', *Neural Plasticity*, 2018. Available at: https://doi.org/10.1155/2018/1892570.

van den Bos, R., Althuizen, J., Tschigg, K., Bomert, M., Zethof, J., Filk, G. and Gorissen, M. (2019) 'Early life exposure to cortisol in zebrafish (Danio rerio): similarities and differences in behaviour and physiology between larvae of the AB and TL strains', *Behavioural pharmacology*, 30, pp. 260–271. Available at: https://doi.org/10.1097/fbp.0000000000000470.

Boughton, C.K., Patterson, M., Bewick, G.A., Tadross, J.A., Gardiner, J. v., Beale, K.E.L., Chaudery, F., Hunter, G., Busbridge, M., Leavy, E.M., Ghatei, M.A., Bloom, S.R. and Murphy, K.G. (2010) 'Alarin stimulates food intake and gonadotrophin release in male rats', *British Journal of Pharmacology*, 161(3), pp. 601–613. Available at: https://doi.org/10.1111/j.1476-5381.2010.00893.x.

Brown, C.H., Ludwig, M., Tasker, J.G. and Stern, J.E. (2020) 'Somato-dendritic vasopressin and oxytocin secretion in endocrine and autonomic regulation', *Journal of Neuroendocrinology*. Blackwell Publishing Ltd. Available at: https://doi.org/10.1111/jne.12856.

Burgess, H.A. and Granato, M. (2007) 'Sensorimotor gating in larval zebrafish', *Journal of Neuroscience*, 27(18), pp. 4984–4994. Available at: https://doi.org/10.1523/jneurosci.0615-07.2007.

Cannon, W.B. (1915) 'Bodily changes in pain, hunger, fear and rage: An account of recent researches into the function of emotional excitement*'* New York, NY, US: D Appleton & Company. Available at: https://doi.org/10.1037/10013-000.

Cannon, W.B. (1929) 'Organization for physiological homeostasis', *Physiological reviews*, pp. 399–431. Available at: https://doi.org/10.1152/physrev.1929.9.3.399.

Castro, A., Becerra, M., Manso, M.J. and Anadón, R. (2006) 'Calretinin immunoreactivity in the brain of the zebrafish, Danio rerio: Distribution and comparison with some neuropeptides

and neurotransmitter- synthesizing enzymes. I. Olfactory organ and forebrain', *Journal of Comparative Neurology*, 494(3), pp. 435–459. Available at: https://doi.org/10.1002/cne.20782.

Champagne, D.L., Hoefnagels, C.C.M., de Kloet, R.E. and Richardson, M.K. (2010) 'Translating rodent behavioral repertoire to zebrafish (Danio rerio): Relevance for stress research', *Behavioural Brain Research*, 214(2), pp. 332–342. Available at: https://doi.org/https://doi.org/10.1016/j.bbr.2010.06.001.

Chen, R., Wu, X., Jiang, L. and Zhang, Y. (2017) 'Single-Cell RNA-Seq Reveals Hypothalamic Cell Diversity', *Cell Reports*, 18(13), pp. 3227–3241. Available at: https://doi.org/10.1016/j.celrep.2017.03.004.

Chen, S., Reichert, S., Singh, C., Oikonomou, G., Rihel, J. and Prober, D.A. (2017) 'Light-Dependent Regulation of Sleep and Wake States by Prokineticin 2 in Zebrafish', *Neuron*, 95(1), pp. 153-168.e6. Available at: https://doi.org/10.1016/j.neuron.2017.06.001.

Choi, H.M.T., Schwarzkopf, M., Fornace, M.E., Acharya, A., Artavanis, G., Stegmaier, J., Cunha, A. and Pierce, N.A. (2018) 'Third-generation in situ hybridization chain reaction: multiplexed, quantitative, sensitive, versatile, robust', *Development*, 145(12). Available at: https://doi.org/10.1242/dev.165753.

Clark, K.J., Boczek, N.J. and Ekker, S.C. (2011) 'Stressing zebrafish for behavioral genetics.', *Reviews in the neurosciences*, 22(1), pp. 49–62. Available at: https://doi.org/10.1515/rns.2011.007.

Colwill, Ruth M. and Creton, R. (2011) 'Imaging escape and avoidance behavior in zebrafish larvae', *Reviews in the Neurosciences*, 22(1), pp. 63–73. Available at: https://doi.org/10.1515/rns.2011.008.

Corradi, L. and Filosa, A. (2021) 'Neuromodulation and Behavioral Flexibility in Larval Zebrafish: From Neurotransmitters to Circuits', *Frontiers in molecular neuroscience*, 14. Available at: https://doi.org/10.3389/fnmol.2021.718951.

Cullinan, W.E. (2000) 'GABAA receptor subunit expression within hypophysiotropic CRH neurons: A dual hybridization histochemical study', *Journal of Comparative Neurology*, 419(3), pp. 344–351. Available at: https://doi.org/10.1002/(sici)1096-9861(20000410)419:3<344::aid-cne6>3.0.co;2-z

Davison, J.M., Akitake, C.M., Goll, M.G., Rhee, J.M., Gosse, N., Baier, H., Halpern, M.E., Leach, S.D. and Parsons, M.J. (2007) 'Transactivation from Gal4-VP16 transgenic insertions for tissue-specific cell labeling and ablation in zebrafish.', *Developmental biology*, 304(2), pp. 811–824. Available at: https://doi.org/10.1016/j.ydbio.2007.01.033.

Demin, K.A., Taranov, A.S., Ilyin, N.P., Lakstygal, A.M., Volgin, A.D., de Abreu, M.S., Strekalova, T. and Kalueff, A. v. (2021) 'Understanding neurobehavioral effects of acute and chronic stress in zebrafish', *Stress*. Taylor and Francis Ltd., pp. 1–18. Available at: https://doi.org/10.1080/10253890.2020.1724948.

Demsie, D.G., Altaye, B.M., Weldekidan, E., Gebremedhin, H., Alema, N.M., Tefera, M.M. and Bantie, A.T. (2020) 'Galanin Receptors as Drug Target for Novel Antidepressants:

Review', *Biologics : Targets & Therapy*, 14, p. 37. Available at: https://doi.org/10.2147/btt.s240715.

Deneux, T., Kaszas, A., Szalay, G., Katona, G., Lakner, T., Grinvald, A., Rózsa, B. and Vanzetta, I. (2016) 'Accurate spike estimation from noisy calcium signals for ultrafast three-dimensional imaging of large neuronal populations in vivo', *Nature Communications*, 7(1), p. 12190. Available at: https://doi.org/10.1038/ncomms12190.

Duncan, P.J., Tabak, J., Ruth, P., Bertram, R. and Shipston, M.J. (2016) 'Glucocorticoids Inhibit CRH/AVP-Evoked Bursting Activity of Male Murine Anterior Pituitary Corticotrophs', *Endocrinology*, 157(8), pp. 3108–3121. Available at: https://doi.org/10.1210/en.2016-1115.

Dunn, T.W., Gebhardt, C., Naumann, E.A., Riegler, C., Ahrens, M.B., Engert, F. and del Bene, F. (2016) 'Neural Circuits Underlying Visually Evoked Escapes in Larval Zebrafish', *Neuron*, 89(3), pp. 613–628. Available at: https://doi.org/10.1016/j.neuron.2015.12.021.

Eachus, H., Choi, M.K. and Ryu, S. (2021) 'The Effects of Early Life Stress on the Brain and Behaviour: Insights From Zebrafish Models', *Frontiers in Cell and Developmental Biology*, 9, p. 1209. Available at: https://doi.org/10.3389/fcell.2021.657591/bibtex.

Eskova, A., Frohnhöfer, H.G., Nüsslein-Volhard, C. and Irion, U. (2020) 'Galanin Signaling in the Brain Regulates Color Pattern Formation in Zebrafish', *Current Biology*, 30(2), pp. 298-303.e3. Available at: https://doi.org/10.1016/j.cub.2019.11.033.

Faught, E. and Vijayan, M.M. (2018) 'The mineralocorticoid receptor is essential for stress axis regulation in zebrafish larvae', *Scientific Reports 2018 8:1*, 8(1), pp. 1–11. Available at: https://doi.org/10.1038/s41598-018-36681-w.

Faught, E. and Vijayan, M.M. (2022) 'Coordinated Action of Corticotropin-Releasing Hormone and Cortisol Shapes the Acute Stress-Induced Behavioural Response in Zebrafish', *Neuroendocrinology*, 112(1), pp. 74–87. Available at: https://doi.org/10.1159/000514778.

Filosa, A., Barker, A.J., Dal Maschio, M. and Baier, H. (2016) 'Feeding State Modulates Behavioral Choice and Processing of Prey Stimuli in the Zebrafish Tectum.', *Neuron*, 90(3), pp. 596–608. Available at: https://doi.org/10.1016/j.neuron.2016.03.014.

Fink, G. (2017) 'Stress: Concepts, Definition and History', *The Curated Reference Collection in Neuroscience and Biobehavioral Psychology*, pp. 549–555. Available at: https://doi.org/10.1016/b978-0-12-809324-5.02208-2.

Flik, G., Klaren, P.H.M., van den Burg, E.H., Metz, J.R. and Huising, M.O. (2006) 'CRF and stress in fish', *General and comparative endocrinology*, 146(1), pp. 36–44. Available at: https://doi.org/10.1016/j.ygcen.2005.11.005.

Fontana, B.D., Gibbon, A.J., Cleal, M., Sudwarts, A., Pritchett, D., Miletto Petrazzini, M.E., Brennan, C.H. and Parker, M.O. (2021) 'Moderate early life stress improves adult zebrafish (Danio rerio) working memory but does not affect social and anxiety-like responses', *Developmental Psychobiology*, 63(1), pp. 54–64. Available at : https://doi.org/10.1002/dev.21986.

Förster, D., Arnold-Ammer, I., Laurell, E., Barker, A.J., Fernandes, A.M., Finger-Baier, K., Filosa, A., Helmbrecht, T.O., Kölsch, Y., Kühn, E., Robles, E., Slanchev, K., Thiele, T.R., Baier, H. and Kubo, F. (2017) 'Genetic targeting and anatomical registration of neuronal populations in the zebrafish brain with a new set of BAC transgenic tools', *Scientific Reports*, 7(1), p. 5230. Available at: https://doi.org/10.1038/s41598-017-04657-x.

Freeman, J., Vladimirov, N., Kawashima, T., Mu, Y., Sofroniew, N.J., Bennett, D. v., Rosen, J., Yang, C.T., Looger, L.L. and Ahrens, M.B. (2014) 'Mapping brain activity at scale with cluster computing', *Nature Methods*, 11(9), pp. 941–950. Available at: https://doi.org/10.1038/nmeth.3041.

Freimann, K., Kurrikoff, K. and Langel, U. (2015) 'Galanin receptors as a potential target for neurological disease.', *Expert opinion on therapeutic targets*, 19(12), pp. 1665–1676. Available at: https://doi.org/10.1517/14728222.2015.1072513.

Fuxe, K., Dahlström, A.B., Jonsson, G., Marcellino, D., Guescini, M., Dam, M., Manger, P. and Agnati, L. (2010) 'The discovery of central monoamine neurons gave volume transmission to the wired brain', *Progress in neurobiology*, 90(2), pp. 82–100. Available at: https://doi.org/10.1016/j.pneurobio.2009.10.012.

Gjerstad, Julia K., Lightman, S.L. and Spiga, F. (2018) 'Role of glucocorticoid negative feedback in the regulation of HPA axis pulsatility', *Stress*, 21(5), 403–416. Available at: https://doi.org/10.1080/10253890.2018.1470238.

Glaaser, I.W. and Slesinger, P.A. (2015) 'Structural Insights into GIRK Channel Function', *International review of neurobiology*, 123, pp. 117–160. Available at: https://doi.org/10.1016/bs.irn.2015.05.014.

Godoy, L.D., Rossignoli, M.T., Delfino-Pereira, P., Garcia-Cairasco, N. and de Lima Umeoka, E.H. (2018) 'A Comprehensive Overview on Stress Neurobiology: Basic Concepts and Clinical Implications', *Frontiers in Behavioral Neuroscience*, 12, pp. 1–23. Available at: https://doi.org/10.3389/fnbeh.2018.00127.

Goldstein, D.S. and Kopin, I.J. (2007) 'Evolution of concepts of stress', *Stress*, pp. 109–120. Available at: https://doi.org/10.1080/10253890701288935.

Griffiths, B., Schoonheim, P.J., Ziv, L., Voelker, L., Baier, H. and Gahtan, E. (2012) 'A zebrafish model of glucocorticoid resistance shows serotonergic modulation of the stress response', *Frontiers in Behavioral Neuroscience*, 6, 68. Available at: https://doi.org/10.3389/fnbeh.2012.00068.

Grillon, C. and Baas, J. (2003) 'A review of the modulation of the startle reflex by affective states and its application in psychiatry', *Clinical Neurophysiology*. pp. 1557–1579. Available at: https://doi.org/10.1016/S1388-2457(03)00202-5.

Groeneweg, F.L., Karst, H., de Kloet, E.R. and Joels, M. (2011) 'Rapid non-genomic effects of corticosteroids and their role in the central stress response.', *The Journal of endocrinology*, 209(2), pp. 153–167. Available at: https://doi.org/10.1530/joe-10-0472.

Gundlach, A.L., Burazin, T.C. and Larm, J.A. (2001) 'Distribution, regulation and role of hypothalamic galanin systems: renewed interest in a pleiotropic peptide family', *Clinical and experimental pharmacology & physiology*, 28(1–2), pp. 100–105. Available at: https://doi.org/10.1046/J.1440-1681.2001.03411.X.

Gutierrez-Triana, J.A., Herget, U., Lichtner, P., Castillo-Ramírez, L.A. and Ryu, S. (2014) 'A vertebrate-conserved cis-regulatory module for targeted expression in the main hypothalamic regulatory region for the stress response', *BMC Developmental Biology*, 14(1). Available at: https://doi.org/10.1186/s12861-014-0041-x.

Habecker, B.A., Gritman, K.R., Willison, B.D. and van Winkle, D.M. (2005) 'Myocardial infarction stimulates galanin expression in cardiac sympathetic neurons', *Neuropeptides*, 39(2), pp. 89–95. Available at: https://doi.org/10.1016/j.npep.2004.11.003.

Herget, U. and Ryu, S. (2015) 'Coexpression analysis of nine neuropeptides in the neurosecretory preoptic area of larval zebrafish'. *Frontiers in neuroanatomy*, 9, 2. Available at: https://doi.org/10.3389/fnana.2015.00002.

Herget, U., Wolf, A., Wullimann, M.F. and Ryu, S. (2014) 'Molecular neuroanatomy and chemoarchitecture of the neurosecretory preoptic-hypothalamic area in zebrafish larvae', *Journal of Comparative Neurology*, 522(7), pp. 1542–1564. Available at: https://doi.org/10.1002/cne.23480.

Herman, J.P. and Cullinan, W.E. (1997) 'Neurocircuitry of stress: central control of the hypothalamo-pituitary-adrenocortical axis.', *Trends in neurosciences*, 20(2), 78–84. Available at: https://doi.org/10.1016/s0166-2236(96)10069-2

Herman, J.P., McKlveen, J.M., Ghosal, S., Kopp, B., Wulsin, A., Makinson, R., Scheimann, J. and Myers, B. (2016) 'Regulation of the hypothalamic-pituitary- adrenocortical stress response', *Comprehensive Physiology*. 6(2), 603–621. Available at: https://doi.org/10.1002/cphy.c150015.

Herrera, K.J., Panier, T., Guggiana-Nilo, D., Correspondence, F.E. and Engert, F. (2021) 'Larval Zebrafish Use Olfactory Detection of Sodium and Chloride to Avoid Salt Water In Brief Larval Zebrafish Use Olfactory Detection of Sodium and Chloride to Avoid Salt Water', *Current Biology*, 31, pp. 782–793. Available at: https://doi.org/10.1016/j.cub.2020.11.051.

Hewitt, S.A., Wamsteeker, J.I., Kurz, E.U. and Bains, J.S. (2009) 'Altered chloride homeostasis removes synaptic inhibitory constraint of the stress axis', *Nature Neuroscience*, 12(4), pp. 438–443. Available at: https://doi.org/10.1038/nn.2274.

Hökfelt, T., Barde, S., Xu, Z.Q.D., Kuteeva, E., Rüegg, J., le Maitre, E., Risling, M., Kehr, J., Ihnatko, R., Theodorsson, E., Palkovits, M., Deakin, W., Bagdy, G., Juhasz, G., Prud'homme, H.J., Mechawar, N., Diaz-Heijtz, R. and Ögren, S.O. (2018) 'Neuropeptide and Small Transmitter Coexistence: Fundamental Studies and Relevance to Mental Illness', *Frontiers in neural circuits*, 12. Available at: https://doi.org/10.3389/fncir.2018.00106.

Hökfelt, T. and Tatemoto, K. (2008) 'Galanin - 25 Years with a multitalented neuropeptide', *Cellular and Molecular Life Sciences*, 65(12), pp. 1793–1795. Available at: https://doi.org/10.1007/s00018-008-8152-9.

Holmes, A., Kinney, J.W., Wrenn, C.C., Li, Q., Yang, R.J., Ma, L., Vishwanath, J., Saavedra, M.C., Innerfield, C.E., Jacoby, A.S., Shine, J., Iismaa, T.P. and Crawley, J.N. (2003) 'Galanin GAL-R1 receptor null mutant mice display increased anxiety-like behavior specific to the elevated plus-maze', *Neuropsychopharmacology*, 28(6), pp. 1031–1044. Available at: https://doi.org/10.1038/sj.npp.1300164.

Holmes, P. v., Blanchard, D.C., Blanchard, R.J., Brady, L.S. and Crawley, J.N. (1995) 'Chronic social stress increases levels of preprogalanin mRNA in the rat locus coeruleus', *Pharmacology Biochemistry and Behavior*, 50(4), pp. 655–660. Available at: https://doi.org/10.1016/0091-3057(94)00334-3.

Hwang, W.Y., Fu, Y., Reyon, D., Maeder, M.L., Tsai, S.Q., Sander, J.D., Peterson, R.T., Yeh, J.R.J. and Joung, J.K. (2013) 'Efficient genome editing in zebrafish using a CRISPR-Cas system', *Nature Biotechnology*, 31(3), pp. 227–229. Available at: https://doi.org/10.1038/nbt.2501.

Israel, J.M., Poulain, D.A. and Oliet, S.H.R. (2008) 'Oxytocin-induced postinhibitory rebound firing facilitates bursting activity in oxytocin neurons', *The Journal of neuroscience : the official journal of the Society for Neuroscience*, 28(2), pp. 385–394. Available at: https://doi.org/10.1523/jneurosci.5198-07.2008.

Joëls, M. (2011) 'Impact of glucocorticoids on brain function: Relevance for mood disorders', *Psychoneuroendocrinology*, 36(3), pp. 406–414. Available at: https://doi.org/10.1016/j.psyneuen.2010.03.004.

Juhasz, G., Hullam, G., Eszlari, N., Gonda, X., Antal, P., Anderson, I.M., Hökfelt, T.G.M., Deakin, J.F.W. and Bagdy, G. (2014) 'Brain galanin system genes interact with life stresses in depression-related phenotypes', *Proceedings of the National Academy of Sciences of the United States of America*, 111(16). Available at: https://doi.org/10.1073/pnas.1403649111

Kalsbeek, A., van der Spek, R., Lei, J., Endert, E., Buijs, R.M. and Fliers, E. (2012) 'Circadian rhythms in the hypothalamo-pituitary-adrenal (HPA) axis', *Molecular and cellular endocrinology*, 349(1), pp. 20–29. Available at: https://doi.org/10.1016/j.mce.2011.06.042.

Karlsson, R.M. and Holmes, A. (2006) 'Galanin as a modulator of anxiety and depression and a therapeutic target for affective disease', *Amino acids*, 31(3), pp. 231–239. Available at: https://doi.org/10.1007/S00726-006-0336-8.

Karlsson, R.M., Holmes, A., Heilig, M. and Crawley, J.N. (2005) 'Anxiolytic-like actions of centrally-administered neuropeptide Y, but not galanin, in C57BL/6J mice', *Pharmacology, biochemistry, and behavior*, 80(3), pp. 427–436. Available at: https://doi.org/10.1016/j.pbb.2004.12.009.

Kawakami, K. (2005) 'Transposon tools and methods in zebrafish', *Developmental Dynamics*, 234(2), pp. 244–254. Available at: https://doi.org/10.1002/dvdy.20516.

Kim, D.K., Yun, S., Son, G.H., Hwang, J.I., Park, C.R., Kim, J. il, Kim, K., Vaudry, H. and Seong, J.Y. (2014) 'Coevolution of the spexin/galanin/kisspeptin family: Spexin activates galanin receptor type II and III', *Endocrinology*, 155(5), pp. 1864–1873. Available at: https://doi.org/10.1210/en.2013-2106.

Kim, E., Jeong, I., Kim, S., Kim, H.K., Lee, D.W., Kim, B., Seong, J.Y., Bae, Y.K., Ryu, J.H. and Park, H.C. (2016) 'Distribution of galanin receptor 2b neurons and interaction with galanin in the zebrafish central nervous system', *Neuroscience Letters*, 628, pp. 153–160. Available at: https://doi.org/10.1016/j.neulet.2016.06.025.

Kinney, G.A., Emmerson, P.J. and Miller, R.J. (1998) 'Galanin Receptor-Mediated Inhibition of Glutamate Release in the Arcuate Nucleus of the Hypothalamus', *The Journal of Neuroscience*, 18(10), p. 3489. Available at: https://doi.org/10.1523/jneurosci.18-10-03489.1998.

Klenerova, V., Flegel, M., Skopek, P., Sida, P. and Hynie, S. (2011) 'Galanin modulating effect on restraint stress-induced short- and long-term behavioral changes in Wistar rats', *Neuroscience letters*, 502(3), pp. 147–151. Available at: https://doi.org/10.1016/j.neulet.2011.06.051.

de Kloet, E.R. (2004) 'Hormones and the stressed brain', *Annals of the New York Academy of Sciences*, 1018, pp. 1–15. Available at: https://doi.org/10.1196/annals.1296.001.

de Kloet, E.R., Joëls, M. and Holsboer, F. (2005) 'Stress and the brain: From adaptation to disease', *Nature Reviews Neuroscience*, pp. 463–475. Available at: https://doi.org/10.1038/nrn1683.

Kofler, B., Liu, M.L., Jacoby, A.S., Shine, J. and Iismaa, T.P. (1996) 'Molecular cloning and characterisation of the mouse preprogalanin gene', *Gene*, 182(1–2), pp. 71–75. Available at: https://doi.org/10.1016/S0378-1119(96)00477-5.

Kohl, J., Babayan, B.M., Rubinstein, N.D., Autry, A.E., Marin-Rodriguez, B., Kapoor, V., Miyamishi, K., Zweifel, L.S., Luo, L., Uchida, N. and Dulac, C. (2018) 'Functional circuit architecture underlying parental behaviour', *Nature*, 556(7701), p. 326. Available at: https://doi.org/10.1038/S41586-018-0027-0.

Koller, A., Rid, R., Beyreis, M., Bianchini, R., Holub, B.S., Lang, A., Locker, F., Brodowicz, B., Velickovic, O., Jakab, M., Kerschbaum, H., Önder, K. and Kofler, B. (2016) 'In vitro toxicity of the galanin receptor 3 antagonist SNAP 37889', *Neuropeptides*, 56, pp. 83–88. Available at: https://doi.org/10.1016/j.npep.2015.12.003.

Kordower, J.H., Le, H.K. and Mufson, E.J. (1992) 'Galanin immunoreactivity in the primate central nervous system', *The Journal of comparative neurology*, 319(4), pp. 479–500. Available at: https://doi.org/10.1002/cne.903190403.

Kormos, V. and Gaszner, B. (2013) 'Role of neuropeptides in anxiety, stress, and depression: From animals to humans', *Neuropeptides*, 47(6), pp. 401–419. Available at: https://doi.org/10.1016/j.npep.2013.10.014.

Korn, H. and Faber, D.S. (2005) 'The Mauthner cell half a century later: a neurobiological model for decision-making?', *Neuron*, 47(1), pp. 13–28. Available at: https://doi.org/10.1016/j.neuron.2005.05.019.

Kozoriz, M.G., Kuzmiski, J.B., Hirasawa, M. and Pittman, Q.J. (2006) 'Galanin Modulates Neuronal and Synaptic Properties in the Rat Supraoptic Nucleus in a Use and State Dependent Manner', *Journal of Neurophysiology*, 96(1), pp. 154–164. Available at: https://doi.org/10.1152/jn.01028.2005.

Kunst, M., Laurell, E., Mokayes, N., Kramer, A., Kubo, F., Fernandes, A.M., Förster, D., Dal Maschio, M. and Baier, H. (2019) 'A Cellular-Resolution Atlas of the Larval Zebrafish Brain', *Neuron*, 103(1), pp. 21-38.e5. Available at: https://doi.org/10.1016/j.neuron.2019.04.034.

Kuteeva, E. (2007) 'Brain galanin systems and their role in depression-like behaviour'. PhD Thesis, Karolinska Institutet, Stockholm. Available at: http://hdl.handle.net/10616/39245

Kuteeva, E., Wardi, T., Lundström, L., Sollenberg, U., Langel, Ü., Hökfelt, T. and Ögren, S.O. (2008) 'Differential Role of Galanin Receptors in the Regulation of Depression-Like Behavior and Monoamine/Stress-Related Genes at the Cell Body Level', *Neuropsychopharmacology*, 33(11), pp. 2573–2585. Available at: https://doi.org/10.1038/sj.npp.1301660.

Lang, R., Gundlach, A.L., Holmes, F.E., Hobson, S.A., Wynick, D., Hokfelt, T. and Kofler, B. (2014) 'Physiology, Signaling, and Pharmacology of Galanin Peptides and Receptors: Three Decades of Emerging Diversity', *Pharmacological Reviews*, 67(1), pp. 118–175. Available at: https://doi.org/10.1124/pr.112.006536.

Lara, R.A. and Vasconcelos, R.O. (2021) 'Impact of noise on development, physiological stress and behavioural patterns in larval zebrafish', *Scientific Reports*, 11(1), pp. 1–14. Available at: https://doi.org/10.1038/s41598-021-85296-1.

Lerner, J.T., Sankar, R. and Mazarati, A.M. (2008) 'Galanin – 25 years with a multitalented neuropeptide', *Cellular and Molecular Life Sciences*, 65(12), pp. 1864–1871. Available at: https://doi.org/10.1007/s00018-008-8161-8.

Lerner, J.T., Sankar, R. and Mazarati, A.M. (2010) 'Galanin and epilepsy', *Experientia supplementum*, 102, pp. 183–194. Available at: https://doi.org/10.1007/978-3-0346-0228-0_13.

Li, L., Wei, S., Huang, Q., Feng, D., Zhang, S. and Liu, Z. (2013) 'A novel galanin receptor 1a gene in zebrafish: Tissue distribution, developmental expression roles in nutrition regulation', *Comparative Biochemistry and Physiology -Part B, Biochemistry and Molecular Biology*, 164(3), pp. 159–167. Available at: https://doi.org/10.1016/j.cbpb.2012.12.004.

Lister, J.A., Robertson, C.P., Lepage, T., Johnson, S.L. and Raible, D.W. (1999) 'nacre encodes a zebrafish microphthalmia-related protein that regulates neural-crest-derived pigment cell fate.', *Development*, 126(17), pp. 3757–3767. Available at: https://doi.org/10.1242/dev.126.17.3757.

Liu, Z., Xu, Y., Wu, L. and Zhang, S. (2010) 'Evolution of Galanin Receptor Genes: Insights from the Deuterostome Genomes', *Journal of Biomolecular Structure and Dynamics*, 28(1), pp. 97–106. Available at: https://doi.org/10.1080/07391102.2010.10507346.

Lovett-Barron, M., Andalman, A.S., Allen, W.E., Vesuna, S., Kauvar, I., Burns, V.M. and Deisseroth, K. (2017) 'Ancestral Circuits for the Coordinated Modulation of Brain State', *Cell*, 171(6), pp. 1411-1423.e17. Available at: https://doi.org/10.1016/j.cell.2017.10.021.

Lovett-Barron, M., Chen, R., Bradbury, S., Andalman, A.S., Wagle, M., Guo, S. and Deisseroth, K. (2020) 'Multiple convergent hypothalamus–brainstem circuits drive defensive behavior', *Nature Neuroscience*, 23(8), pp. 959–967. Available at: https://doi.org/10.1038/s41593-020-0655-1.

Ludwig, M., Apps, D., Menzies, J., Patel, J.C. and Rice, M.E. (2017) 'Dendritic release of neurotransmitters', *Comprehensive Physiology*, 7(1), pp. 235–252. Available at: https://doi.org/10.1002/cphy.c160007.

Ludwig, M. and Leng, G. (2006) 'Dendritic peptide release and peptide-dependent behaviours', *Nature Reviews Neuroscience*, pp. 126–136. Available at: https://doi.org/10.1038/nrn1845.

Lundberg, J.M. and Hökfelt, T. (1983) 'Coexistence of peptides and classical neurotransmitters', *Trends in Neurosciences*, 6(C), pp. 325–333. Available at: https://doi.org/10.1016/0166-2236(83)90149-2.

Ma, X., Tong, Y.-G., Schmidt, R., Brown, W., Payza, K., Hodzic, L., Pou, C., Godbout, C., Hökfelt, T. and Xu, Z.-Q.D. (2001) 'Effects of galanin receptor agonists on locus coeruleus neurons', *Brain Research*, 919(1), pp. 169–174. Available at: https://doi.org/https://doi.org/10.1016/s0006-8993(01)03033-5.

Ma, Y., Miracca, G., Yu, X., Harding, E.C., Miao, A., Yustos, R., Vyssotski, A.L., Franks, N.P. and Wisden, W. (2019) 'Galanin Neurons Unite Sleep Homeostasis and α2-Adrenergic Sedation', *Current Biology*, 29(19), p. 3315. Available at: https://doi.org/10.1016/j.cub.2019.07.087.

Mains, R.E., Cullen, E.I., May, V. and Eipper, B.A. (1987) 'The role of secretory granules in peptide biosynthesis', *Annals of the New York Academy of Sciences*, 493(1), pp. 278–291. Available at: https://doi.org/10.1111/j.1749-6632.1987.tb27213.x.

Mangieri, L.R., Jiang, Z., Lu, Y., Xu, Yuanzhong, Cassidy, R.M., Justice, N., Xu, Yong, Arenkiel, B.R. and Tong, Q. (2019) 'Defensive Behaviors Driven by a Hypothalamic-Ventral Midbrain Circuit', *eNeuro*, 6(4). Available at: https://doi.org/10.1523/eneuro.0156-19.2019.

de Marco, R.J., Groneberg, A.H., Yeh, C.M., Castillo Ramírez, L.A. and Ryu, S. (2013) 'Optogenetic elevation of endogenous glucocorticoid level in larval zebrafish', *Frontiers in Neural Circuits*, 7, p. 82. available at: https://doi.org/10.3389/fncir.2013.00082.

de Marco, R.J., Groneberg, A.H., Yeh, C.-M., Treviño, M. and Ryu, S. (2014) 'The behavior of larval zebrafish reveals stressor-mediated anorexia during early vertebrate development.', *Frontiers in behavioral neuroscience*, 8, p. 367. Available at: https://doi.org/10.3389/fnbeh.2014.00367.

de Marco, R.J., Thiemann, T., Groneberg, A.H., Herget, U. and Ryu, S. (2016) 'Optogenetically enhanced pituitary corticotroph cell activity post-stress onset causes rapid

organizing effects on behaviour', *Nature Communications*, 7, p. 12620. Available at: https://doi.org/10.1038/ncomms12620.

Marvin, J.S., Shimoda, Y., Magloire, V., Leite, M., Kawashima, T., Jensen, T.P., Kolb, I., Knott, E.L., Novak, O., Podgorski, K., Leidenheimer, N.J., Rusakov, D.A., Ahrens, M.B., Kullmann, D.M. and Looger, L.L. (2019) 'A genetically encoded fluorescent sensor for in vivo imaging of GABA', *Nature Methods*, 16(8), pp. 763–770. Available at: https://doi.org/10.1038/s41592-019-0471-2.

Mazarati, A.M., Baldwin, R.A., Shinmei, S. and Sankar, R. (2005) 'In vivo interaction between serotonin and galanin receptors types 1 and 2 in the dorsal raphe: implication for limbic seizures', *Journal of neurochemistry*, 95(5), pp. 1495–1503. Available at: https://doi.org/10.1111/J.1471-4159.2005.03498.X.

Melander, T., Hökfelt, T. and Rökaeus, A. (1986) 'Distribution of galaninlike immunoreactivity in the rat central nervous system', *The Journal of comparative neurology*, 248(4), pp. 475–517. Available at: https://doi.org/10.1002/cne.902480404.

Mommsen, T.P., Vijayan, M.M. and Moon, T.W. (1999) 'Cortisol in teleosts: dynamics, mechanisms of action, and metabolic regulation', *Reviews in Fish Biology and Fisheries*, 9(3), pp. 211–268. Available at: https://doi.org/10.1023/a:1008924418720.

Moncrieff, J., Cooper, R.E., Stockmann, T., Amendola, S., Hengartner, M.P. and Horowitz, M.A. (2022) 'The serotonin theory of depression: a systematic umbrella review of the evidence', *Molecular Psychiatry 2022*, pp. 1–14. Available at: https://doi.org/10.1038/s41380-022-01661-0.

Myers, B., Mark Dolgas, C., Kasckow, J., Cullinan, W.E. and Herman, J.P. (2014) 'Central stress-integrative circuits: Forebrain glutamatergic and GABAergic projections to the dorsomedial hypothalamus, medial preoptic area, and bed nucleus of the stria terminalis', *Brain Structure and Function*, 219(4), pp. 1287–1303. Available at: https://doi.org/10.1007/s00429-013-0566-y.

Myers, B., McKlveen, Jessica M and Herman, J.P. (2012) 'Neural Regulation of the Stress Response: The Many Faces of Feedback', *Cellular and molecular neurobiology*. Available at: https://doi.org/10.1007/s10571-012-9801-y.

Myers, B., Scheimann, J.R., Franco-Villanueva, A. and Herman, J.P. (2017) 'Ascending mechanisms of stress integration: Implications for brainstem regulation of neuroendocrine and behavioral stress responses', *Neuroscience and Biobehavioral Reviews*, pp. 366–375. Available at: https://doi.org/10.1016/j.neubiorev.2016.05.011.

Nakai, J., Ohkura, M. and Imoto, K. (2001) 'A high signal-to-noise Ca^{2+} probe composed of a single green fluorescent protein', *Nature Biotechnology*, 19(2), pp. 137–141. Available at: https://doi.org/10.1038/84397.

Nicolaides, N.C., Charmandari, E., Chrousos, G.P. and Kino, T. (2014) 'Circadian endocrine rhythms: the hypothalamic–pituitary–adrenal axis and its actions', *Annals of the New York Academy of Sciences*, 1318(1), p. 71. Available at: https://doi.org/10.1111/nyas.12464.

Nusbaum, M.P., Blitz, D.M. and Marder, E. (2017) 'Functional consequences of neuropeptide and small-molecule co-transmission', *Nature Reviews Neuroscience*, pp. 389–403. Available at: https://doi.org/10.1038/nrn.2017.56.

Ögren, S.O., Kuteeva, E., Elvander-Tottie, E. and Hökfelt, T. (2010) 'Neuropeptides in learning and memory processes with focus on galanin', *European journal of pharmacology*, 626(1), pp. 9–17. Available at: https://doi.org/10.1016/j.ejphar.2009.09.070.

Ohtaki, T., Kumano, S., Ishibashi, Y., Ogi, K., Matsui, H., Harada, M., Kitada, C., Kurokawa, T., Onda, H. and Fujino, M. (1999) 'Isolation and cDNA cloning of a novel galanin-like peptide (GALP) from porcine hypothalamus', *The Journal of biological chemistry*, 274(52), pp. 37041–37045. Available at: https://doi.org/10.1074/jbc.274.52.37041.

O'Neal, H.A., van Hoomissen, J.D., Holmes, P. v. and Dishman, R.K. (2001) 'Prepro-galanin messenger RNA levels are increased in rat locus coeruleus after treadmill exercise training', *Neuroscience Letters*, 299(1–2), pp. 69–72. Available at: https://doi.org/10.1016/s0304-3940(00)01780-8.

Orger, M.B., Gahtan, E., Muto, A., Page-Mccaw, P., Smear, M.C. and Baier, H. (2004) 'Behavioral Screening Assays in Zebrafish'. *Methods in cell biology*, 77, pp. 53–68. Available at: https://doi.org/10.1016/s0091-679x(04)77003-x

Park, H.-C., Hong, S.-K., Kim, H.-S., Kim, S.-H., Yoon, E.-J., Kim, C.-H., Miki, N. and Huh, T.-L. (2000) 'Structural comparison of zebrafish Elav/Hu and their differential expressions during neurogenesis', *Neuroscience Letters*, 279(2), pp. 81–84. Available at: https://doi.org/https://doi.org/10.1016/s0304-3940(99)00940-4.

Pérez, S.E., Wynick, D., Steiner, R.A. and Mufson, E.J. (2001) 'Distribution of galaninergic immunoreactivity in the brain of the mouse', *The Journal of comparative neurology*, 434(2), pp. 158–185. Available at: https://doi.org/10.1002/cne.1171.

Picciotto, M.R., Brabant, C., Einstein, E.B., Kamens, H.M. and Neugebauer, N.M. (2010) 'Effects of galanin on monoaminergic systems and HPA axis: Potential mechanisms underlying the effects of galanin on addiction- and stress-related behaviors', *Brain Research*, pp. 206–218. Available at: https://doi.org/10.1016/j.brainres.2009.08.033.

Pieribone, V.A., Xu, Z.-Q., Zhang, X., Grillner, S., Bartfai, T. and Hökfelt, T. (1995) 'Galanin induces a hyperpolarization of norepinephrine-containing locus coeruleus neurons in the brainstem slice', *Neuroscience*, 64(4), pp. 861–874. Available at: https://doi.org/https://doi.org/10.1016/0306-4522(94)00450-j.

Pnevmatikakis, E.A. and Giovannucci, A. (2017) 'NoRMCorre: An online algorithm for piecewise rigid motion correction of calcium imaging data', *Journal of Neuroscience Methods*, 291, pp. 83–94. Available at: https://doi.org/10.1016/j.jneumeth.2017.07.031.

Podlasz, P., Jakimiuk, A., Chmielewska-Krzesinska, M., Kasica, N., Nowik, N. and Kaleczyc, J. (2016) 'Galanin regulates blood glucose level in the zebrafish: a morphological and functional study', *Histochemistry and Cell Biology*, 145(1), pp. 105–117. Available at: https://doi.org/10.1007/s00418-015-1376-5.

Podlasz, P., Jakimiuk, A., Kasica-Jarosz, N., Czaja, K. and Wasowicz, K. (2018) 'Neuroanatomical Localization of Galanin in Zebrafish Telencephalon and Anticonvulsant Effect of Galanin Overexpression', *ACS Chemical Neuroscience*, 9(12), pp. 3049–3059. Available at: https://doi.org/10.1021/acschemneuro.8b00239.

Podlasz, P., Sallinen, V., Chen, Y.C., Kudo, H., Fedorowska, N. and Panula, P. (2012) 'Galanin gene expression and effects of its knock-down on the development of the nervous system in larval zebrafish', *Journal of Comparative Neurology*, 520(17), pp. 3846–3862. Available at: https://doi.org/10.1002/cne.23131.

Portugues, R., Feierstein, C.E., Engert, F. and Orger, M.B. (2014) 'Whole-brain activity maps reveal stereotyped, distributed networks for visuomotor behavior', *Neuron*, 81(6), pp. 1328–1343. Available at: https://doi.org/10.1016/j.neuron.2014.01.019.

Portugues, R., Severi, K.E., Wyart, C. and Ahrens, M.B. (2013) 'Optogenetics in a transparent animal: circuit function in the larval zebrafish', *Current Opinion in Neurobiology*, 23(1), pp. 119–126. Available at: https://doi.org/10.1016/j.conb.2012.11.001.

Qualls-Creekmore, E., Yu, S., Francois, M., Hoang, J., Huesing, C., Bruce-Keller, A., Burk, D., Berthoud, H.-R., Morrison, C.D. and Münzberg, H. (2017) 'Galanin-Expressing GABA Neurons in the Lateral Hypothalamus Modulate Food Reward and Noncompulsive Locomotion', *The Journal of Neuroscience*, 37(25), pp. 6053–6065. Available at: https://doi.org/10.1523/jneurosci.0155-17.2017.

Randlett, O., Wee, C.L., Naumann, E.A., Nnaemeka, O., Schoppik, D., Fitzgerald, J.E., Portugues, R., Lacoste, A.M.B., Riegler, C., Engert, F. and Schier, A.F. (2015) 'Whole-brain activity mapping onto a zebrafish brain atlas.', *Nature methods*, 12(11), pp. 1039–1046. Available at: https://doi.org/10.1038/nmeth.3581.

Ray, W.J., Molnar, C., Aikins, D., Yamasaki, A., Newman, M.G., Castonguay, L. and Borkovec, T.D. (2009) 'Startle response in Generalized Anxiety Disorder', *Depression and Anxiety*, 26(2), pp. 147–154. Available at: https://doi.org/https://doi.org/10.1002/da.20479.

Reichert, S., Pavón Arocas, O. and Rihel, J. (2019) 'The Neuropeptide Galanin Is Required for Homeostatic Rebound Sleep following Increased Neuronal Activity', *Neuron*, 104(2), pp. 370-384.e5. Available at: https://doi.org/10.1016/j.neuron.2019.08.010.

Reichmann, F. and Holzer, P. (2016) 'Neuropeptide Y: A stressful review', *Neuropeptides*, 55, p. 99. Available at: https://doi.org/10.1016/j.npep.2015.09.008.

Rokaeus, A. and Brownstein, M.J. (1986) 'Construction of a porcine adrenal medullary cDNA library and nucleotide sequence analysis of two clones encoding a galanin precursor', *Proceedings of the National Academy of Sciences of the United States of America*, 83(17), pp. 6287–6291. Available at: https://doi.org/10.1073/pnas.83.17.6287.

Ryu, S. and de Marco, R.J. (2017) 'Performance on innate behaviour during early development as a function of stress level', *Scientific Reports*, 7(1). Available at: https://doi.org/10.1038/s41598-017-08400-4.

Santic, R., Fenninger, K., Graf, K., Schneider, R., Hauser-Kronberger, C., Schilling, F.H., Kogner, P., Ratschek, M., Jones, N., Sperl, W. and Kofler, B. (2006) 'Gangliocytes in neuroblastic tumors express alarin, a novel peptide derived by differential splicing of the galanin-like peptide gene', *Journal of Molecular Neuroscience 2006 29:2*, 29(2), pp. 145–152. Available at: https://doi.org/10.1385/jmn:29:2:145.

Sapolsky, R.M., Romero, L.M. and Munck, A.U. (2000) 'How do glucocorticoids influence stress responses? Integrating permissive, suppressive, stimulatory, and preparative actions.', *Endocrine reviews*, 21(1), pp. 55–89. Available at: https://doi.org/10.1210/edrv.21.1.0389.

Sawchenko, P.E., Imaki, T. and Vale, W. (1992) 'Co-localization of neuroactive substances in the endocrine hypothalamus.', *Ciba Foundation symposium*, 168. Available at: https://doi.org/10.1002/9780470514283.ch3.

Sawchenko, P.E., Swanson, L.W. and Vale, W.W. (1984) 'Co-expression of corticotropin-releasing factor and vasopressin immunoreactivity in parvocellular neurosecretory neurons of the adrenalectomized rat.', *Proceedings of the National Academy of Sciences of the United States of America*, 81(6), p. 1883. Available at: https://doi.org/10.1073/pnas.81.6.1883.

Sheng, J.A., Bales, N.J., Myers, S.A., Bautista, A.I., Roueinfar, M., Hale, T.M. and Handa, R.J. (2021) "The Hypothalamic-Pituitary-Adrenal Axis: Development, Programming Actions of Hormones, and Maternal-Fetal Interactions," *Frontiers in behavioral neuroscience*, 14. Available at: https://doi.org/10.3389/fnbeh.2020.601939.

Schmid, B. and Haass, C. (2013) 'Genomic editing opens new avenues for zebrafish as a model for neurodegeneration', *Journal of Neurochemistry*, 127(4), pp. 461–470. Available at: https://doi.org/10.1111/jnc.12460.

Sciolino, N.R., Smith, J.M., Stranahan, A.M., Freeman, K.G., Edwards, G.L., Weinshenker, D. and Holmes, P. v. (2015) 'Galanin Mediates Features of Neural and Behavioral Stress Resilience Afforded by Exercise', *Neuropharmacology*, 89, p. 255. Available at: https://doi.org/10.1016/j.neuropharm.2014.09.029.

Scott, E.K., Mason, L., Arrenberg, A.B., Ziv, L., Gosse, N.J., Xiao, T., Chi, N.C., Asakawa, K., Kawakami, K. and Baier, H. (2007) 'Targeting neural circuitry in zebrafish using GAL4 enhancer trapping', *Nature methods*, 4(4), pp. 323–326. Available at: https://doi.org/10.1038/nmeth1033.

Selye, H. (1936) 'A Syndrome produced by Diverse Nocuous Agents', *Nature*, 138(3479), p. 32. Available at: https://doi.org/10.1038/138032a0.

Selye, H. (1950) 'Stress and the general adaptation syndrome', *British medical journal*, 1(4667), pp. 1383–1392. Available at: https://doi.org/10.1136/bmj.1.4667.1383.

Selye, H. (1976) 'Stress without Distress', *Psychopathology of Human Adaptation*, pp. 137–146. Available at: https://doi.org/10.1007/978-1-4684-2238-2_9.

Shams, S., Khan, A. and Gerlai, R. (2020) 'Early social deprivation does not affect cortisol response to acute and chronic stress in zebrafish', *Stress*, 24(3), pp. 273–281. Available at: https://doi.org/10.1080/10253890.2020.1807511.

Sharkey, L.M., Madamba, S.G., Siggins, G.R. and Bartfai, T. (2008) 'Galanin alters GABAergic neurotransmission in the dorsal raphe nucleus', *Neurochemical Research*, 33(2), pp. 285–291. *Neurochemical research, 33*(2), 285–291. Available at: https://doi.org/10.1007/s11064-007-9524-5

Shiozaki, K., Kawabe, M., Karasuyama, K., Kurachi, T., Hayashi, A., Ataka, K., Iwai, H., Takeno, H., Hayasaka, O., Kotani, T., Komatsu, M. and Inui, A. (2020) 'Neuropeptide Y deficiency induces anxiety-like behaviours in zebrafish (Danio rerio)', *Scientific Reports*, 10(1). Available at: https://doi.org/10.1038/S41598-020-62699-0.

Singh, C., Rihel, J. and Prober, D.A. (2017) 'Neuropeptide Y Regulates Sleep by Modulating Noradrenergic Signaling', *Current biology*, pp. 3796-3811.e5. Available at: https://doi.org/10.1016/j.cub.2017.11.018.

Skofitsch, G. and Jacobowitz, D.M. (1985) 'Immunohistochemical mapping of galanin-like neurons in the rat central nervous system', *Peptides*, 6(3), pp. 509–546. Available at: https://doi.org/10.1016/0196-9781(85)90118-4.

Smith, A.S., Tabbaa, M., Lei, K., Eastham, P., Butler, M.J., Linton, L., Altshuler, R., Liu, Y. and Wang, Z. (2016) 'Local oxytocin tempers anxiety by activating GABAA receptors in the hypothalamic paraventricular nucleus', *Psychoneuroendocrinology*, 63, p. 50. Available at: https://doi.org/10.1016/j.psyneuen.2015.09.017.

Smith, K.E., Walker, M.W., Artymyshyn, R., Bard, J., Borowsky, B., Tamm, J.A., Yao, W.J., Vaysse, P.J.J., Branchek, T.A., Gerald, C. and Jones, K.A. (1998) 'Cloned human and rat galanin GALR3 receptors. Pharmacology and activation of G-protein inwardly rectifying K+ channels', *The Journal of biological chemistry*, 273(36), pp. 23321–23326. Available at: https://doi.org/10.1074/jbc.273.36.23321.

Sollenberg, U., Bartfai, T. and Langel, Ü. (2005) 'Galnon – a low-molecular weight ligand of the galanin receptors', *Neuropeptides*, 39(3), pp. 161–163. Available at: https://doi.org/10.1016/j.npep.2004.12.019.

Steenbergen, P.J., Richardson, M.K. and Champagne, D.L. (2011) 'The use of the zebrafish model in stress research', *Progress in Neuro-Psychopharmacology and Biological Psychiatry*, 35(6), pp. 1432–1451. Available at: https://doi.org/10.1016/j.pnpbp.2010.10.010.

Stoop, R. (2012) 'Neuromodulation by Oxytocin and Vasopressin', *Neuron*, 76(1), pp. 142–159. Available at: https://doi.org/10.1016/j.neuron.2012.09.025.

Sumbre, G. and de Polavieja, G.G. (2014) 'The world according to zebrafish: how neural circuits generate behavior.', *Frontiers in neural circuits*, p. 91. Available at: https://doi.org/10.3389/fncir.2014.00091.

Sun, Q.Q., Baraban, S.C., Prince, D.A. and Huguenard, J.R. (2003) 'Target-Specific Neuropeptide Y-Ergic Synaptic Inhibition and Its Network Consequences within the Mammalian Thalamus', *The Journal of Neuroscience*, 23(29), p. 9639. Available at: https://doi.org/10.1523/jneurosci.23-29-09639.2003.

Tasker, J.G. and Herman, J.P. (2011) 'Mechanisms of rapid glucocorticoid feedback inhibition of the hypothalamic-pituitary-adrenal axis', *Stress (Amsterdam, Netherlands)*, 14(4), pp. 398–406. Available at: https://doi.org/10.3109/10253890.2011.586446.

Tatemoto, K., Rökaeus, Å., Jörnvall, H., McDonald, T.J. and Mutt, V. (1983) 'Galanin - a novel biologically active peptide from porcine intestine', *FEBS letters*, 164(1), pp. 124–128. Available at: https://doi.org/10.1016/0014-5793(83)80033-7.

Thiele, T.R., Donovan, J.C. and Baier, H. (2014) 'Descending control of swim posture by a midbrain nucleus in zebrafish.', *Neuron*, 83(3), pp. 679–691. Available at: https://doi.org/10.1016/j.neuron.2014.04.018.

Thisse, C. and Thisse, B. (2008) 'High-resolution in situ hybridization to whole-mount zebrafish embryos.', *Nature protocols*, 3(1), pp. 59–69. Available at: https://doi.org/10.1038/nprot.2007.514.

Tillage, Rachel P., Foster, S.L., Lustberg, D., Liles, L.C., McCann, K.E. and Weinshenker, D. (2021) 'Co-released norepinephrine and galanin act on different timescales to promote stress-induced anxiety-like behavior', *Neuropsychopharmacology*, 46(8), pp. 1535–1543. Available at: https://doi.org/10.1038/s41386-021-01011-8.

Tillage, R.P., Wilson, G.E., Liles, L.C., Holmes, P. v and Weinshenker, D. (2020) 'Chronic Environmental or Genetic Elevation of Galanin in Noradrenergic Neurons Confers Stress Resilience in Mice', *The Journal of Neuroscience*, 40(39), p. 7464. Available at: https://doi.org/10.1523/jneurosci.0973-20.2020.

Timmermans, S., Souffriau, J. and Libert, C. (2019) 'A general introduction to glucocorticoid biology', *Frontiers in Immunology*, 10. Available at: https://doi.org/10.3389/fimmu.2019.01545/full.

Tortorella, C., Neri, G. and Nussdorfer, G.G. (2007) 'Galanin in the regulation of the hypothalamic-pituitary-adrenal axis (review)', *International Journal of Molecular Medicine*, 19(4), pp. 639–647.

Ulrich-Lai, Y. and Herman, J. (2009) 'Neural regulation of endocrine and autonomic stress responses', *Nature Reviews Neuroscience*, pp. 397–409. Available at: https://doi.org/10.1038/nrn2647.

Vale, W., Rivier, C., Yang, L., Minick, S. and Guillemin, R. (1978) 'Effects of Purified Hypothalamic Corticotropin-Releasing Factor and Other Substances on the Secretion of Adrenocorticotropin and β-Endorphin-Like Immunoactivities in Vitro', *Endocrinology*, 103(5), pp. 1910–1915. Available at: https://doi.org/10.1210/endo-103-5-1910.

Vale, W., Spiess, J., Rivier, C. and Rivier, J. (1981) 'Characterization of a 41-residue ovine hypothalamic peptide that stimulates secretion of corticotropin and beta-endorphin', *Science*, 213(4514), pp. 1394–1397. Available at: https://doi.org/10.1126/science.6267699.

Vila-Porcile, É., Xu, Z.Q.D., Mailly, P., Nagy, F., Calas, A., Hökfelt, T. and Landry, M. (2009) 'Dendritic synthesis and release of the neuropeptide galanin: Morphological evidence from

studies on rat locus coeruleus neurons', *Journal of Comparative Neurology*, 516(3), pp. 199–212. Available at: https://doi.org/10.1002/cne.22105.

Wang, L. and Armstrong, W.E. (2012) 'Tonic regulation of GABAergic synaptic activity on vasopressin neurones by cannabinoids', *Journal of neuroendocrinology*, 24(4), pp. 664–673. Available at: https://doi.org/10.1111/j.1365-2826.2011.02239.x.

Wang, S., He, C., Maguire, M.T., Clemmons, A.L., Burrier, R.E., Guzzi, M.F., Strader, C.D., Parker, E.M. and Bayne, M.L. (1997) 'Genomic organization and functional characterization of the mouse GalR1 galanin receptor', *FEBS Letters*, 411(2–3), pp. 225–230. Available at: https://doi.org/10.1016/s0014-5793(97)00695-9.

Webling, K.E.B., Runesson, J., Bartfai, T. and Langel, Ü. (2012) 'Galanin receptors and ligands', *Frontiers in Endocrinology*, 3, p. 146. Available at: https://doi.org/10.3389/fendo.2012.00146/bibtex.

Wee, C.L., Song, E., Nikitchenko, M., Herrera, K.J., Wong, S., Engert, F. and Kunes, S. (2022) 'Social isolation modulates appetite and avoidance behavior via a common oxytocinergic circuit in larval zebrafish', *Nature Communications*, 13(1), pp. 1–17. Available at: https://doi.org/10.1038/s41467-022-29765-9.

Weikum, E.R., Knuesel, M.T., Ortlund, E.A. and Yamamoto, K.R. (2017) 'Glucocorticoid receptor control of transcription: precision and plasticity via allostery.', *Nature reviews. Molecular cell biology*, 18(3), pp. 159–174. Available at: https://doi.org/10.1038/nrm.2016.152.

Weinshenker, D. and Holmes, P. v. (2016) 'Regulation of neurological and neuropsychiatric phenotypes by locus coeruleus-derived galanin', *Brain Research*, pp. 320–337. Available at: https://doi.org/10.1016/j.brainres.2015.11.025.

Wendelaar Bonga, S.E. (1997) 'The stress response in fish', *Physiological reviews*, 77(3), pp. 591–625. Available at: https://doi.org/10.1152/physrev.1997.77.3.591.

Wied, D. de and Kloet, E.R.D. (1987) 'Pro-opiomelanocortin (POMC) as Homeostatic Control System', *Annals of the New York Academy of Sciences*, 512(1), pp. 328–337. Available at: https://doi.org/10.1111/j.1749-6632.1987.tb24971.x.

Wilkinson, M. and Brown, R.E. (2015) 'Neuropeptides I: classification, synthesis and co-localization with classical neurotransmitters', in *An Introduction to Neuroendocrinology*. Cambridge University Press, pp. 257–285. Available at: https://doi.org/10.1017/cbo9781139045803.012.

Woods, I.G., Schoppik, D., Shi, V.J., Zimmerman, S., Coleman, H.A., Greenwood, J., Soucy, E.R. and Schier, A.F. (2014) 'Neuropeptidergic signaling partitions arousal behaviors in zebrafish', *Journal of Neuroscience*, 34(9), pp. 3142–3160. Available at: https://doi.org/10.1523/jneurosci.3529-13.2014.

World Health Organization (2022) *COVID-19 pandemic triggers 25% increase in prevalence of anxiety and depression worldwide*. Available at: https://www.who.int/news/item/02-03-

2022-covid-19-pandemic-triggers-25-increase-in-prevalence-of-anxiety-and-depression-worldwide

Wrenn, C.C. and Holmes, A. (2006) 'The role of galanin in modulating stress-related neural pathways.', *Drug news & perspectives*, 19(8), pp. 461–467. Available at: https://doi.org/10.1358/dnp.2006.19.8.1043963.

Wu, Z., Autry, A.E., Bergan, J.F., Watabe-Uchida, M. and Dulac, C.G. (2014) 'Galanin neurons in the medial preoptic area govern parental behaviour', *Nature*, 509(7500), pp. 325–330. Available at: https://doi.org/10.1038/nature13307.

Wyart, C., Bene, F. del, Warp, E., Scott, E.K., Trauner, D., Baier, H. and Isacoff, E.Y. (2009) 'Optogenetic dissection of a behavioural module in the vertebrate spinal cord', *Nature*, 461(7262), pp. 407–410. Available at: https://doi.org/10.1038/nature08323.

Yang, D., Zhou, Q., Labroska, V., Qin, S., Darbalaei, S., Wu, Y., Yuliantie, E., Xie, L., Tao, H., Cheng, J., Liu, Q., Zhao, S., Shui, W., Jiang, Y. and Wang, M.W. (2021) 'G protein-coupled receptors: structure- and function-based drug discovery', *Signal Transduction and Targeted Therapy*, 6(1), pp. 1–27. Available at: https://doi.org/10.1038/s41392-020-00435-w.

Yeh, C.M. (2015) 'The basal NPO crh fluctuation is sustained under compromised glucocorticoid signaling in diurnal zebrafish', *Frontiers in Neuroscience*, 9, p. 436. Available at: https://doi.org/10.3389/fnins.2015.00436/bibtex.

Yeh, C.-M., Glöck, M. and Ryu, S. (2013) 'An optimized whole-body cortisol quantification method for assessing stress levels in larval zebrafish.', *PloS one*, 8(11), p. e79406. Available at: https://doi.org/10.1371/journal.pone.0079406.

Zhu, P.C., Thureson-Klein, Å. and Klein, R.L. (1986) 'Exocytosis from large dense cored vesicles outside the active synaptic zones of terminals within the trigeminal subnucleus caudalis: a possible mechanism for neuropeptide release', *Neuroscience*, 19(1), pp. 43–54. Available at: https://doi.org/10.1016/0306-4522(86)90004-7.

Zini, S., Roisin, M.-P., Langel, U., Bartfai, T. and Ben-Ari, Y. (1993) 'Galanin reduces release of endogeneous excitatory amino acids in the rat hippocampus', *European Journal of Pharmacology: Molecular Pharmacology*, 245(1), pp. 1–7. Available at: https://doi.org/https://doi.org/10.1016/0922-4106(93)90162-3.

Ziv, L., Muto, A., Schoonheim, P.J., Meijsing, S.H., Strasser, D., Ingraham, H.A., Schaaf, M.J.M., Yamamoto, K.R. and Baier, H. (2012) 'An affective disorder in zebrafish with mutation of the glucocorticoid receptor', *Molecular Psychiatry*, 18(6), pp. 681–691. Available at: https://doi.org/10.1038/mp.2012.64.

Zorrilla, E.P., Brennan, M., Sabino, V., Lu, X. and Bartfai, T. (2007) 'Galanin type 1 receptor knockout mice show altered responses to high-fat diet and glucose challenge', *Physiol Behav*, 91(5), pp. 479–485. Available at: https://doi.org/10.1016/j.physbeh.2006.11.011.

8 Publications

This monographic thesis is based on the following publication:

Corradi L, Bruzzone M, Sawamiphak S, dal Maschio M, Filosa A. Hypothalamic Galanin-producing neurons regulate stress in zebrafish through a peptidergic, self-inhibitory loop. *Current Biology* (2022).

Other publications:

Corradi L, Zaupa M, Sawamiphak S, Filosa A. Quantification of neuronal activity induced by stress using pERK immunostaining in zebrafish larvae. *STAR Protoc* (accepted).

Corradi L, Filosa A. Neuromodulation and Behavioral Flexibility in Larval Zebrafish: From Neurotransmitters to Circuits. *Front Mol Neurosci* (2021).

Apaydin DC, Jaramillo PAM, **Corradi L**, Cosco F, Rathjen FG, Kammertoens T, Filosa A, Sawamiphak S. Early-Life Stress Regulates Cardiac Development through an IL-4-Glucocorticoid Signaling Balance. *Cell Rep* (2020).

9 Appendix

9.1 List of abbreviations

AC	Adenylate Cyclase
ACTH/Acth	Adrenocorticotropin Hormone
ASR	Acoustic Startle Response
AVP/Avp	Arginine Vasopressin
bp	Base Pair
Ca^{2+}	Calcium
cAMP	3′, 5′-Cyclic Adenosine Monophosphate
CaM	Calmodulin
CNS	Central Nervous System
COVID-19	Coronavirus disease 2019
CRISPR	Clustered Regularly Interspaced Short Palindromic Repeats
CRH/Crh	Corticotropin Releasing Hormone
dpf	Days Post Fertilization
ERK	Extracellular Signal-Regulated Kinase
fps	Frames Per Second
GABA	Gamma-Aminobutyric Acid
Gad2	Glutamate Decarboxylase 2
GAL/Galn	Galanin
GALP	Galanin Like Peptide
GC	Glucocorticoid
GECI	Genetically encoded calcium indicator
GFP	Green Fluorescent Protein
GIRK	G-protein Coupled Inwardly Rectifying Potassium
GMAP	Galanin Message Associated Peptide
GPCR	G protein-coupled receptor
HB	Hybridization buffer
HCR	Hybridization Chain Reaction

HPA	Hypothalamic Pituitary Adrenal
HPI	Hypothalamic Pituitary Interrenal
IP3	Inositol triphosphate
K^+	Potassium
LDCV	Large Dense Core Vescicle
LC	Locus Coeruleus
LMP	Low Melting Point
MAPK	Mitogen-Activated Protein Kinase
NaCl	Sodium Chloride
NPY/Npy	Neuropeptide Y
NTR	Nitroreductase
OXT	Oxytocin
PAM	Protospacer Associated Motif
PLC	Phospholipase C
PTX	Pertussis Toxin
pHyp	Posterior Hypothalamus
POA/PoA	Preoptic Area
PoC	Post Optic Commissure
PVN	Paraventricular Nucleus
RT-PCR	Reverse Transcript Polymerase Chain Reaction
SAM	Sympathetic Adreno Medullar
SEM	Standard Error of the Mean
sgRNA	Single Guide RNA
UAS	Upstream Activation Sequence

9.2 List of figures

9.3 Nomenclature guide

Galanin

Species	Gene symbol	Protein symbol
Zebrafish (*Danio rerio*)	***galn****	**Galn**
Mouse/Rat (*Mus musculus*)	***Gal***	**GAL**
Rat (*Rattus norvegicus*)	***Gal***	**GAL**
Human (*Homo sapiens*)	***GAL***	**GAL**

Galanin receptors

Species	Gene symbol	Protein symbol
Zebrafish (*Danio rerio*)	***galnR****	**GalnR**
Mouse/Rat (*Mus musculus*)	***Galr***	**GALR**
Rat (*Rattus norvegicus*)	***Galr***	**GALR**
Human (*Homo sapiens*)	***GALR***	**GALR**

*In 2020 the genes encoding Galanin and its receptors in zebrafish were renamed as *gal* and *galr* to conform with the human nomenclature. In this dissertation I decided to use the synonyms *galn/galnR* which were in use when I started my project and are still commonly used.

Acknowledgments

Thanks to my supervisor Dr. Alessandro Filosa for his support and guidance even in the hardest times. I did not choose a city, an institute, or even a project but I chose a mentor, which it proved to be the best choice. Thanks to Dr. Suphansa Sawamiphak, for her supervision, her brilliant mind and determination, which have always been a source of inspiration.

I would like to express my gratitude to Prof. Dr. Mathias Wernet and Dr. Niccolo Zampieri for their participation in my committee meetings and their inputs to this project.

Thanks to Prof. Marco dal Maschio and Matteo Bruzzone for the great collaboration and help with some of the results showed in this study.

Thanks to Prof. Pertti Panula for the plasmid used for the antisense *galn* probe.

A huge thanks to Anne Banerjee for all her continuous technical, professional, and personal help and to Margherita Zaupa for her help with Matlab and for the cloning of the *UAS:tdTomato-CAAX* plasmid used in this study.

Thanks to Bhakti, to Paul, to all my colleagues and to the former lab members. I also would like to thank Bastiaan Pierik, Steffen Tornow, the Microscope Facility, and the zebrafish care takers of the MDC.

Thanks to Dilem and Onur Apaydin who contributed to this project with that every day help which I would not even know how to acknowledge properly as it was never a favor from a colleague, but always a kindness from a friend.

Last but not the least, I would like to thank all my friends in Berlin who were family in these last years, with whom I shared unforgettable lockdowns, Christmas, and Easter, who took care of me when I fell (literally and metaphorically) and never let me feel alone.

"Non temete i momenti difficili.
Il meglio scaturisce da lì."

Rita Levi Montalcini